U.S. DEPARTMENT OF COMMERCE
National Technical Information Service
PB-253 008

MULTISPAN ELEVATED GUIDEWAY DESIGN FOR PASSENGER TRANSPORT VEHICLES

VOLUME I. TEXT

MASSACHUSETTS INSTITUTE OF TECHNOLOGY

PREPARED FOR
TRANSPORTATION SYSTEMS CENTER

APRIL 1975

Technical Report Documentation Page

1. Report No.	2. Government Accession No.	3. Recipient's Catalog No.
FRA-OR&D-75-43.I		

4. Title and Subtitle
MULTISPAN ELEVATED GUIDEWAY DESIGN FOR PASSENGER TRANSPORT VEHICLES
Volume I. Text

5. Report Date
April 1975

6. Performing Organization Code

7. Author(s)
D.N. Wormley, C.C. Smith, A.J. Gilchrist

8. Performing Organization Report No.
DOT-TSC-FRA-75-4.I

9. Performing Organization Name and Address
Massachusetts Institute of Technology
Department of Mechanical Engineering*
Cambridge MA 02139

10. Work Unit No. (TRAIS)
RR518/R5318

11. Contract or Grant No.
DOT-TSC-349-1

12. Sponsoring Agency Name and Address
U.S. Department of Transportation
Federal Railroad Administration
Office of Research and Development
Washington DC 20590

13. Type of Report and Period Covered
Final Report
July - December 1974

14. Sponsoring Agency Code

15. Supplementary Notes
*Under contract to: U.S. Department of Transportation
Transportation Systems Center
Kendall Square
Cambridge MA 02142

16. Abstract

Analysis techniques, a design procedure and design data are described for passenger vehicle, simply supported, single span and multiple span elevated guideway structures. Analyses and computer programs are developed to determine guideway deflections, moments and stresses and vehicle accelerations resulting from a two-dimensional vehicle with finite pad length front and rear suspensions traversing a multispan elevated guideway. A preliminary design procedure is described to estimate guideway beam structural requirements so that a vehicle-guideway system will meet specified levels of passenger comfort. Design data for 150 mph and 300 mph intercity 40,000, 80,000 and 120,000 lb. air cushion vehicle single and multiple span (span lengths of 50 to 150 ft.) guideways is summarized. For both urban and intercity operating regimes, the data indicates that improvements in the vehicle suspension and the use of multiple span structures rather than single span structures may result in reduced guideway material requirements. The nomenclature is contained in Appendix H, Volume II.

17. Key Words	18. Distribution Statement
Elevated Guideways Vehicle Guideway Interactions Air Cushion Vehicles Magnetically Levitated Vehicles	DOCUMENT IS AVAILABLE TO THE PUBLIC THROUGH THE NATIONAL TECHNICAL INFORMATION SERVICE, SPRINGFIELD, VIRGINIA 22161 PRICES SUBJECT TO CHANGE

19. Security Classif. (of this report)	20. Security Classif. (of this page)	21. No. of Pages	22. Price
Unclassified	Unclassified	137	6.00-2.25

Form DOT F 1700.7 (8-72) Reproduction of completed page authorized

PREFACE

This work was supported by the U. S. Department of Transportation, Transportation Systems Center under contract DOT-TSC-349 in support of the Federal Railroad Administration Office of Research and Development and the Urban Mass Transportation Administration.

The authors wish to acknowledge the many fruitful technical discussions held with Dr. H. H. Richardson, of the Department of Mechanical Engineering, Massachusetts Institute of Technology and with Dr. H. Weinstock, who served as technical monitor of the contract for the Transportation Systems Center. We also wish to acknowledge the contribution of Mr. J. Edward Snyder who assisted in preparing the computer programs developed and Miss Leslie Buckley who prepared the report manuscript.

TABLE OF CONTENTS

VOLUME I

LIST OF ILLUSTRATIONS

VOLUME I

LIST OF TABLES

VOLUME I

VOLUME II

1. INTRODUCTION

1.1 Background

In the past few years substantial interest has developed in advanced, innovative urban and intercity mass ground transportation because of the need for transportation of people and commodities with increased energy efficiency, acceptable environmental impact, convenience and economy. Systems under current development include 20-60 mph personal rapid transit systems [1]*, advanced 60-150 mph rail transit systems [2-4], and high speed 100-300 mph air cushion and magnetically levitated vehicle systems [5-9]. The economic feasibility of implementing these advanced systems depends significantly upon the development of guideways which minimize construction and maintenance costs while meeting system performance specifications since a major fraction of total system cost is represented by guideway construction and maintenance.

In urban environments and some intercity corridors, substantial portions of a system guideway will be elevated to negotiate rights of way and topological barriers, utilize air space and provide safety. This report focuses upon the design of elevated structures for tracked, levitated vehicles. Guideway design for these systems offers both a number of problems and opportunities [10-14] which have not been considered in

---

*Numbers in [ ] refer to references listed in the Bibliography

classical highway and rail transit elevated structure design. Because of the distributed low unit pressure suspension loadings which characterize levitated vehicle systems and the high vehicle speeds which may occur in intercity systems, the vehicle induced loads on the guideway may be significantly different in conventional and levitated vehicle systems. Also while in classical highway and rail bridge design passenger comfort criteria have been specified indirectly in terms of a maximum permissible guideway midspan deflection to span length ratio such as the 1/800 specification in [15], for advanced systems the Department of Transportation has established passenger comfort requirements directly in terms of permissible levels of vehicle acceleration. To design a guideway-vehicle system to meet an acceleration specification requires consideration of vehicle characteristics and of the vehicle-guideway dynamic interaction. In this report, an integrated vehicle-guideway design procedure is developed.

1.2 Vehicle-Elevated Guideway Design Literature

Vehicle-elevated guideway design literature prior to 1969, primarily describes analytical techniques to determine guideway deflections due to the passage of constant and pulsating forces, masses and simple, one-dimensional vehicles. In the last few years, parametric data, basic analyses and computer simulations of vehicle-guideway interactions for tracked levitated vehicles have been developed. Both the early and more recent work concerning beam-type guideways is reviewed in some detail

in [26].[1] In [26] work is reviewed based upon [10, 19, 22 and 25] which determines single and multispan guideway dynamic deflections due to the passage of constant traveling point force or pressure pad vehicle models. These studies have shown that dynamic amplification factors resulting from a single constant force passage are within 20% of the quasi-static case for vehicle velocities $v < 0.5\, \ell_s f^*$ for single span guideways and for $v < \ell_s f^*$ for continuous span guideways where ℓ_s is the span length and f^* the span natural frequency. For speeds above these values, span dynamic effects are important with the single span guideway amplification factor approaching 1.76 at $v \simeq 1.3\, \ell_s f_1$ and the continuous guideway approaching a resonant condition for $v \simeq 2.0\, \ell_s f^*$. This report extends the single moving force amplification factor data to include deflection and moment (stress) amplification factors for multispan guideways excited by multiple finite length suspension pads and shows that, for specific vehicle to span length ratios, the multispan resonance at $v = 2.0\, \ell_s f^*$ may be suppressed.

Analyses and simulation programs of multi-dimensional point contact suspension vehicles crossing single and multiple span guideways are described in [16, 17, and 18]. The simulation program listed in [18] is complemented by [19] which discusses continuous guideway span design for cases which are either stress or deflection limited.

---

[1] In [27] through-truss and cable stayed structures are reviewed for systems in which span lengths exceeding 200 ft. are required.

Analyses which include vehicle models with finite length suspension pads are discussed in [21--25 and 31]. In [22, 23, and 24] numerical solution procedures are developed which allow simulation of a multipad air cushion vehicle with a three stage passive suspension traversing cambered and uncambered single span guideways. In [21] a computer program which determines the accelerations of a two-dimensional vehicle with finite pad length suspensions crossing a single span guideway is developed using an approximate constant suspension force analysis similar to that summarized in Chapter 3.

Recent guideway design studies have illustrated the relative importance of structural loading design constraints in comparison to passenger comfort design constraints for specific urban and intercity air cushion vehicles [11-13]. Reference [13] has shown for 50-150 ft. span guideways that the passenger comfort constraint represents a more severe guideway design constraint for typical 150 mph air cushion systems than stress constraints resulting from vehicle loading. This study [13] and complementary studies [11, 12, 14 and 25] have highlighted the need to develop efficient guideway design procedures and parametric data for urban and intercity levitated vehicle systems which include passenger comfort constraints directly.

1.3 Scope of the Study

The primary objective of this study is the development of parametric design data and a preliminary design procedure for

tracked, levitated vehicle system guideways. The beam-like guideway configurations illustrated in Figure 1.1 are considered including (1) the single span guideway, (2) the multispan guideway in which continuous beams span several supports, and (3) the continuous span guideway in which a single continuous beam spans all supports. A primary advantage of a multispan structure compared to a single-span structure is that for the same span material and cross section the multi- or continuous span deflection, due to a given static load, is less than that generated in an equivalent single span structure. As summarized in Figure 1.1 a multispan beam with 3 or more spans sustains 70% of the deflection of a single span due to a static load while a continuous span sustains 53% of a single span deflection. Equivalently, a multi- or continuous span structure may provide the same deflection as a single span system and use less span material or have greater distance between span supports. In multi- and continuous span structures, span-to-span coupling may result in possible dynamic resonance conditions for which dynamic deflections are greater than in single spans. In the study, multispan resonance conditions are evaluated.

Since the level of passenger comfort desired for levitated vehicle systems [11-14] represents a guideway design constraint which is more stringent than vehicle induced stress constraints, techniques are developed to estimate directly guideway structural properties required for the vehicle-guideway system to provide a specified level of passenger comfort and then stress

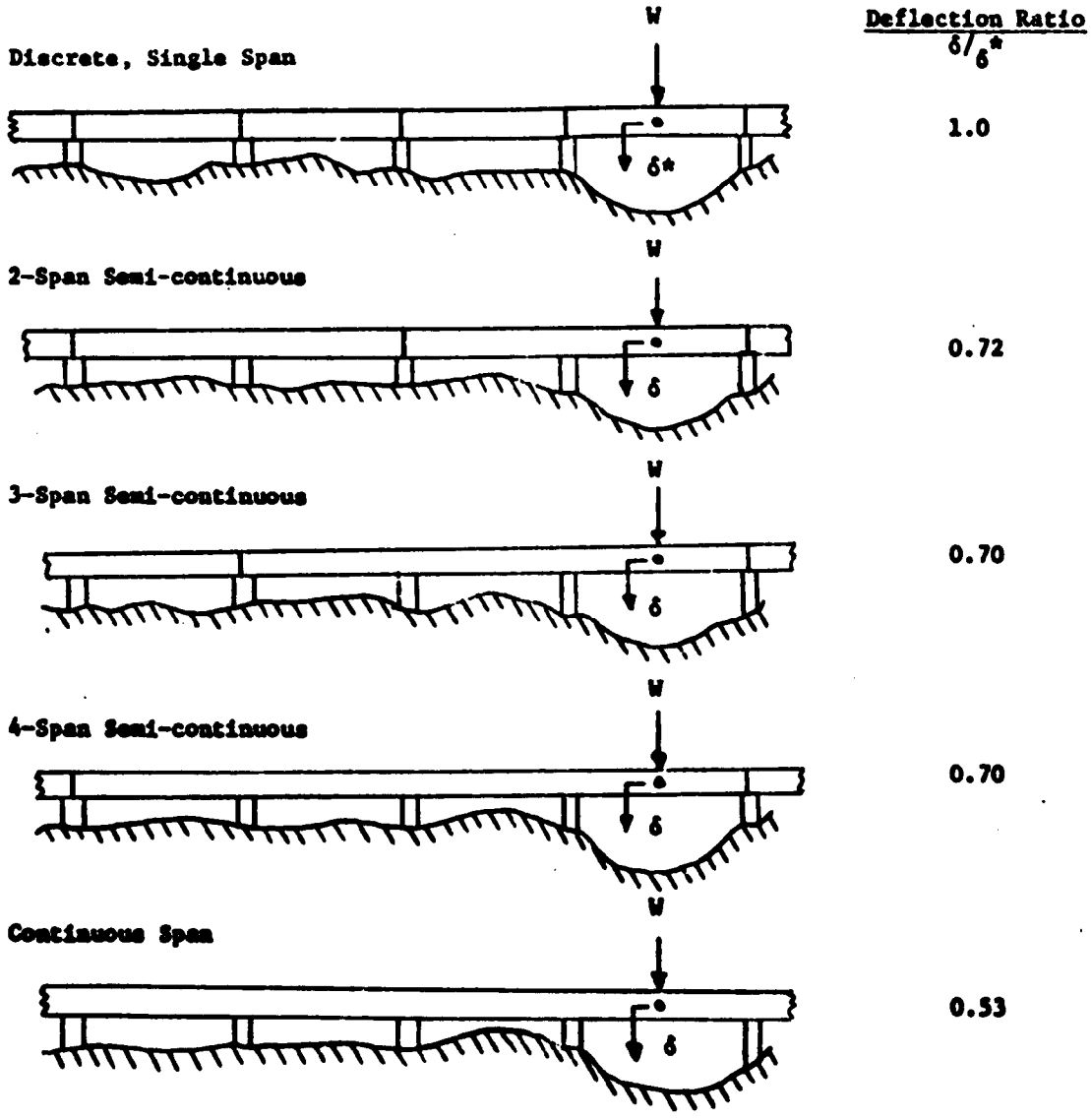

Fig. 1-1. Single, Multispan and Continuous Span Configurations

levels are checked. The passenger comfort constraint considered is an extension of the one hour ride comfort criteria of the International Standards Organization which specifies a permissible level of rms passenger compartment acceleration as a function of frequency.*

1.4 Summary of the Study

As a result of this study the following models and design procedures have been developed for the evaluation and design of passenger transport vehicle-guideway systems:

(1) Fully Coupled Vehicle-Guideway Model Simulation

This model allows determination of the response of a completely coupled vehicle guideway system as a function of time. The vehicle model includes vehicle body mass and pitch inertia, front and rear secondary suspensions with stiffness and damping characteristics and primary suspensions with stiffness and finite pad length characteristics. The guideway model includes single and multispan cambered beams with distributed stiffness, mass and damping properties supported on rigid piers.** In the model the time varying vehicle accelerations and suspension deflections and forces are computed as well as span deflections, moments and stresses. The model is described in Chapter 2 and instructions for the computer simulation program based upon fourth order numerical integration of the model equations are given in Appendix C.

---

* The specification is displayed in Figure 4.1 and requires a rms acceleration level of less than 0.04 g's in the 3--12 hertz frequency range. The design procedures developed are applicable to any form of specification which involves rms accelerations as a function of frequency.

** The influence of pier-support motion upon vehicle-guideway dynamic interactions is shown to be negligible in Appendix B for the systems considered in this study.

(2) Partially Coupled Vehicle-Guideway Model Simulation

The partially coupled simulation model provides determination of vehicle acceleration versus time, rms acceleration versus frequency, suspension deflections and guideway deflections, moments and stresses. The model allows coupling between the vehicle and the guideway but assumes that the vehicle suspension forces on the guideway are constant and equal to the vehicle weight. All other features of the vehicle-guideway model are similar to those of the model described above. This partially coupled model is described in Chapter 3 and Appendix G in which it is shown to be valid for vehicles with high levels of passenger comfort (0.07g peak acceleration or less) which operate at span encounter frequencies, i.e. vehicle velocity divided by span length v/ℓ_s, less than the vehicle suspension natural frequency, f_v, for both conventional and levitated vehicles with unsprung to sprung mass ratios of 0 to 0.66 and/or for the full range of tracked levitated vehicle operation for vehicles with the small unsprung to sprung mass ratios characteristic of passenger carrying air cushion vehicles, i.e. less than 0.1 This partially coupled simulation is implemented in the computer program described in Appendix D which allows computation of system characteristics in less than one quarter the time required for the full simulation described above.*

(3) A Vehicle-Guideway System Design Procedure

A systematic procedure has been developed to design transport vehicle guideways. This procedure is based upon the partially coupled vehicle-guideway model and results in the determination of guideway main support beam structural properties required so that for a given type of vehicle specified levels of vehicle passenger comfort (and guideway stress) are met. The procedure is described in Chapter 4 and may be performed with the aid of the design charts using a desk calculation or may be performed with the computer program described in Appendix E.

*In many of the cases run in this study the partially coupled model running time was less than one eighth of the fully coupled simulation time.

In addition to the simulation models, design methods and associated working computer programs, design data for general vehicle-elevated guideway systems has been developed in Chapter 3 which shows:

(1) For vehicle operating speeds

(a) less than 0.5 $\ell_s f^*$ for single span structures

(b) less than $\ell_s f^*$ for multiple span structures

(c) less than 1.5 $\ell_s f^*$ for continuous span structures

the span deflections, due to a vehicle passage, are quasi-static and multispan deflections (for 3 or greater spans) are 70% while continuous span deflections are 53% of comparable single span structures. In these operating ranges multiple and continuous spans require less material and/or fewer supports than single span guideways.

(2) For vehicle operating speeds v that approach 2 $\ell_s f^*$ resonance conditions may occur in multiple and continuous spans. The span deflections are influenced strongly by span damping and for a damping ratio of 0.02, maximum deflections in three and continuous spans caused by the passage of a concentrated force are respectively 3.7 and 4.6 times the quasi-static deflections.

(3) Vehicles with a suspension separation length in the vicinity of 0.8 ℓ_s may effectively suppress the multi-span resonance condition described in (2).

(4) As vehicle loads are distributed across suspension pads, guideway deflections are reduced. In the quasi-static operating range, vehicles crossing single spans with pad lengths 50% and 100% of a span length reduce span deflections respectively by more than 20% and 40% compared to concentrated force vehicles.

Specific design data has been developed for 40,000, 80,000 and 120,000 lb. 150 mph and 300 mph air cushion vehicle guideways. This data was developed using the

design program of Appendix E for prestressed concrete twin I beam structures traversed by vehicles which meet the passenger comfort specifications of Figure 4.1, i.e. rms vehicle body accelerations are less than 0.045 g's in the 2.5-12 hertz frequency range. The conclusions reached from this specific study include:

(1) For all designs, the passenger comfort constraint is more stringent than vehicle induced stress constraints. The maximum induced span dynamic stress is less than 775 psi for both low and high speed vehicle systems. The guideway designs are directly dependent upon the passenger comfort level required. For an 80,000 lb. 150 mph vehicle with 2 hertz suspension natural frequency traversing a single 100 ft. span guideway, if the permissible rms acceleration is increased from 0.045 g's to 0.09 g's span material requirements may be reduced by 15%.

(2) For system designs constrained by passenger comfort, vehicle characteristics may strongly influence guideway requirements. Vehicle suspension natural frequency and damping, vehicle body mass distribution (pitch inertia) and vehicle suspension attachment point location may all influence span requirements as well as total vehicle size and weight, vehicle speed and suspension pad length. For an 80,000 lb. vehicle crossing a 100 ft. single span system at 300 mph, a reduction in suspension natural frequency from 2.0 to 1.0 hertz allows a reduction in span requirements of 29% while an increase in pitch inertia from that of a uniform mass distribution to a body with an effective mass distribution concentrated at the suspension attachment points allows a reduction in span material of 14%.

(3) Span configuration and camber may strongly influence span structural requirements. In all cases studied the use of multiple span guideways required less span material than single span structures designed for the same operational vehicle. For an 80,000 lb. vehicle with a 2.0 hertz suspension crossing 100 ft. spans at 300 mph, a two span system requires 91% and a three span system 87% of the material of a single span system.

The use of cambered spans for single and three span systems can result respectively in 11% and 12% material reduction in comparison to uncambered spans and can, also, provide a tolerance of ± 33% variation in camber due to thermal effects from the precamber amplitude and still meet ride quality specifications for 150 mph vehicles.

The systematic application of the integrated vehicle-guideway design techniques developed in this study is illustrated for 150 and 300 mph 80,000 lb. air cushion vehicles crossing twin I beam prestressed concrete span guideways in Figs. 1-2 and 1-3. All of the designs illustrated meet the rms acceleration specification cited above and yield guideway stresses due to a vehicle passage which are less than 750 psi. Figs. 1-2 and 1-3 show that the use of successive improvements in vehicle design through:

(1) Reduction of suspension natural frequency

(2) Redistribution of vehicle body mass

and in span design through:

(1) Use of multiple spans

(2) Use of camber

allow a reduction in span height from 7.1 to less than 3.0 ft. in the 150 mph case and from 11 to 4 ft. in the 300 mph case and provide an increased tolerance to thermal camber. Through the successive use of integrated vehicle-guideway design techniques, designs for advanced transport systems may be identified which meet system performance specifications and as illustrated for air cushion vehicle guideway designs, may have reduced guideway material requirements.

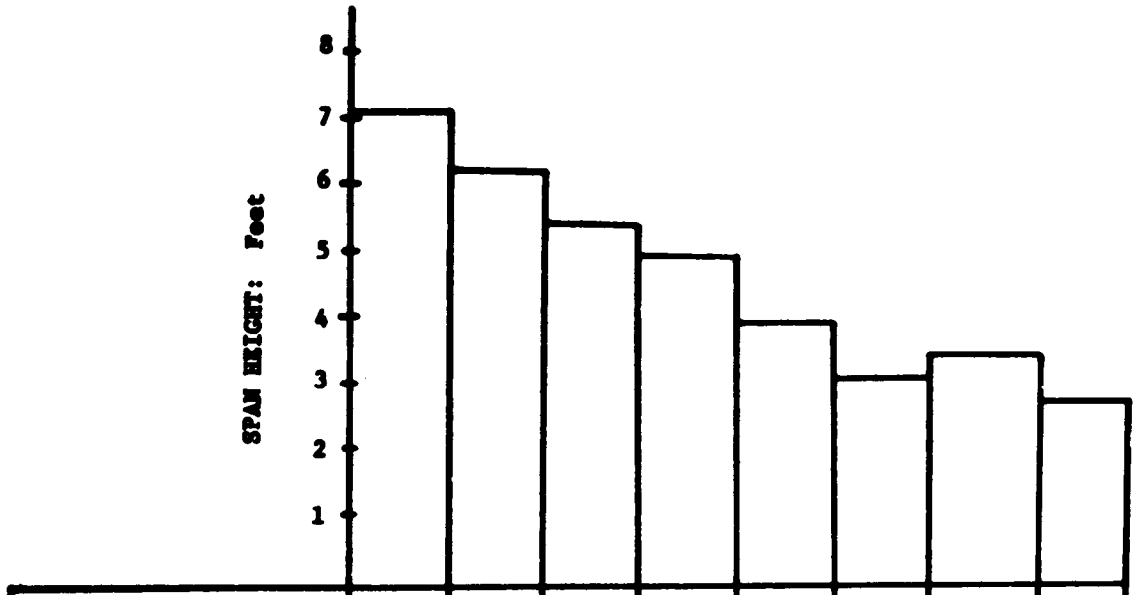

Suspension Frequency: hertz	2.0	2.0	1.0	1.0	1.0	1.0	1.0	1.0
Vehicle Inertia Ratio $\bar{I}_v$	1.0	1.0	1.0	1.0	3.0	3.0	3.0	3.0
Number of Spans	1	3	1	3	1	3	1	3
Camber: $\bar{A}_c$ Minimum							0.2	0.16
Camber: $\bar{A}_c$ Nominal							0.6	0.4
Camber: $\bar{A}_c$ Maximum	0	0	0	0	0	0	1.0	0.64

Fig. 1-2. Reduction in Span Height Requirements for 150 mph Air Cushion Vehicle Concrete Guideways as a Function of Design Improvements

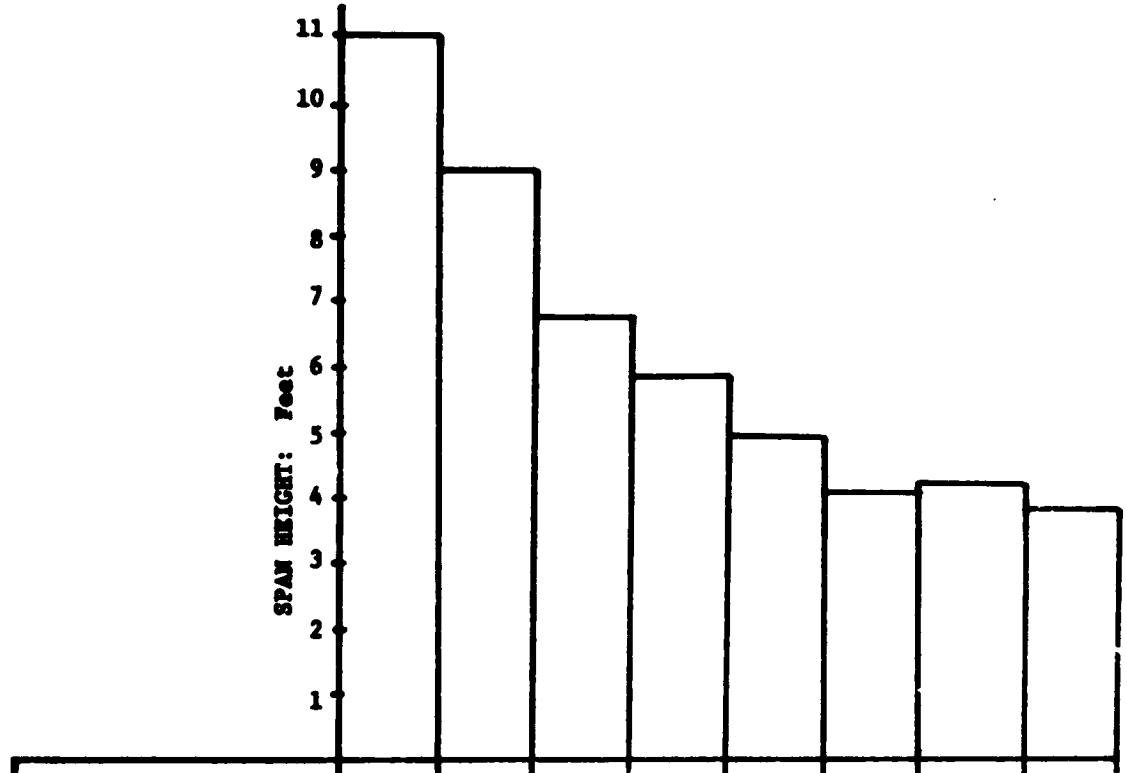

Suspension Frequency: hertz	2.0	2.0	1.0	1.0	1.0	1.0	1.0	1.0
Vehicle Inertia Ratio $\bar{I}_v$	1.0	1.0	1.0	1.0	3.0	3.0	3.0	3.0
Number of Spans	1	3	1	3	1	3	1	3
Camber: $\bar{A}_c$ Minimum Nominal Maximum	0	0	0	0	0	0	0.25 0.60 0.95	0.2 0.45 0.7

Fig. 1-3. Reduction in Span Height Requirements for 300 mph Air Cushion Vehicle Concrete Guideways as a Function of Design Improvements

2. GUIDEWAY-VEHICLE INTERACTION SYSTEM MODELS

2.1 The Vehicle-Guideway System

The general vehicle-guideway system model considered in this study is illustrated in Figure 2.1. The model is formulated for the vertical motion between the vehicle and the guideway. The vertical motion of the guideway is excited by the full vehicle weight while lateral and longitudinal motions are excited by only a fraction of vehicle weight; therefore, primary attention is devoted to the vertical interaction problem. The basic design techniques developed for the vertical interaction problem may be extended to lateral vehicle-guideway interaction design.

2.2 The Guideway Model

The model for the guideway is formulated in a general manner so that it is compatible with a variety of vehicles which may use air cushion, magnetic or wheel suspensions. For typical guideway systems of interest, span length to width ratios are large enough so that individual spans may be considered as beams rather than as plates. The model considers a structure consisting of a finite series of beams which may be continuous across a finite number of supports.* Each beam is represented by its general structural mass, stiffness, and damping properties so that a variety of detailed structure shapes (box, I, T, inverted T, channel or other shapes) and materials may be considered.

*A guideway model for the limiting case of a completely continuous beam is discussed in [28 and 29]

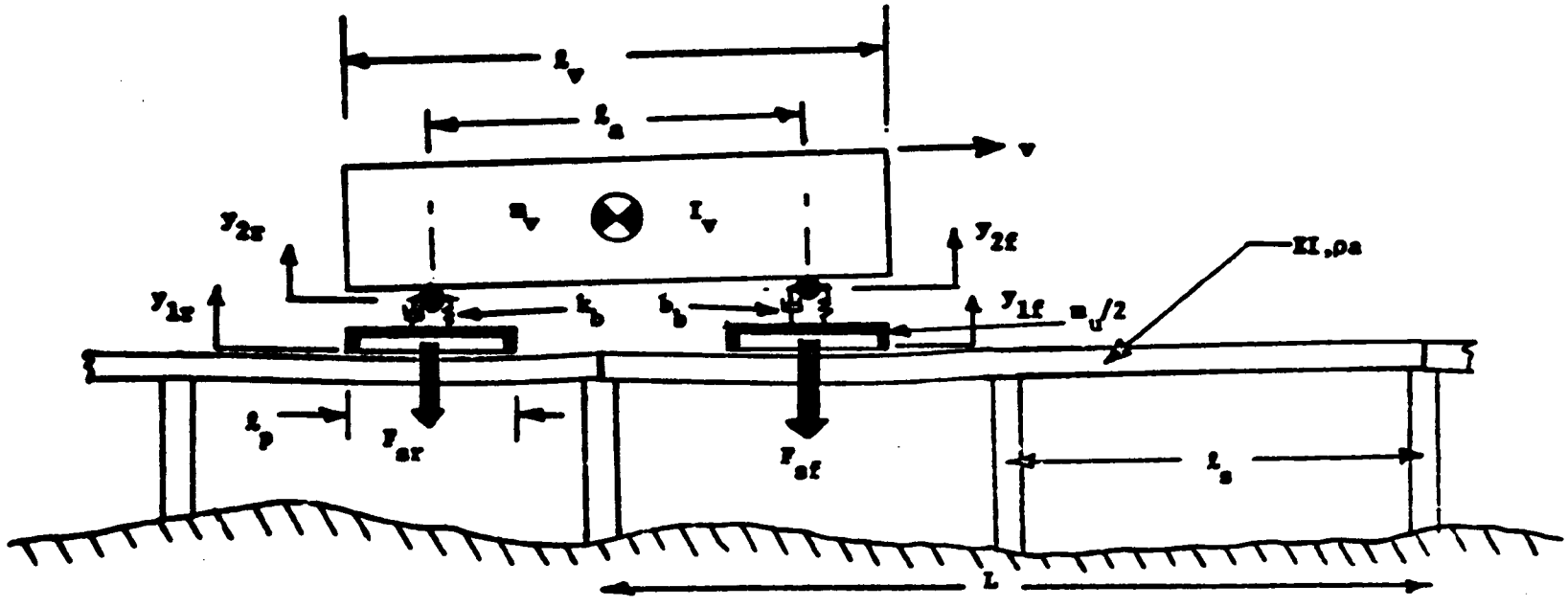

Fig. 2-1. Multiple Suspension Vehicle Traversing a Multispan Guideway

The spans are considered to rest freely upon rigid pier supports. An evaluation of pier and foundation flexibility, mass and damping properties is summarized in Appendix B. The work has shown that for representative structures designed in accordance with standard civil engineering practice, the motions of the pier supports, due to a vehicle passage, will be small, typically less than 10% of the motion of the guideway beam and will not, in representative cases, strongly influence vehicle motion and vehicle-guideway interactions.

When only the vertical span and vehicle motion are considered, the influence of a vehicle upon a span may be represented by a general force distribution f (x,t) which may vary spatially along the span and is a function of time while the influence of the span dynamic motion upon a vehicle may be represented by the time varying guideway deflection profile y(x, t) which is assumed to be constant across a span width. The complete guideway profile presented to the vehicle consists of the guideway time varying profile y (x,t) plus the initial guideway profile $y_c(x)$ which is a function of only spatial location. The initial profile $y_c(x)$ may arise from possible misalignment, thermal camber, or intentional precamber. The profile is assumed to be time invariant during a vehicle passage. Thus, the complete guideway profile presented to the vehicle y_t is:

$$y_t = y(x,t) + y_c(x) \tag{2.1}$$

A number of analytical techniques, including (1) lumped mass methods, (2) direct numerical methods and (3) modal analysis have been developed to model beam-like structures. These techniques are reviewed in [10]. In this study the modal analysis technique is used in which the space and time varying motion of a span y(x,t) is represented as the summation of the span natural modes of vibration:

$$y(x,t) = \sum_{m=1}^{\infty} A_m(t)\ \phi_m(x) \qquad (2.2)$$

Where $\phi_m(x)$ are the modal shape functions determined from the boundary conditions and the Bernoulli-Euler beam equation and $A_m(t)$ are time varying functions determined from solution of the beam equation with the forcing function f(x,t). In practice the method is well suited for distributed systems which have small inherent damping such as guideway beams where damping is typically less than 5% of critical damping [10]. The technique is particularly attractive in this study because it provides an efficient*, general technique in which single and multiple span systems excited by a general force distribution f(x,t) arising from vehicle passage may be considered in a uniform and consistent manner. The detailed derivation of the guideway modal equations is described in Appendix A.

2.3 The Vehicle Model

The vehicle model for this study illustrated in Figure 2.1 may represent air cushion, magnetic or wheel vehicles. It is a two-

*For many of the systems considered, only a few modes in the summation of (2.2) are required to represent the guideway adequately as discussed in Section 2.5.

dimensional, rigid body vehicle with mass m_v and inertia I which is capable of both heave and pitch motion and is supported upon identical front and rear suspensions separated by a length ℓ_a. Each suspension consists of a secondary stiffness k_b and damping b_b, an unsprung mass m_u and a primary stiffness k_{sr}*. The suspension force is assumed to be uniformly distributed on the guideway over the suspension pad length ℓ_p. The total suspension force is represented by the force generated in the resultant primary suspension spring k_{sr} whose effective displacement is based upon the distance between the pad midpoint and the point on the guideway directly beneath the pad midpoint.

For an air cushion vehicle the stiffness k_{sr} represents the air pad stiffness, m_u the pad mass and k_b and b_b secondary suspension parameters which may be implemented as a classical secondary suspension or as a flexible skirt. In a similar manner for a magnetic suspension k_{sr} represents the magnetic gap stiffness, m_u the unsprung magnet mass and k_b and b_b secondary suspension stiffness and damping parameters. For wheeled vehicles k_{sr} represents the tire or wheel stiffness, m_u the unsprung wheel mass and k_b and b_b secondary suspension stiffness and damping parameters. The suspension pad length ℓ_p may be selected as a significant fraction of the vehicle length to represent typical air cushion vehicle pads and magnetic suspension modules or as a very small fraction of vehicle length to represent a tire footprint length or wheel contact length. The equations of motion describing the vehicle model are derived in Appendix A.

*m_u is the total vehicle unsprung mass while k_{sr}, k_b and b_b are respectively the primary and secondary stiffness and damping for each suspension.

2.4 Vehicle-Guideway Interaction Model Parameters

From the guideway and vehicle equations derived in Appendix A, a set of fundamental nondimensional parameters may be derived to characterize the vehicle-guideway model. The parameters required for a vehicle with identical front and rear suspensions crossing a guideway with equally spaced identical spans are summarized in Table 2.1. In Table 2.1 the crossing velocity frequency V_c characterizes the vehicle speed and is the ratio of the vehicle span crossing frequency v/ℓ_s to the natural frequency f* of the first mode of vibration of a simple pinned end beam of length ℓ_s.

$$f^* = \frac{\pi}{2\ell_s^2}\sqrt{\frac{EI}{\rho A}} \tag{2.3}$$

The crossing frequency ratio is small for low vehicle speeds and increases as the vehicle speed increases. At a value of $V_c = 1.0$, the vehicle crosses the span in a period equal to the time it takes a span to undergo one full period of vibration. At values of $V_c > 2.0$ the vehicle crosses the span in a time less than the span can complete one half cycle and the vehicle begins to "outrun" the span. Typical values of V_c for tracked, levitated vehicles are tabulated in Table 2.1. For typical 150 mph systems $0 < V_c < 1$ while for 300 mph systems $0 < V_c < 2$.

The value of f in (2.3) is also the first mode frequency for a multiple span pinned end beam.

TABLE 2.1

Fundamental Vehicle-Guideway Interaction Parameters

Parameter	Definition	Typical Values for Tracked, Levitated Vehicle Systems
V_c: Crossing Velocity Frequency Ratio	$\frac{v}{f^* \ell_s}$	0 → 1 (150 mph urban system) 0 → 2 (300 mph intercity system)
Ω: Span to Vehicle Suspension Frequency Ratio	$2\pi f^* \Big/ \sqrt{\frac{2k_b}{m_v}}$	1 → 10
M: Vehicle to Span Mass Ratio	$(m_u + m_v)/\rho a \ell_s$	0.1 → 1.0
L_a: Vehicle Suspension Length Ratio	ℓ_a/ℓ_s	0 → 3
L_p: Pad Length to Span Length Ratio	ℓ_p/ℓ_s	0 → 1
K: Vehicle Primary to Secondary Suspension Stiffness Ratio	k_{sr}/k_b	5 -- 50*
M_u: Vehicle Unsprung to Sprung Mass Ratio	m_u/m_v	.02 → .3
$\bar{I}_v$: Vehicle Nondimensional Inertia	$I_v/m_v \ell_a^2/12$	0.75 → 1.25
ξ_v: Vehicle Suspension Damping Ratio	$b_b \omega_v/2k_b$	0.15 → 0.75
ξ_m: Span Damping Ratio	$b_m/2\rho a \omega_m$	0.005 → 0.1
k: Number of Semi-Continuous Spans	-----	1 -- 5

*These values assume that both a primary and a secondary suspension is used. If a carriage suspension is used, such as the tracked air cushion research vehicle, or some magnetic vehicles, M_u, may exceed 0.3.

Values of the other parameters required to define the vehicle-guideway system for typical tracked, levitated vehicle systems are also summarized in Table 2.1.

2.5 Solution of the Interaction Model Equations

A computer program using a fourth order Runge-Kutta integration routine has been developed to solve the fully coupled vehicle guideway interaction equations. The program description and listing are contained in Appendix C. The program input parameters required to specify a vehicle-guideway system are the nondimensional parameters summarized in Table 2.1. The program is set up to treat single and 2 and 3 multispan systems and prints out front, midpoint and rear vehicle accelerations in g's and nondimensional midspan moments and deflections as a function of time as the vehicle traverses a guideway system at constant speed.

In the guideway model the number of modes required to represent the guideway must be selected. As shown in [10], the number of modes required to represent the guideway depends upon the vehicle crossing frequency ratio V_c. For all of the typical system designs considered in this study $V_c < 2.0$. For cases $V_c < 2.0$, the contribution of each mode m to the span deflection in a single span system is approximately proportional to $1/m^4$, and in the calculation of the midspan deflection, the third mode* contribution is approximately $1/81 \simeq 1.2\%$.

---

*The even modes have no contribution to the midspan deflection of a single pinned end span.

For a k span guideway in which the number of modes is selected as an integer multiple of k*, the contribution of each higher set of modes to the deflection is approximately proportional to $1/(\frac{m}{k})^4$.

The contribution of each mode to the moment in a single span system is approximately $1/m^2$, thus the third mode contribution to the midspan moment is 1/9, 11% and the use of a finite number of modes to represent the guideway results in greater errors in the moment calculation than the deflection calculation.

For a k span guideway with m selected as an integer multiple of k the contribution of each mode to the moment is approximately $1/(\frac{m}{k})^2$.

For the design examples considered in this study k modes (m = k) have been used to represent the guideway. In this study guideway moments and the resulting stresses due to a vehicle passage have not provided stringent design constraints; however, for design cases in which moments and stresses provide stringent design constraints, the use of more modes to represent the guideway may be warranted so that higher accuracy in the moment and stress calculation is achieved.

*In a k span guideway the eigenvalues occur in clusters of k eigenvalues in each band with the first, k + 1, 2k + 1, etc. eigenvalues corresponding to the single span eigenvalues.

To indicate the accuracy resulting from the selection of k modes to represent the guideway, the data in Table 2.2 has been computed for a typical air cushion vehicle-guideway system using the full simulation program listed in Appendix C.

In the table, the maximum steady--state values of the system variables which occur as an 80,000 lb. air cushion vehicle with air cushions covering 75% of the vehicle length crosses 100 ft. single and three span guideways have been tabulated for crossing frequency ratios of 1.0 and 2.0.

For the maximum values of span deflections, suspension deflections and vehicle accelerations, the difference in using m = k modes and either m = 2k or m = 3k modes is less than 2%. For the moments the maximum difference is greater, and for the single span system at V_c = 1.0 a 6% difference exists between using a one - and a three-mode approximation.

For all of the data the level of accuracy obtained using m = k modes compared with m = 3k modes is sufficient for the design examples considered in this study and is adopted.

TABLE 2.2

INFLUENCE OF THE NUMBER OF MODES ON MAXIMUM VALUES OF SYSTEM VARIABLES

Crossing Frequency: V_c	1.0						2.0					
Number of Spans: k	1			3			1			3		
Number of Modes: n	1	2	3	3	6	9	1	2	3	3	6	9
Midspan Deflection: Y_m	.89	.89	.88	.54	.54	.53	1.10	1.10	1.10	1.54	1.54	1.54
Midspan Moment: $\bar{M}_{cm}$	.89	.89	.83	.57	.58	.56	1.10	1.10	1.11	1.61	1.60	1.57
Front Suspension Deflection: Y_{of}	.76	.76	.76	.50	.50	.50	.44	.45	.45	.64	.63	.63
Rear Suspension Deflection: Y_{or}	.76	.76	.76	.46	.46	.46	1.03	1.04	1.05	1.36	1.37	1.37
Front Acceleration: $\ddot{y}_{2f}$ (g's)	.10	.10	.10	.072	.074	.073	.17	.17	.17	.19	.20	.20
Rear Acceleration: $\ddot{y}_{2r}$ (g's)	.13	.13	.13	.087	.087	.087	.20	.20	.20	.27	.27	.27

System Parameters:

$$M = 0.15,\ U = 2.2,\ L_a = 0.5,\ L_p = 0.3,\ K = 10,\ M_u = 0.0,\ \bar{I}_v = 1.0,\ \xi_v = 0.25,\ \xi_m = 0.0$$

3. GUIDEWAYS EXCITED BY CONSTANT FORCE VEHICLES

3.1 The Constant Force Vehicle Model

The study of a guideway excited by a constant force vehicle model, which is a limiting case of the complete vehicle-guideway interaction model, illustrates a number of fundamental vehicle-guideway dynamic characteristics. This case is considered in the following paragraphs.

The influence of the two-dimensional vehicle upon a guideway span is represented by the front F_{sf} and rear F_{sr} suspension forces defined in (A.66) and (A.67). These forces may be expressed in terms of the front $\ddot{y}_{2f}$ and rear $\ddot{y}_{2r}$ sprung mass accelerations and front $\ddot{y}_{1f}$ and rear $\ddot{y}_{1r}$ unsprung mass accelerations as:

$$F_{sf} = \frac{-m_v g}{2}\left[1 + \frac{m_u}{m_v} + \frac{m_u}{m_v}\frac{\ddot{y}_{1f}}{g} + \frac{(\ddot{y}_{2f} + \ddot{y}_{2r})}{2g} + \frac{2I_v}{m_v \ell_a^2}\frac{(\ddot{y}_{2f} - \ddot{y}_{2r})}{g}\right] \quad (3.1)$$

$$F_{sr} = \frac{-m_v g}{2}\left[1 + \frac{m_u}{m_v} + \frac{m_u}{m_v}\frac{\ddot{y}_{1r}}{g} + \frac{(\ddot{y}_{2f} + \ddot{y}_{2r})}{2g} + \frac{2I_v}{m_v \ell_a^2}\frac{(\ddot{y}_{2f} - \ddot{y}_{2r})}{g}\right] \quad (3.2)$$

A primary goal in advanced vehicle design is to achieve passenger compartment accelerations in the range of 0.05g or less. For vehicles which meet this goal, $\ddot{y}_{2f/g} \approx \ddot{y}_{2r/g} < 0.05$ and for which the unsprung mass inertia forces are small, i.e.

$$\frac{m_u}{m_u}\frac{\ddot{y}_{1f}}{g} \approx \frac{m_u}{m_u}\frac{\ddot{y}_{1r}}{g} < 0.05,$$

the front and rear suspension forces on the guideway deviate from constant values equal to half the vehicle total weight by less than 10% and may be approximated as:

$$F_{sf} = -\frac{1}{2} m_v g \left[1 + \frac{m_u}{m_v}\right] \tag{3.3}$$

$$F_{sr} = -\frac{1}{2} m_v g \left[1 + \frac{m_u}{m_v}\right] \tag{3.4}$$

When (3.3) and (3.4) provide a good approximation to the vehicle suspension forces, the guideway deflections, moments and stresses may be computed independent of vehicle dynamics, and parametric plots, may be used to determine maximum guideway loads, deflections and stresses for many cases of interest; also, once the deflections are computed they may be used directly to determine the vehicle dyamic response accurately for the partially coupled model. The use of a constant force model which partially decouples the vehicle-guideway equations leads to considerable simplification in the vehicle-guideway design task.

The approximations leading to the constant force model of (3.3) and (3.4) involve both sprung mass and unsprung mass inertia forces. As noted in (3.1) and (3.2) if the sprung mass acceleration forces are directly limited to 0.05g by passenger comfort requirements, only if the unsprung mass inertia forces become a significant fraction of the vehicle total weight will the suspension forces very significantly from the constant values of (3.3) and (3.4).

For a number of low speed PRT and higher speed urban and intercity systems, air cushion and electromagnetic suspension vehicles have been proposed with very low $m_u/m_v < 0.1$ or no unsprung mass. For these low unsprung mass systems, if high ride quality is achieved, the sprung and unsprung mass inertia forces in (3.1) and (3.2) are small and the constant force approximations of (3.3) and (3.4) are valid for preliminary design over the complete range of operating conditions considered in this report.

For some types of PRT system wheeled vehicles, unsprung mass ratios exceeding 0.15 have been proposed while the tracked levitated research vehicle [6] and electromagnetic suspension vehicles* [30--31] have been proposed with unsprung mass ratios in the 0.33--0.66 range. The range of operating conditions for which the constant force approximations are valid for these large unsprung mass systems is discussed in Section 3.4 where direct comparisons of the fully coupled and the partially coupled models are presented. The work presented in Section 3.5 and Appendix G shows that for vehicles with unsprung mass ratios less than 0.66, if the crossing velocity V_c is less than 1.5, the suspension force variation is less than 15% if $v/\ell_s < f_v$ and the sprung mass acceleration is limited to less than 0.07g. Thus, a considerable operating range of interest exists for

*The unsprung mass depends to some extent upon the type of propulsion, its coupling to the vehicle and presence of a chasis housing the suspension and propulsion elements.

vehicles with large unsprung mass ratios and high levels of passenger comfort for which the constant suspension force model is sufficiently accurate for preliminary design. Additional parametric data is presented to show the levels of force variation which occur for $v/\ell_s > f_v$ as a function unsprung mass ratio, suspension unsprung to sprung mass frequency ratio and crossing velocity ratio. For cases $v/\ell_s > 5\ f_v$, $M_u = 1.0$, it is shown that the force variation may exceed 50% and the partially coupled model agrees poorly with a fully coupled model. These operating ranges in which significant force variation occurs are identified where a fully coupled model is required to determine vehicle guideway interactions.

3.2 Determination of Span Deflections and Moments

In the constant force vehicle model the guideway motion is uncoupled from the vehicle dynamics and depends only upon the vehicle weight, speed and pad configuration. The nondimensional equations describing a multispan guideway excited by a constant force vehicle model may be derived directly from Appendix A in terms of the nondimensional span dynamic deflection Y as:

$$Y(x,\tau) = \sum_{m=1}^{\infty} \alpha_m(\tau)\, \bar{\phi}_m(x) \tag{3.5}$$

where for each mode α_m is determined from:

$$\frac{d^2\alpha_m}{d\tau^2} + 2\xi_m \bar{\omega}_m \frac{d\alpha_m}{dt} + \bar{\omega}^2_m\, \alpha_m = -\frac{1}{4}\left[\psi_m(X_{vf},L_p) + \psi_m(X_{vr},L_p)\right] \tag{3.6}$$

where it is noted $\bar{F}_{sf} = \bar{F}_{sr} = -\frac{1}{2}$ has been used in the derivation

of (3.6) and where the mode shape functions $\bar{\phi}_m$ and forcing functions ψ_m are derived in Appendix A.

Using the solution of (3.6) the nondimensional guideway deflection $Y(x,\tau)$ due to the passage of a constant force vehicle may be determined directly from (3.5). In addition, the nondimensional bending moment $\bar{M}_t$, which for a given span configuration is directly proportional to the nondimensional stress, may be computed directly from (A.79).

The maximum guideway deflections, moments and stresses due to a constant force vehicle passage have been determined to illustrate guideway dynamic performance characteristics. The values of the maximum midspan deflection and moment which occur on any span in a k span system are presented, i.e., Y_m and $\bar{M}_{tm}$ have been determined as:

Y_m = Maximum of $[Y(1/2, \tau)|_{i=1}, \ldots\ldots\ldots\ldots Y(1/2,\tau)|_{i=k}]$

$\bar{M}_{tm}$ = Maximum of $[\bar{M}_t\ (1/2, \tau)|_{i=1}, \ldots\ldots\ldots\ldots \bar{M}_t(1/2,\tau)|_{i=k}]$

where all spans in a k span system are searched for the maximum values for a given vehicle passage and where:

$Y(1/2,\tau)|_i$ = nondimensional midspan deflection of the i^{th} span in a k span system.

$\bar{M}_t\ (1/2,\tau)|_i$ = nondimensional midspan moment of the i^{th} span in a k span system.

The nondimensional maximum midspan deflection Y_m and moment $\bar{M}_{tm}$ are functions of the following parameters:

1. Span Configuration*: k multiple spans
2. Span Damping: ξ_m
3. Vehicle Configuration
   (a) Pad Separation distance: $L_a = \ell_a/\ell_s$
   (b) Pad Length: $L_p = \ell_p/\ell_s$
4. Vehicle Guideway Nondimensional Crossing Velocity: V_c

Data illustrating the influence of these parameters on Y_m and $\bar{M}_{tm}$ is presented in Figures 3.1 to 3.11. The data for the k multispan guideways (k,finite) has been obtained with the computer program listed in Appendix D using k normal modes for each configuration. The data presented for the continous span ($k=\infty$) systems has been obtained from [28 and 29].

Data in Figure 3.1 shows the nondimensional maximum midspan deflection which occurs in single (k=1), multiple (k=3) and continuous ($k=\infty$) spans due to the passage of a single concentrated force. For all three span systems for $V_c<0.5$, the maximum deflections are almost independent of V_c and equal to the deflections calculated from static beam theory. In this operating range, $Y_m \approx 1.0$ for single spans while for three span and continuous spans it is reduced to

*For all the data, the k spans in a given configuration are assumed to be of equal length and identical in cross section properties.

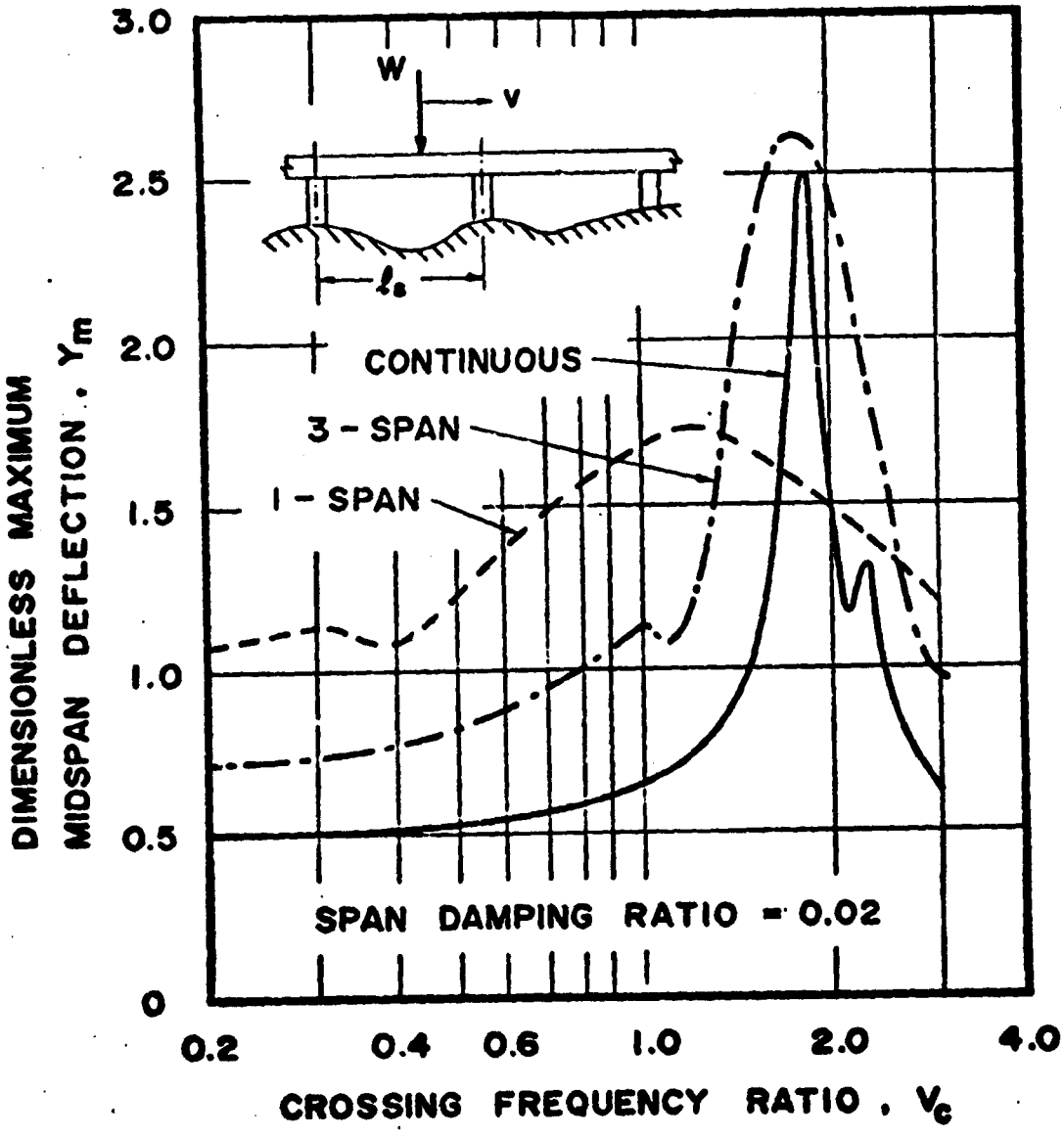

Fig. 3-1. Span Response to a Single Traveling Force

0.7 and 0.53, respectively due to the transfer of moments across support points in the multi and continuous span systems. For guideway designs which are deflection limited, and operate in this quasi-static region, the use of multiple spans would allow either a reduction in span cross section required or an increase in span length (therefore fewer supports)compared to use of single spans.

In the range $0.5 < V_c < 1.0$, Figure 3.1 shows that Y_m increases with V_c for the single and 3-span system while the deflection of the continuous system remains essentially at its static value. Thus, the continuous system has both a reduction in static deflection and an increased operating range over which its behavior is quasi-static compared with single and multi-span systems. For a 100 ft. length, 3 hertz natural frequency span, the response of single and multiple span systems is quasi-static for vehicle speeds up to 100 mph while for continuous spans it is quasi-static up to 200 mph.

For $V_c > 1.0$ dynamic effects become important for all span systems with the single span reaching a maximum deflection of 1.76 at $V_c = 1.33$ and the three- and continuous-span systems reaching maxima of 2.6 and 2.4, respectively, near $V_c = 2$. The ratio of the peak deflection to the static value at $V_c = 0$ increases as the number of spans increases, from 3.7 for a three-span to 4.6 for a continuous guideway. This increased dynamic amplification, as the number of spans increases, occurs because in multiple span systems the excitation on one span can propagate

to and excite adjacent spans. In single spans the vehicle force only excites the span on which it is located; each span is at rest before the force arrives and its deflection is limited by the transient passage of the force. As the number of spans increases, the peak deflection occurs at values closer to $V_c = 2$ which corresponds to the resonant excitation of the system at its first-mode natural frequency (span crossing time coincides with a half cycle of free vibration).

Data in Figures 3.2 and 3.3 illustrate the influence of span damping on values of Y_m and $\bar{M}_{tm}$ for single concentrated force vehicles crossing 1,3 and 5 span systems. For values of $V_c < 1.0$ increasing the span damping from 0 to 0.1 has very little influence on either deflections or moments, however, near $V_c = 2.0$, span damping significantly influences the dynamic response. At a resonant condition, span damping of 0.1 reduces the deflection and moment of a single span by 12%, of a three span system by 35% and of a five span system by 43% in comparison to systems with zero damping.

The data in Figures 3.4 to 3.7 illustrates that for all crossing frequency values, Y_m and $\bar{M}_{tm}$ are decreased as the pad length increases. For $V_c < 0.4$ in the single span case, Y_m and $\bar{M}_{tm}$ are reduced to 80% for $L_p = 0.5$ and to 60% for $L_p = 1.0$ of the zero pad length values, while for the three span case Y_m and $\bar{M}_{tm}$ are reduced to 85% for $L_p = 0.5$ and to 57% for $L_p = 1.0$ of the zero pad length values.

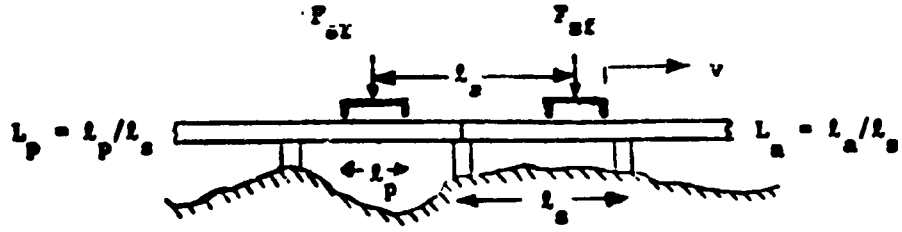

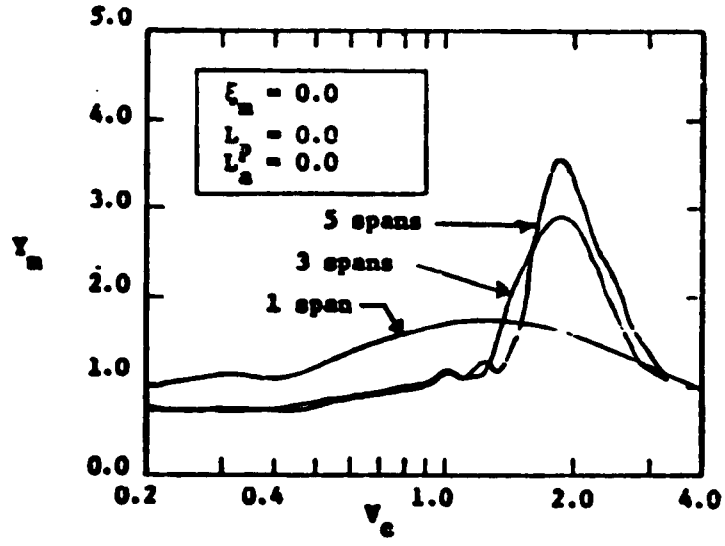

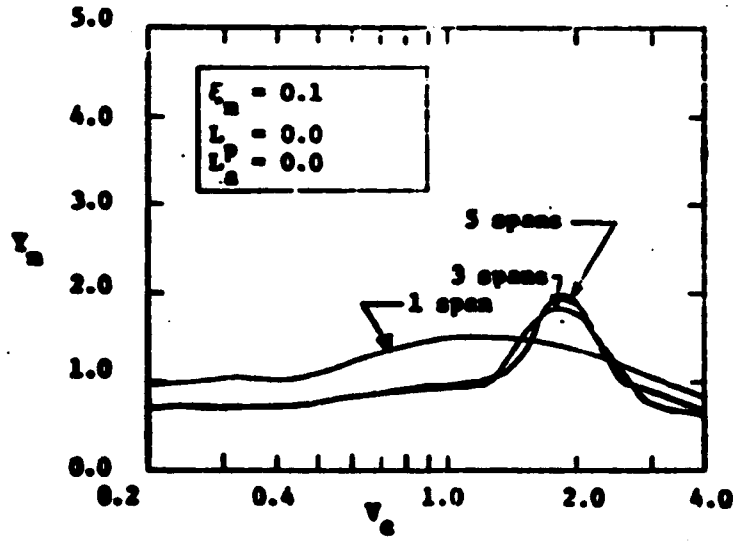

Fig. 3-2. Nondimensional Maximum Midspan Deflection Y_m Versus Crossing Frequency Ratio V_c

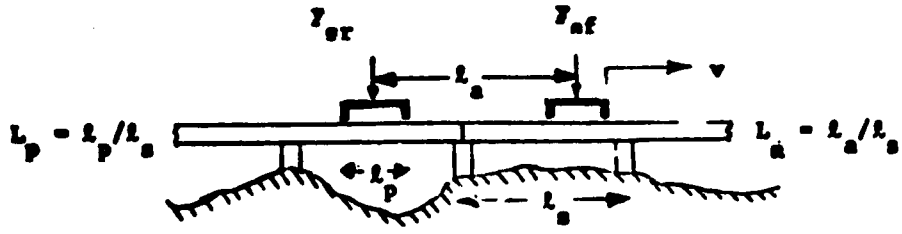

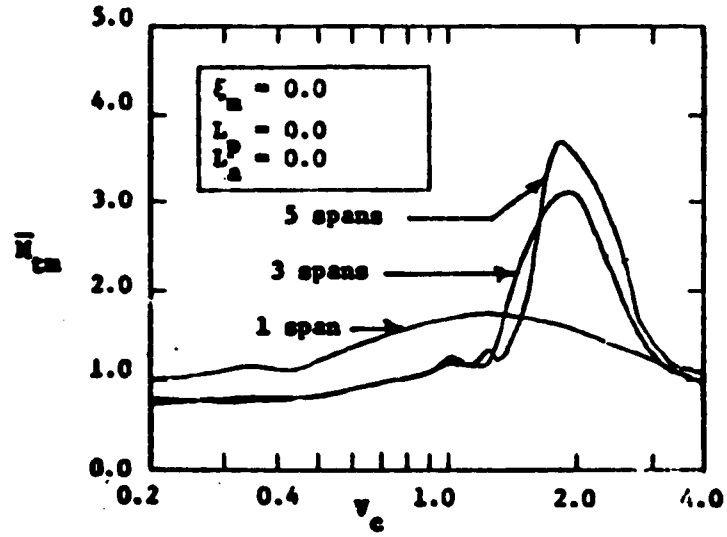

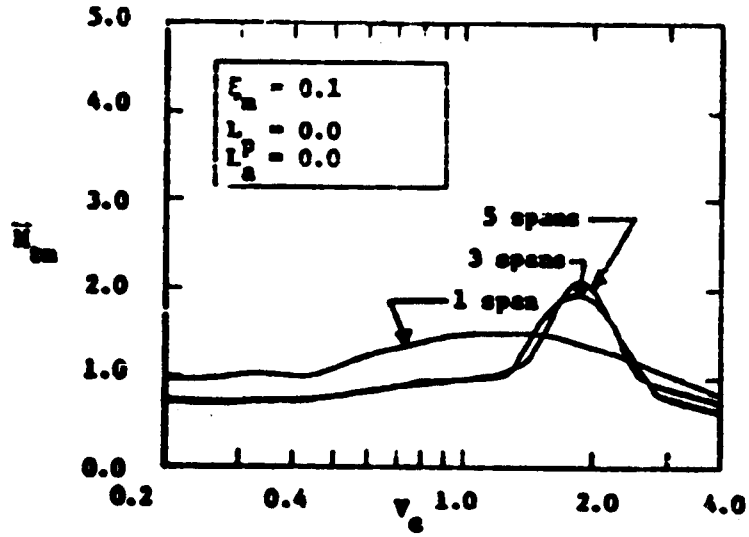

Fig. 3-3. Nondimensional Maximum Moment $\bar{M}_{cm}$ Versus Crossing Frequency Ratio V_c

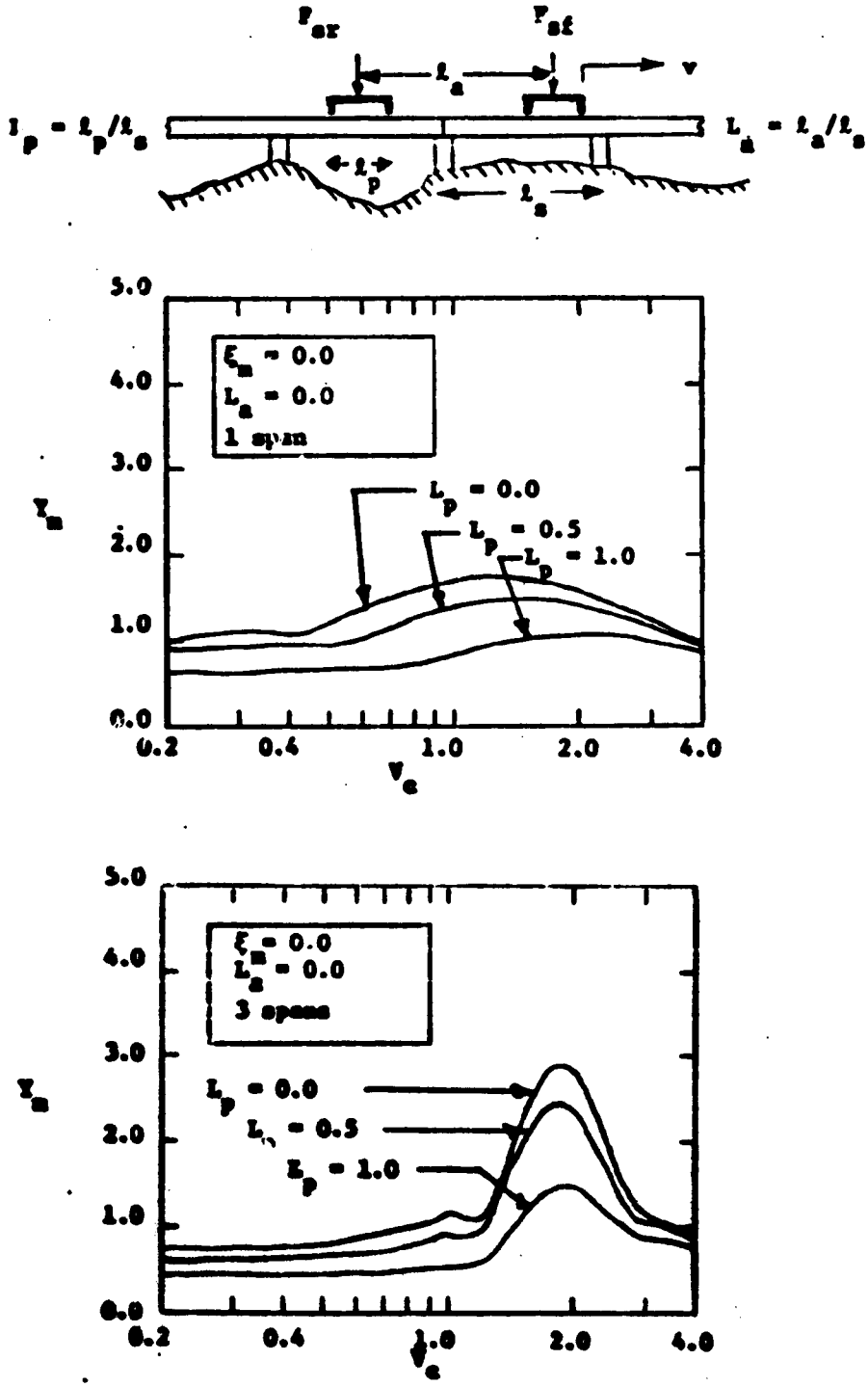

Fig. 3-4. Nondimensional Maximum Midspan Deflection Y_m Versus Crossing Frequency Ratio V_c

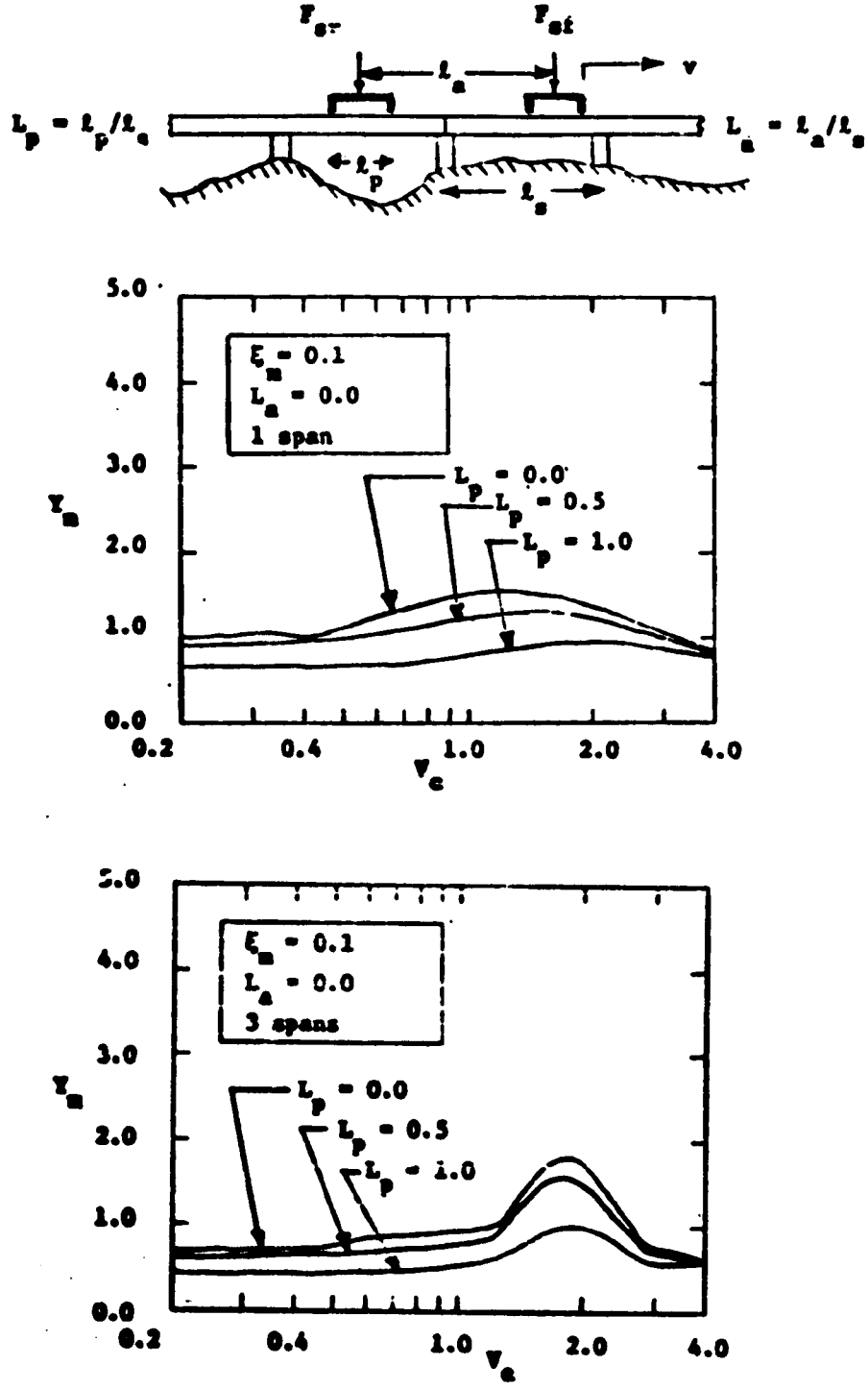

Fig. 3-5. Nondimensional Maximum Midspan Deflection Y_m Versus Crossing Frequency Ratio V_c

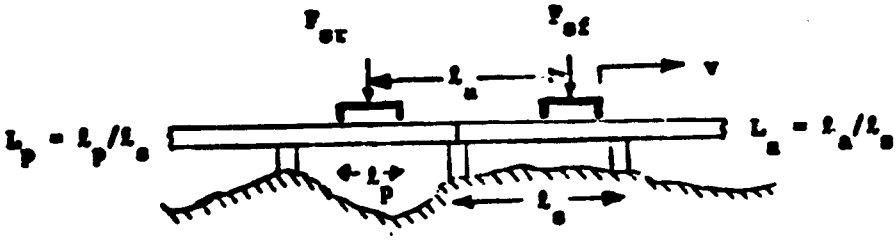

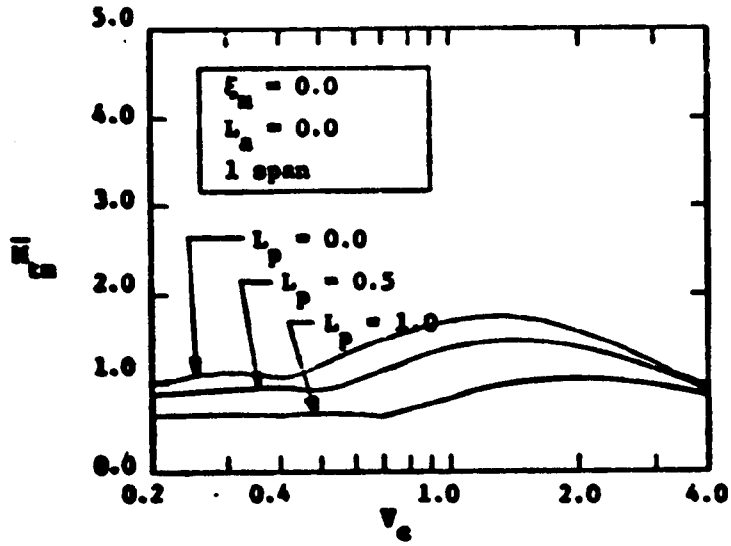

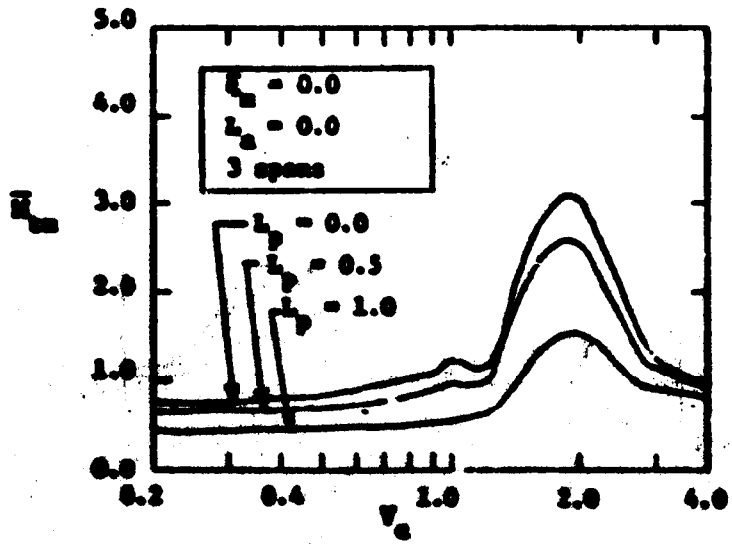

Fig. 3-4. Nondimensional Maximum Midspan Moment $\bar{M}_{tm}$ Versus Crossing Frequency Ratio V_c

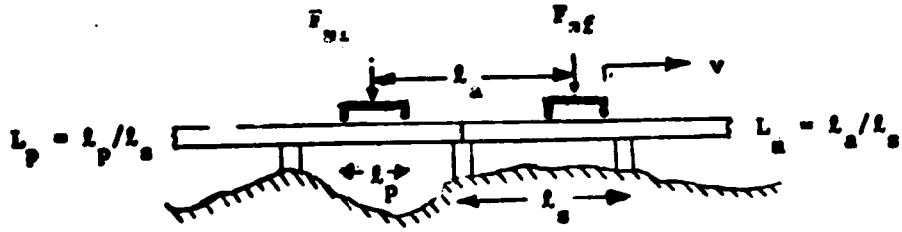

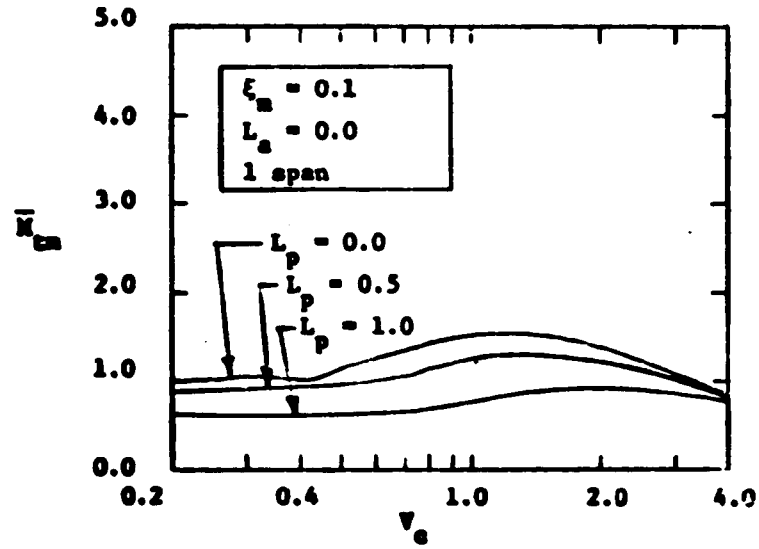

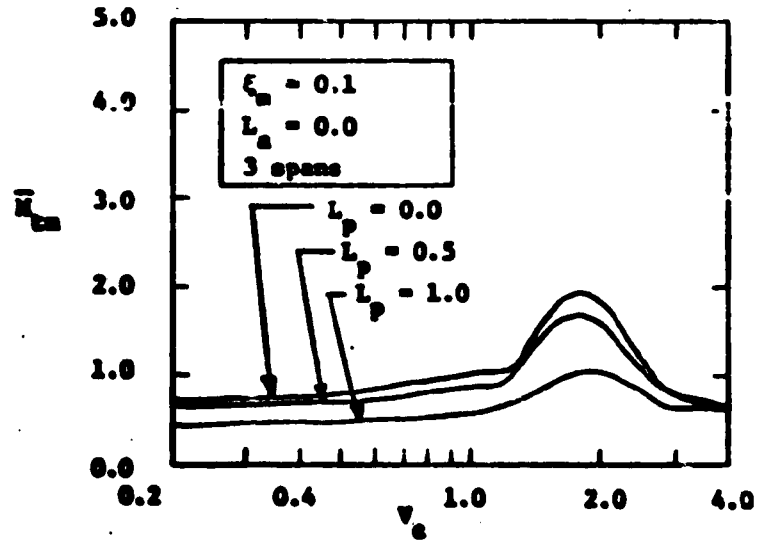

Fig. 3-7. Nondimensional Maximum Midspan Moment $\bar{M}_{cm}$ Versus Crossing Frequency Ratio V_c

At higher crossing frequency ratios as the pad length is increased the values of Y_m and $\bar{M}_{tm}$ are also decreased. At the three span resonant condition, Y_m and $\bar{M}_{tm}$ are decreased by 14% for $L_p = 0.5$ and by 50% for $L_p = 1.0$ for zero span damping and by 11% for $L_p = 0.5$ and by 44% for $L_p = 1.0$ for 0.1 span damping compared to the zero pad length case.

The pad length has an additional influence upon the values of Y_m and $\bar{M}_{tm}$; as the pad length is increased, the crossing frequency ratio V_c at which span dynamic effects become important is increased. The values of Y_m and $\bar{M}tm$ are almost independent of V_c and equal to the static case values for $V_c < 0.4$ at $L_p = 0.$ and for $V_c < 0.7$ at $L_p = 1.0$ for the single span case and in the three span case for $V_c < 0.5$ at $L_p = 0$, and for $V_c < 1.0$ at $L_p = 1.0$. Thus, for a given span system a vehicle with a distributed suspension force on the guideway not only produces smaller moments (stresses) and deflections, but may also be run at higher speeds before span dynamic effects become significant in comparison to a vehicle with a more concentrated suspension force.

Figures 3.8 to 3.11 illustrate the influence of vehicle length upon span deflection and moment for the cases of $L_a = 0.8$ and $L_a = 1.6$ with pad lengths of 0 and 50%. At low crossing frequency ratios, $V_c < 0.4$, the data for the single and three span systems indicate that Y_m and $\bar{M}_{tm}$ are reduced by 50% for both $L_a = 0.8$ and $L_a = 1.6$ in comparison to the zero length vehicle.

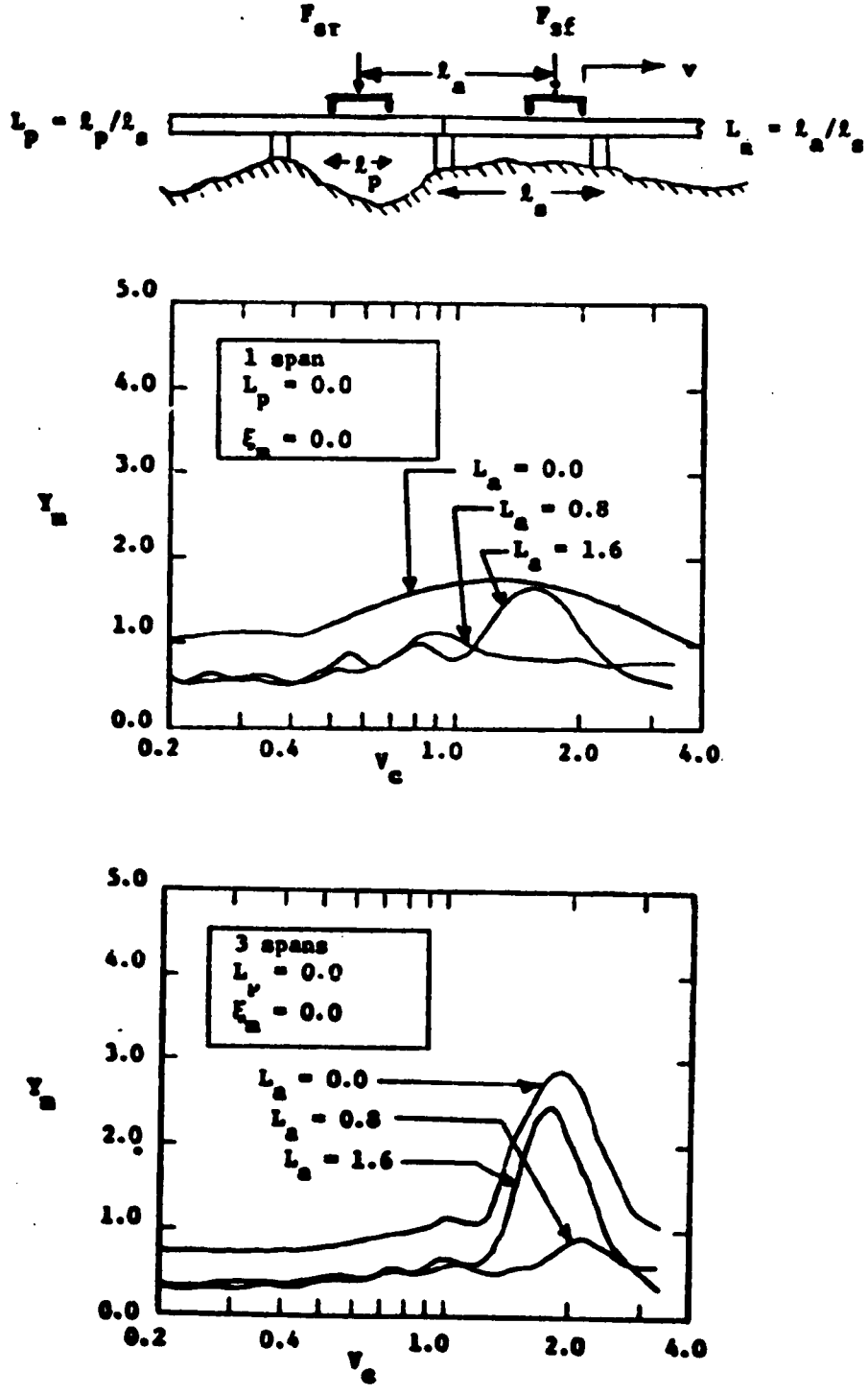

Fig. 3-8. Nondimensional Maximum Midspan Deflection Y_m Versus Crossing Frequency Ratio V_c

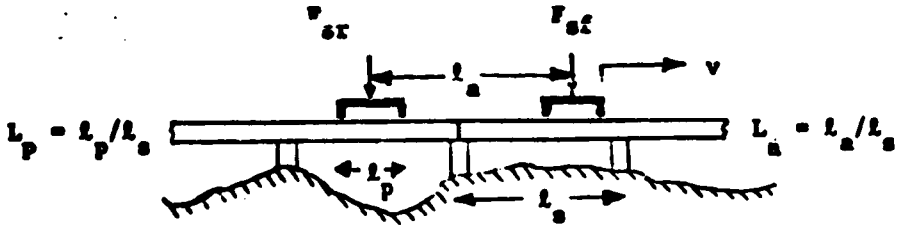

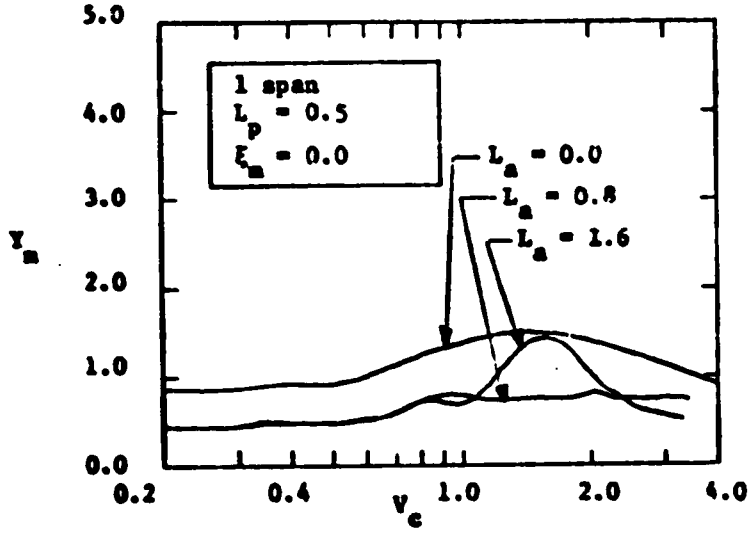

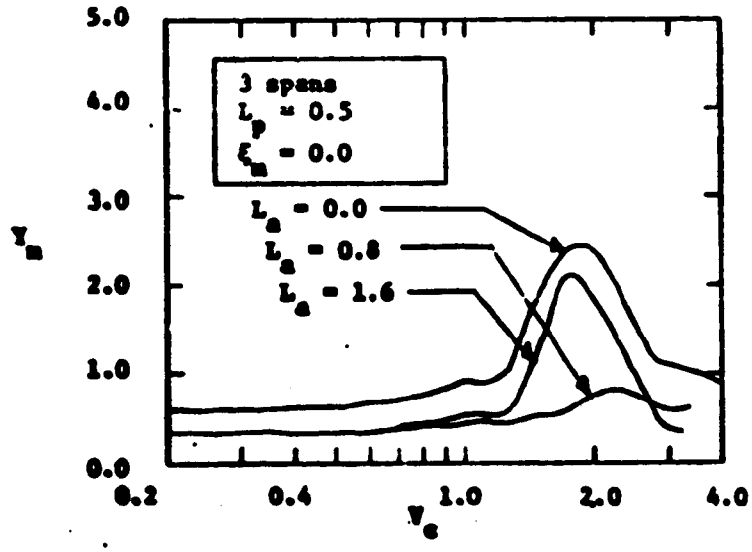

Fig. 3-9. Nondimensional Maximum Midspan Deflection Y_m Versus Crossing Frequency Ratio V_c

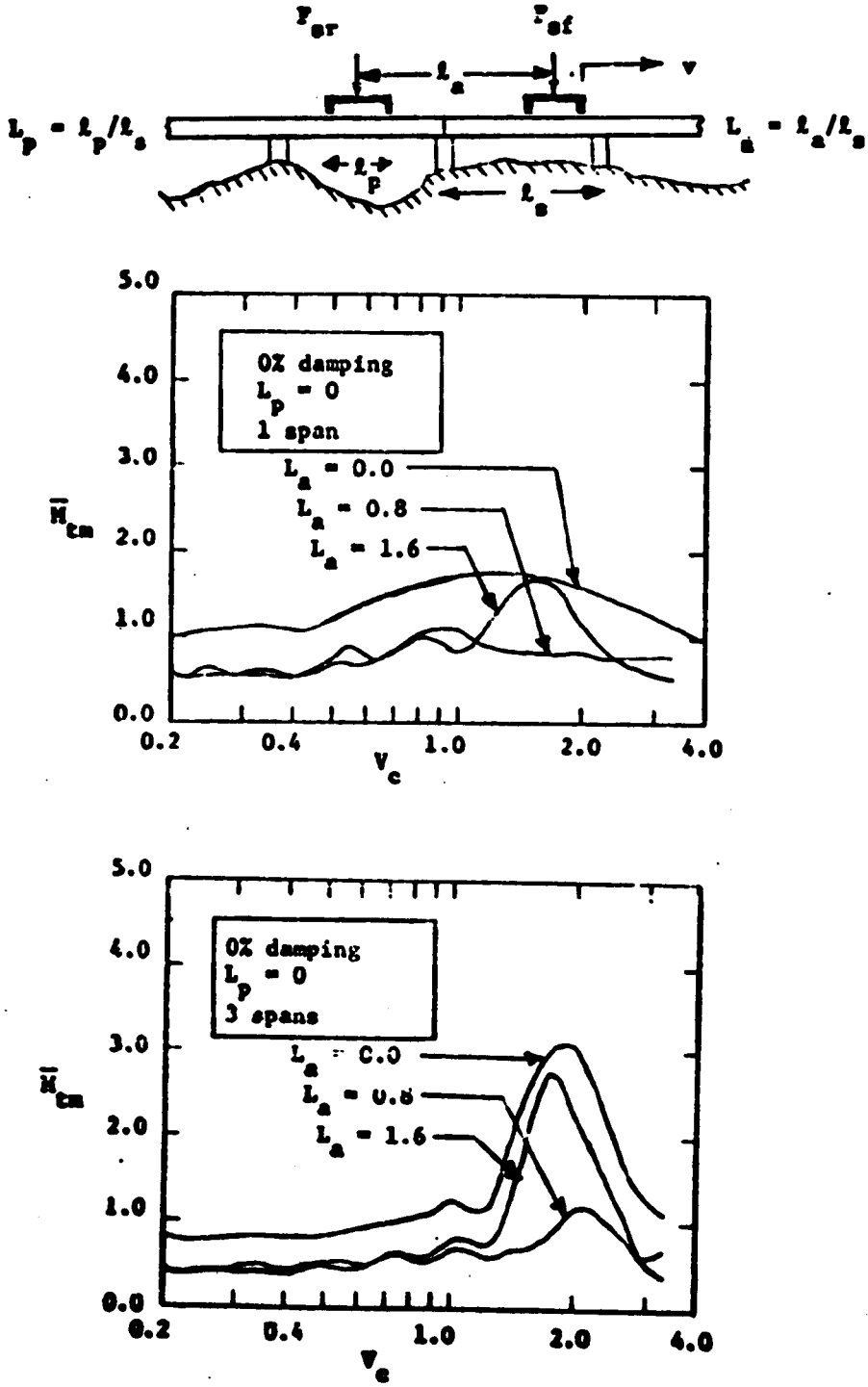

Fig. 3-10. Nondimensional Maximum Midspan Moment $\bar{M}_{cm}$ Versus Crossing Frequency Ratio V_c

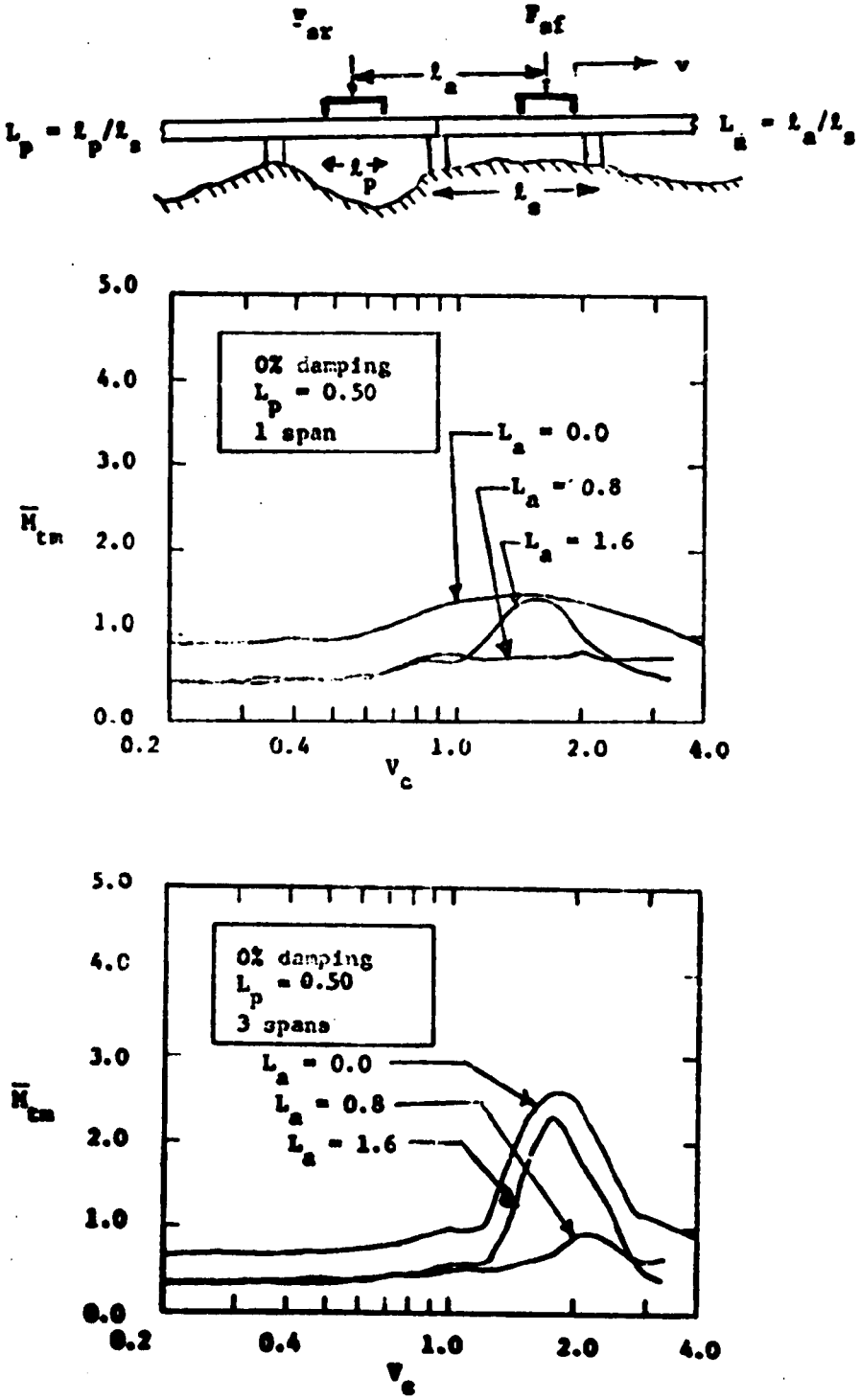

Fig. 3-11. Nondimensional Maximum Midspan Moment $\bar{M}_{tm}$ Versus Crossing Frequency Ratio V_c

If $L_a > 0.5$ only half the vehicle weight is at the midspan while the other half is off the span, thus the deflection is reduced by 50% in comparison to a zero length vehicle.

When a vehicle with two suspensions is considered, the repetitive forcing of the span by first the front suspension and then the rear suspension leads to a number of crossing frequency ratios V_c at which local relative maximums in Y_m and $\bar{M}_{tm}$ may occur as illustrated in the zero pad length data. For vehicles with pad length ratios of 50% these local maximums are essentially eliminated and for $V_c < 0.8$ the values of Y_m and $\bar{M}_{tm}$ for $L_a = 0.8$ and 1.6 are equal and are 50% of the corresponding values for $L_a = 0.0$.

At values of $1 > V_c$ a span resonant condition may occur which is significantly influenced by vehicle length. For both the single and three span systems, the longer vehicle, $L_a = 1.6$, has a significant increase in Y_m and $\bar{M}_{tm}$, i.e. $Y_m = 2.4$ and $\bar{M}_{tm} = 2.8$ at $V_c = 1.9$ while the vehicle $L_a = 0.8$ and $L_p = 0.0$ has very little increase in Y_m and $\bar{M}_{tm}$, i.e. maximum values of $Y_m = 0.8$ and $\bar{M}_{tm} = 1.2$ at $V_c = 2.2$. This marked difference in behavior between the low crossing frequency ratio cases, $V_c < 1.0$, in which data for the two vehicle lengths are similar and the high crossing frequency ratio cases $V_c > 1.0$ in which the data is significantly different occurs because the phasing between the front and rear suspensions is not as significant a factor for $V_c < 1.0$ as it is at a nearly

resonant condition where $V_c \simeq 2.0$. For the vehicle $L_a = 0.8$ at $V \simeq 2.0$, the rear suspension approaches the midspan at a time when the span is moving upward with a positive velocity and tends to decrease the deflection. For the vehicle, $L_a = 1.6$ at $V_c \simeq 2.0$, the rear suspension approaches the midspan at a time when the span has sustained almost a full cycle of oscillation and is nearly at its maximum upward deflection and thus reinforces the oscillation.

3.3 Vehicle Excitation

As the span is excited by the vehicle passage and undergoes a dynamic deflection, the vehicle is excited by the span dynamic deflection beneath the suspensions. For the two-dimensional vehicle model the influence of the span upon the vehicle may be represented by the nondimensional deflections under the front and rear suspension attachment points, i.e. $Y_{of}(x,\tau)$ and $Y_{or}(x,\tau)$. These deflections are periodic for a vehicle traveling at constant velocity. For a single span system the deflections are periodic for each span crossing, while for a k span semi-continuous system they are periodic every k span crossing.

At low crossing frequency values, $V_c < 0.4$, in which the span responds in a quasi-static manner, the suspension deflections may be calculated from the classical beam theory of (3.5) and (3.6) for deflection under a distributed load traveling across the beam*.

---

*Figure G.5 presents the time history of the suspension point in contact with the guideway for a constant traveling force. The influence of the small amplitude oscillation of the lightly damped span about its static equilibrium point is shown for low speed vehicles.

For two suspensions, superposition may be used to calculate the deflection due to both forces. In the quasi-static case, the front and rear suspension deflections reach maximum values which are equal to maximum midspan guideway deflection values given in Figures 3.1 to 3.11 for $V_c \simeq 0.2$ and are simply related.

As the crossing frequency increases span dynamic effects become important and the front and rear suspension deflections differ in magnitude. Data to illustrate these dynamic effects have been determined for the constant force vehicle model with $L_a = 0.8$ for crossing frequency ratios of $V_c = 1.0$ and 2.0. The data is presented in Figures 3.12 to 3.15 as plots of Y_{of} and Y_{or} versus nondimensional time, τ, with $\tau = 0$ corresponding to the front suspension midpoint at the position $X = 0$ for the first span of a k span system.

The data in Figure 3.12 shows the difference between the front and rear deflections for $V_c = 1.0$; Y_{of} which until the second suspension reaches the span results from the front suspension forcing an initially at rest span, decreases monotonically with increasing time from $\tau = 0.6$ until a maximum negative value of -0.8 is reached and then increases monotonically until $Y_{of} = 0$ at $\tau = 2\pi/V_c$. Y_{or}, which results from the rear suspension forcing a span which has already been excited by the front suspension, sustains both positive and negative deflections and reaches a maximum negative value of -0.7. For the suspension

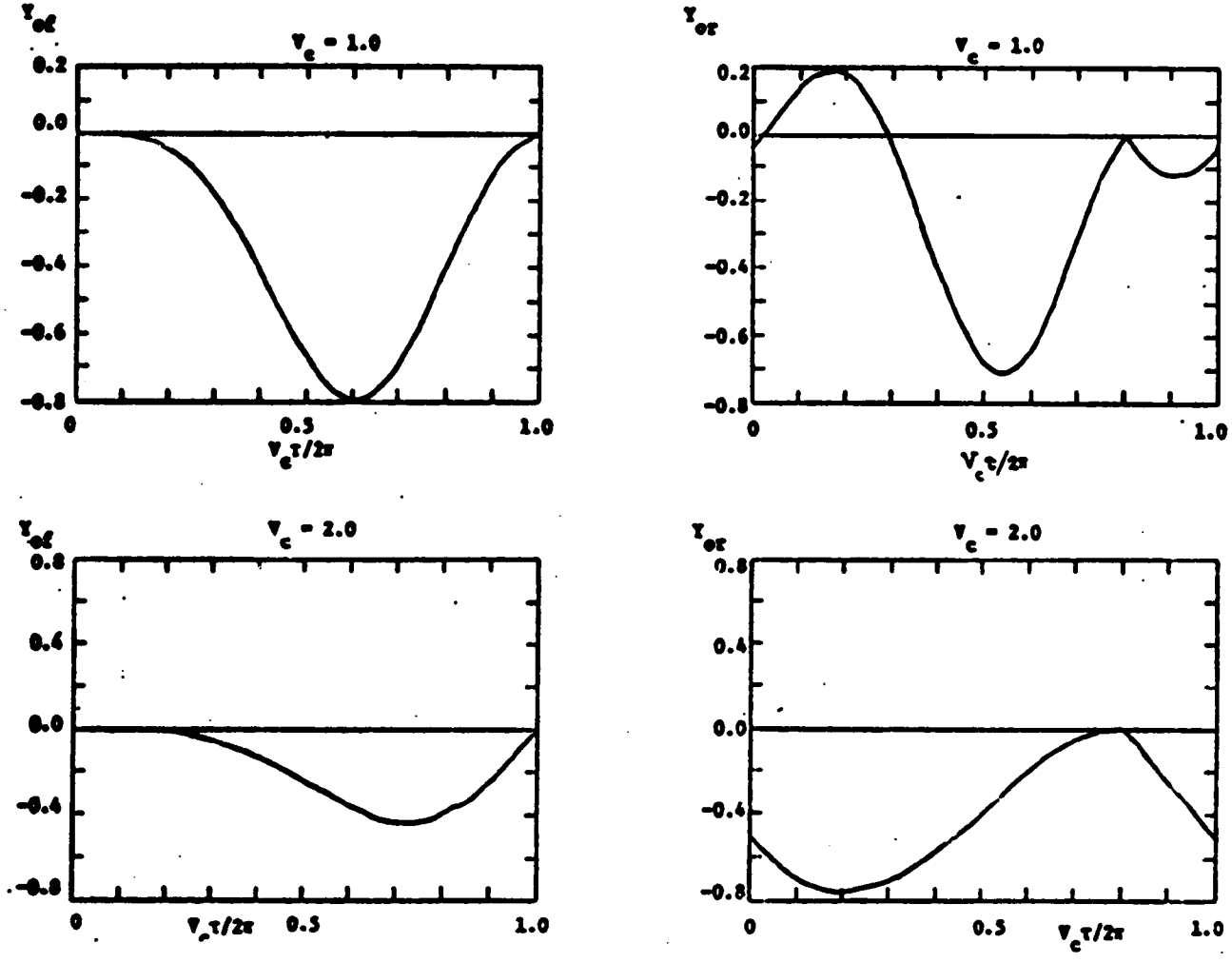

Fig. 3-12. Nondimensional Front and Rear Vehicle Suspension Deflections, Y_{of} and Y_{or}, Versus Nondimensional Time $V_c\tau/2\pi$, for L_a=0.8, L_p=0.0 and ξ_m=0.0 on a Single Span Guideway

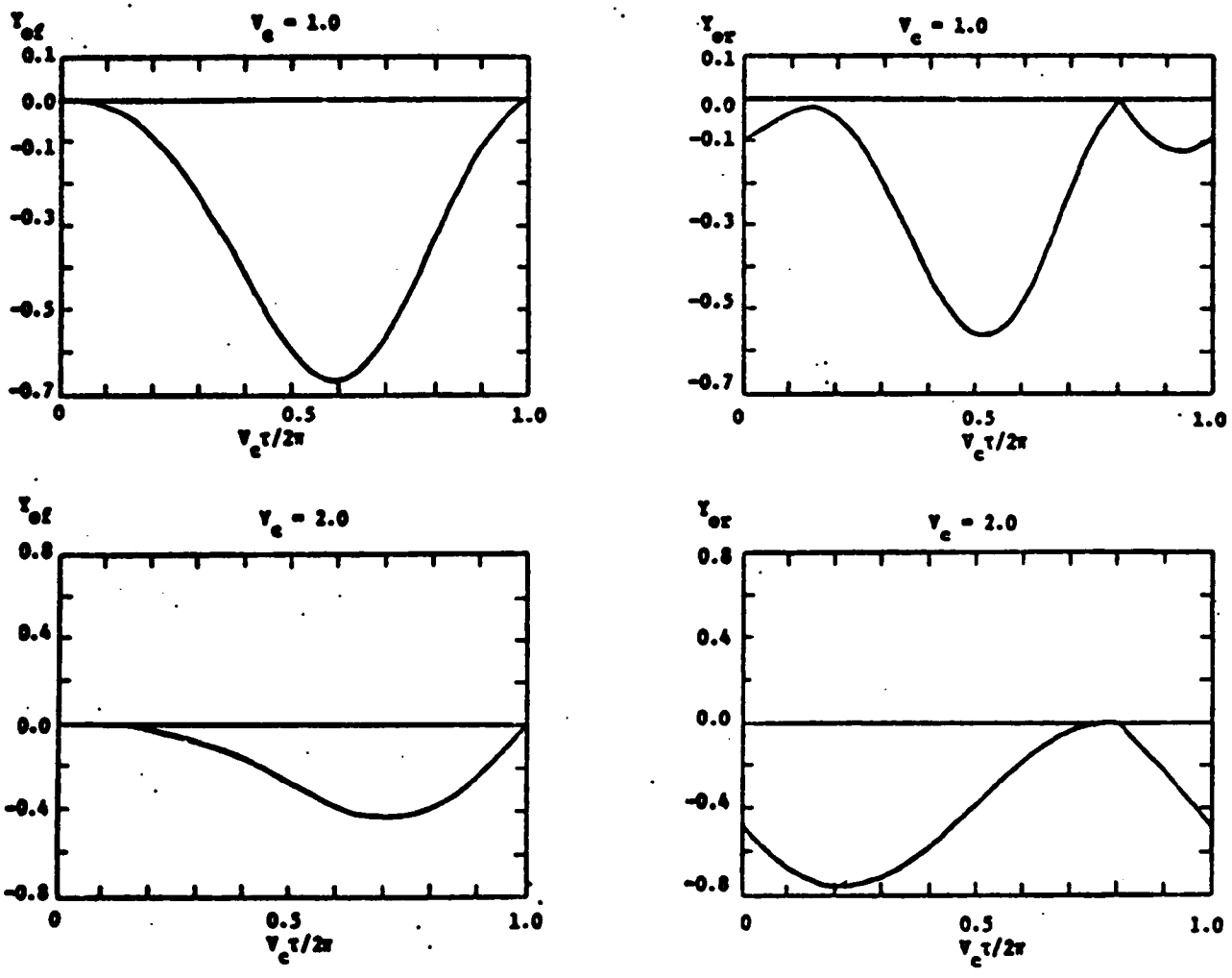

Fig. 3-13. Nondimensional Front and Rear Vehicle Suspension Deflections, Y_{of} and Y_{or}, Versus Nondimensional Time, $V_c\tau/2\pi$, for L_a=0.8, L_p=0.5 and ξ_m=0.0 on a Single Span Guideway

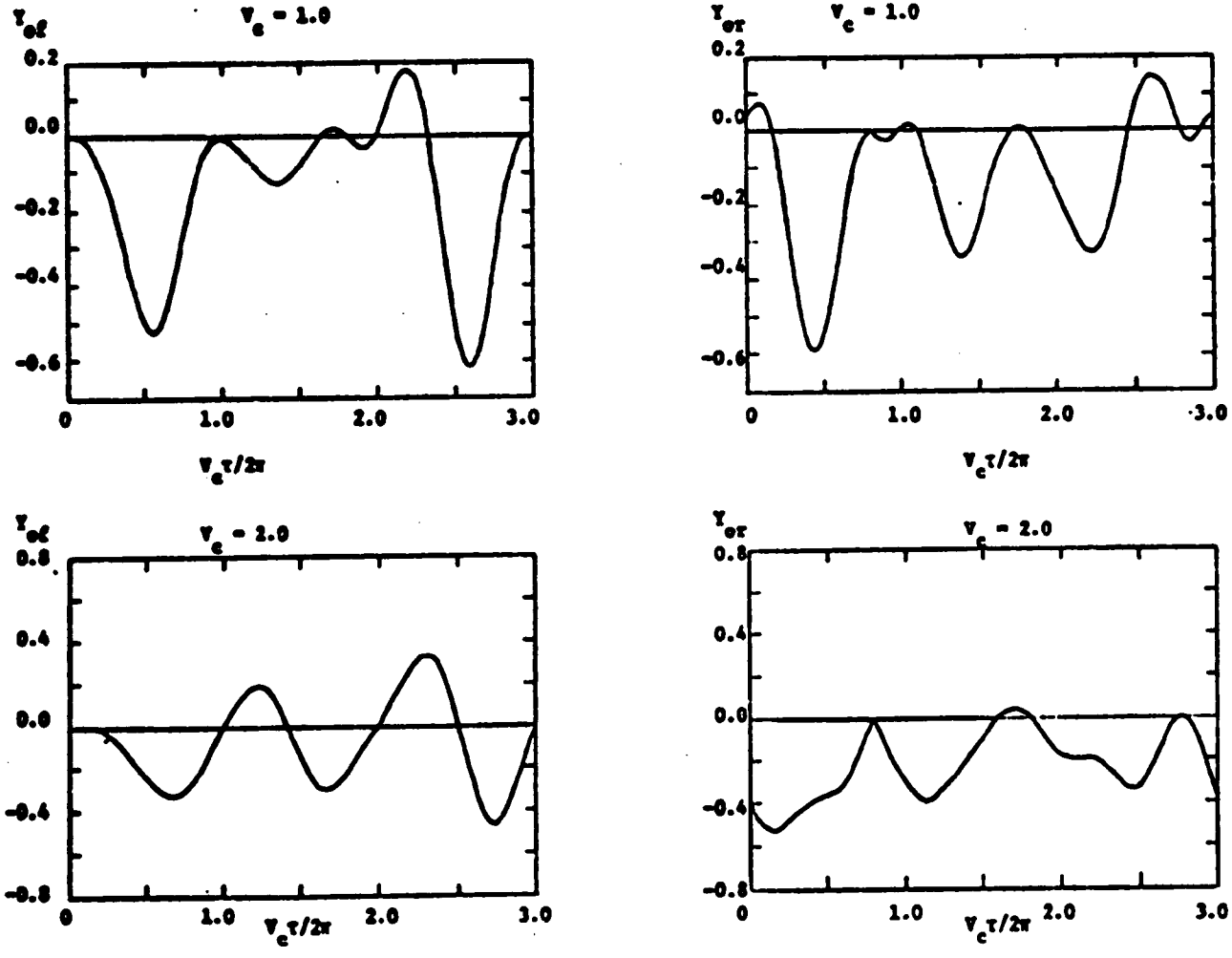

Fig. 3-14. Nondimensional Front and Rear Vehicle Suspension Deflections, Y_{of} and Y_{or}, Versus Nondimensional Time, $V_c\tau/2\pi$, for L_a=0.8, L_p=0.0, ξ_m=0.0 on a Three-Span Semi-Continuous Guideway

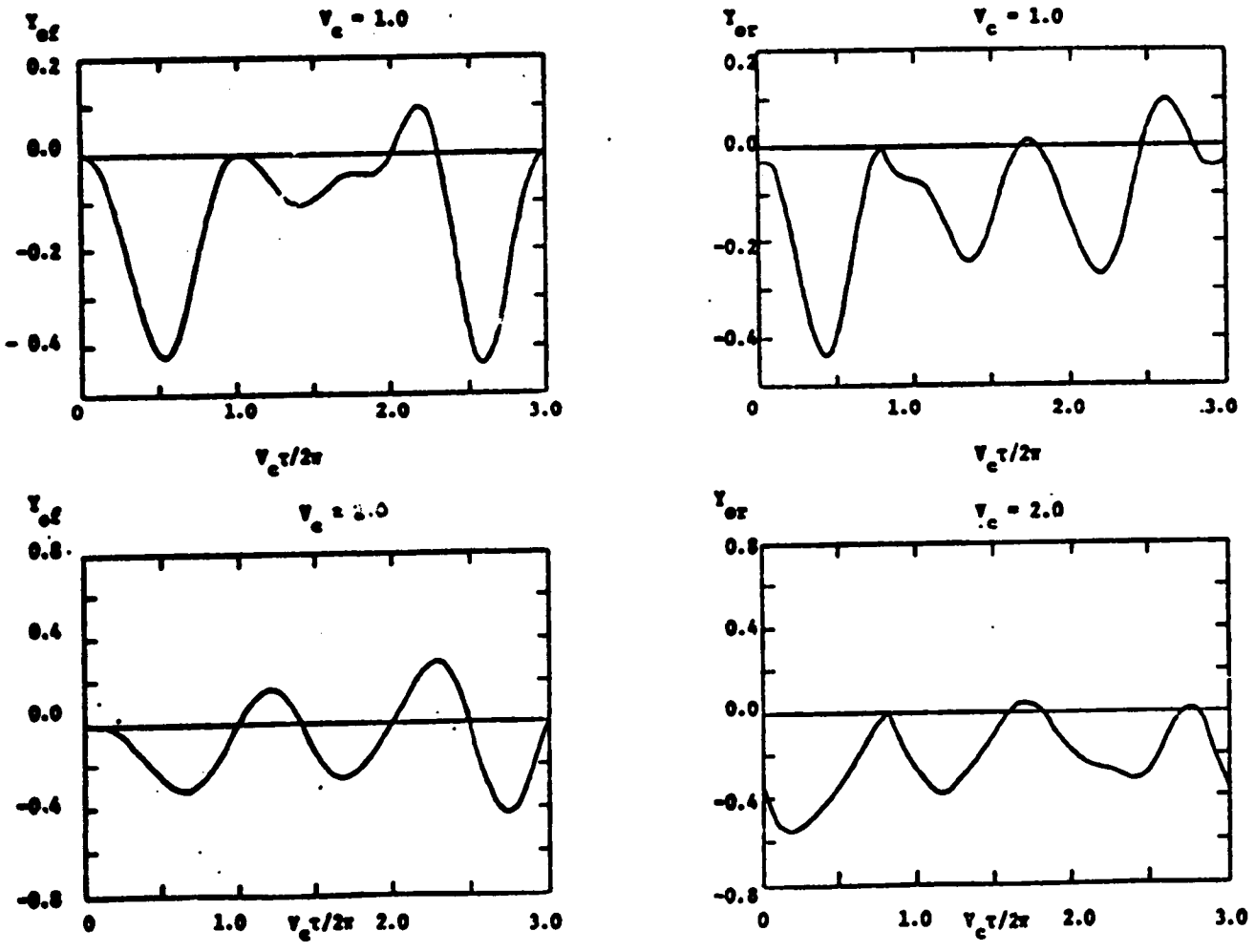

Fig. 3-15. Nondimensional Front and Rear Vehicle Suspension Deflections, Y_{of} and Y_{or}, Versus Nondimensional Time $V_c\tau/2\pi$, for L_a=0.8, L_p=0.5 and ξ_m=0.0 on a Three-Span Semi-Continuous Guideway

length L_a = 0.8 the rear suspension reaches a support at τ = 0.8 $(\frac{2\pi}{V_c})$ where Y_{or} = 0.0.

At a higher velocity, V_c = 2.0, the front suspension "outruns" the span and the maximum deflection is -0.4 while the rear suspension reaches a maximum deflection -0.78 crossing the span which has already been excited by the front suspension.

A comparison of Figure 3.12 for zero pad length with Figure 3.13 for 50% pad length indicates that at V_c = 1.0, the deflections are somewhat similar in waveform to the case L_p = 0 with the maximum deflections reduced for L_p = 0.5 by 15% for the front suspension and by 8% for the rear suspension compared to the case L_p = 0. For the higher speed case, V_c = 2.0, there is less than 5% difference between the suspension deflections for L_p = 0.0 and the corresponding deflections for L_p = 0.5.

The data in Figure 3.14 illustrates the front and rear suspension deflections which occur on a 3 span semi-continuous system for L_p = 0.0. The maximum deflections for the lower speed, V_c = 1.0, for the front suspension and for the rear suspension are respectively 22% and 17% less than the corresponding single span results of Figure 3.12. For the higher speed case, V_c = 2.0, the maximum deflections for the front and rear suspensions are respectively 20% more and 4% less than the corresponding single span data.

A comparison of the three span data in Figure 3.14 for L_p = 0.0 and 3.15 for L_p = 0.5 at V_c = 1.0 indicates that a 50% pad length reduces the maximum front and rear suspension deflections by 27% and 21% respectively compared to the zero pad length case.

At the higher speed, $V_c = 2.0$, the 0.5 pad length front and rear suspension maximum deflections are respectively only 6% and 4% less than the maximum suspension deflections of the zero pad length vehicle.

3.4 Computation of Vehicle Dynamics Using the Constant Force Vehicle Approximation

An efficient method of determining the steady-state time histories and rms accelerations and deflections of a vehicle may be formulated based upon the constant force vehicle approximation. This method of computation allows a factor or more reduction in computer time compared to a fully coupled numerical integration solution method. For vehicles in which the sprung and unsprung mass acceleration forces are small enough so that the front and rear suspension forces F_{sf} and F_{sr} of (3.1) and (3.2)may be represented as the constant forces in (3.3) and (3.4), vehicle dynamic motion may be computed accurately in the following manner when a linear vehicle model is considered:

(1) The guideway motion is determined from the constant force vehicle model and the nondimensional deflections under the vehicle front and rear suspensions are determined.

(2) The suspension nondimensional deflections, which are periodic functions, are represented in terms of a finite Fourier cosine and sine series.

(3) Using a vehicle description in terms of transfer functions and the Fourier representation of the suspension deflections, the vehicle nondimensional acceleration time histories and rms accelerations, as a function of frequency,are determined.

This description of the vehicle-guideway system allows full coupling between the guideway deflection and the vehicle dynamic motion, but assumes the vehicle forces on the guideway are due only to vehicle weight with the variation in dynamic suspension forces acting on the guideway neglected.

The vehicle front and rear suspension deflections may be determined directly as described in Section 3.2 using the program listed in Appendix D. These deflections are periodic over k spans for a k span system and may be represented in terms of a Fourier series as:

$$Y_{ofn} = a_{fo} + \sum_{i=1}^{n} [a_{fi} \cos \omega_i t + b_{fi} \sin \omega_i t] \qquad (3.7)$$

$$Y_{orn} = a_{ro} + \sum_{i=1}^{n} [a_{ri} \cos \omega_i t + b_{ri} \sin \omega_i t] \qquad (3.8)$$

where:

Y_{ofn} (Y_{orn}) = n^{th} order Fourier series representation of Y_{of} (Y_{or})

a_{fi}, a_{ri}, b_{fi}, b_{ri} = non dimensional Fourier series coefficients

$\omega_i = \frac{2\pi i v}{k\ell_s}$ = crossing frequency of k span system

The Fourier series coefficients may be defined in terms of $X = vt/\ell_s$ and $X_d = vt/\ell_s - \ell_a/\ell_s = vt/\ell_s - L_a$:

$$a_{fo} = \frac{1}{k} \int_0^k Y_{of}(X)\, dX \tag{3.9}$$

$$a_{ro} = \frac{1}{k} \int_{-L_a}^{k-L} Y_{or}(X_d)\, dX_d \tag{3.10}$$

and for i = 1 to n

$$a_{fi} = \frac{2}{k} \int_0^k Y_{of}(X) \cos\left[\frac{2\pi iX}{k}\right] dX \tag{3.11}$$

$$a_{ri} = \frac{2}{k} \int_{-L_a}^{k-L_a} Y_{or}(X_d) \cos\left[\frac{2\pi iX_d}{k}\right] dX_d \tag{3.12}$$

$$b_{fi} = \frac{2}{k} \int_0^k Y_{of}(X) \sin\left[\frac{2\pi iX}{k}\right] dX \tag{3.13}$$

$$b_{ri} = \frac{2}{k} \int_{-L_a}^{k-L_a} Y_{or}(X_d) \sin\left[\frac{2\pi iX_d}{k}\right] dX_d \tag{3.14}$$

The nondimensional Fourier coefficients for the front and rear suspension displacements have been determined by implementing (3.9) through (3.14) with direct numerical integration as a part of the digital computer program listed in Appendix D. The Fourier coefficients are determined so that the representations of Y_{ofn} and Y_{orn} reproduce the exact phase relation of the front and rear vehicle suspension deflections as they occur on the vehicle.

If periodic guideway camber or misalignment is present, it is added to the contribution to Y_{of} and Y_{or} provided by the guideway dynamic motion and the resulting complete suspension motion, Fourier analyzed. The program in Appendix D computes Fourier coefficients for both initially flat guideways and also for guideways with a specified, periodic initial (camber) shape.

With the representation of the vehicle front and rear suspension motion by (3.7) and (3.8), the acceleration at any point on the vehicle may be computed using vehicle transfer functions. In general, it is convenient to define two components of acceleration - the vehicle heave acceleration at the center of mass and the vehicle (pitch) angular acceleration about the center mass. These accelerations may be computed as:

$$\hat{\ddot{Y}}_c = 0.5\, T_h\, (Y_{of} + Y_{or}) \tag{3.15}$$

$$\hat{\ddot{\delta}} = 0.5\, T_p\, (Y_{of} + Y_{or}) \tag{3.16}$$

where:

$\hat{\ddot{Y}}_c = \ddot{y}_{cg}/(\omega_v^2\, y^*)$ = nondimensional vehicle center of mass acceleration

$\hat{\ddot{\delta}} = \ddot{\delta}/(\omega_v^2)$ = nondimensional vehicle angular acceleration about the center of mass

T_h = nondimensional vehicle heave transfer function

T_p = nondimensional vehicle pitch angle transfer function

ω_v = vehicle heave natural frequency

The accelerations at other points on the vehicle may be computed directly from these accelerations. For example, the nondimensional acceleration on the vehicle body at the front $\ddot{\hat{Y}}_{2f}$ and rear $\ddot{\hat{Y}}_{2f}$ suspension attachment points are:

$$\ddot{\hat{Y}}_{2f} = \ddot{\hat{Y}}_c + \ddot{\hat{\delta}} \frac{\ell_a}{2y^*} \tag{3.17}$$

$$\ddot{\hat{Y}}_{2r} = \ddot{\hat{Y}}_c - \ddot{\hat{\delta}} \frac{\ell_a}{2y^*} \tag{3.18}$$

where $0.5\ \ell_a$ is the suspension attachment length from the vehicle center of mass. Accelerations at other points on the vehicle may be computed by replacing $0.5\ \ell_a$ by the appropriate distance from the center of mass to the point of interest.

By noting that Y_{or} and Y_{of} may be represented by the Fourier series of (3.7) and (3.8) and that the heave and pitch transfer functions may be represented in terms of their magnitude and phase, the steady-state heave and pitch accelerations as a function of time for each frequency may be expressed as:*

$$\begin{aligned}\ddot{\hat{Y}}_{ci} = {} & 0.5 \mid T_h (j\hat{\Omega}_i) \mid \cos \hat{\Omega}_i t \left[(a_{fi} + a_{ri}) \cos \theta_{hi} + (b_{fi} + b_{ri}) \sin \theta_{hi}\right] \\ & + 0.5 \mid T_h (j\hat{\Omega}_i) \mid \sin \hat{\Omega}_i t \left[- (a_{fi} + a_{ri}) \sin \theta_{hi} + (b_{fi} + b_{ri}) \cos \theta_{hi}\right]\end{aligned} \tag{3.19}$$

---

*In determining the vehicle accelerations, the contribution of the average deflection represented by a_{ro}, b_{ro}, a_{fo}, b_{fo} is zero.

$$\ddot{\hat{\delta}}_i = 0.5 \mid T_p\,(j\hat{\omega}_i) \mid \cos \hat{\omega}_i t \left[(a_{fi} - a_{ri}) \cos \theta_{pi} + (b_{fi} - b_{ri}) \sin \theta_{pi}\right] + 0.5 \mid T_p\,(j\hat{\omega}_i) \mid \sin \hat{\omega}_i t \left[-(a_{fi} - a_{ri}) \sin \theta_{pi} + (b_{fi} - b_{ri}) \cos \theta_{pi}\right] \quad (3.20)$$

where: $\ddot{\hat{Y}}_{ci}$ = heave acceleration at frequency $\hat{\omega}_i$

$\ddot{\hat{\delta}}_i$ = pitch acceleration at frequency $\hat{\omega}_i$

θ_{hi} = phase angle of $T_h\,(j\hat{\omega}_i)$

θ_{pi} = phase angle of $T_p\,(j\hat{\omega}_i)$

$\hat{\omega}_i = \frac{2\pi i v}{k \omega_v \ell_s}$

$\hat{t} = \omega_v t$

$j = \sqrt{-1}$

The steady-state heave and pitch accelerations versus time are determined by summing over all frequencies as:

$$\ddot{\hat{Y}}_c = \sum_{i=1}^{n} \ddot{\hat{Y}}_{ci} \quad (3.21)$$

$$\ddot{\hat{\delta}} = \sum_{i=1}^{n} \ddot{\hat{\delta}}_i \quad (3.22)$$

The rms accelerations at a given frequency $\hat{\omega}_i$ may also be readily determined using (3.19) and (3.20) from the relationships:

$$\tilde{\ddot{Y}}_{ci} = \sqrt{\frac{1}{T_i}\int_o^{T_i}\left[\hat{\ddot{Y}}_{ci}\right]^2 dt} \qquad (3.23)$$

$$\tilde{\ddot{\delta}}_i = \sqrt{\frac{1}{T}\int_o^{T_i}\left[\hat{\ddot{Y}}_{ci}\right]^2 dt} \qquad (3.24)$$

where:

$\tilde{\ddot{Y}}_{ci}$ = rms nondimensional heave acceleration at frequency $\hat{\omega}_i$

$\tilde{\ddot{\delta}}_i$ = rms nondimensional pitch acceleration at frequency $\hat{\omega}_i$

$T_i = \omega_i / 2\pi$

For a vehicle described in terms of the heave and pitch transfer functions, the steady-state acceleration versus time and rms acceleration at any given frequency may be determined directly using (3.19) -- (3.24). For the two-dimensional vehicle model described in Chapter 2, the vehicle heave and pitch transfer functions are summarized in Appendix A.

3.5 Comparison of the Partially and Fully Coupled Model Simulations

To illustrate the degree of approximation resulting from the constant force vehicle model in comparison to a completely coupled model, vehicle accelerations, suspension forces on the guideway, and guideway deflections under the vehicle suspensions have been computed with the fully coupled vehicle model and with the constant force model described above. The results are presented in Figures 3.16--3.19 for the two vehicle systems defined in Table 3.1 where a sufficient number of span crossings have occured prior to those presented so that a steady-state periodic response is achieved.* The vehicle parameters have been selected to yield maximum vehicle body accelerations for Vehicle A in the range of 0.05 and Vehicle B in the range of 0.1g and correspond to vehicles with a relatively large unsprung to sprung mass ratio of 0.25.** The other vehicle parameters are typical of advanced TLV systems.

---

*For the full simulation 5-10 span crossings are typically required to achieve steady-state. The number of terms used in the Fourier series representation is 2k+1.

**The sprung mass secondary suspension natural frequency is 1.0 hertz; the unsprung mass-primary suspension spring natural frequency is 6.3 hertz, and the span crossing frequency is 4.4 hertz.

TABLE 3.1

SIMULATION VEHICLE GUIDEWAY SYSTEM PARAMETERS*

Parameter	Vehicle-Guideway System A	Vehicle-Guideway System B
V_c	0.75	0.95
Ω	5.89	4.65
M	0.24	0.28
L_a	0.5	0.5
L_p	0.3	0.3
K	10.0	10.0
M_u	0.25	0.25
$\bar{I}_v$	1.0	1.0
ξ_v	0.25	0.25
ξ_m	0.0	0.0

*In both systems 75,000 lb. vehicles with 1.0 hertz suspension natural frequencies are considered crossing 100 ft. spans. System A has an 8.34 ft. high span cross-section to yield ≈ 0.05g vehicle acceleration while System B has a 6.43 ft. high span cross-section to yield≈ 0.1g vehicle acceleration at 300 mph.

Guideway midspan and vehicle suspension pad displacements and suspension forces on the guideway are presented in Figures 3.16 and 3.17. For the 0.05g vehicle the suspension forces differ in magnitude from constant values of 0.5 by less than 0.05, while for the 0.1g vehicle the suspension forces differ in magnitude from constant values by less than 0.1. The beam maximum nondimensional midspan deflection computed from the full simulation is 0.736 and from the constant force model 0.74 for the 0.05g vehicle, while for the 0.1g vehicle it is 0.88 from the full simulation and 0.91 from the constant force model. The time histories of the deflections sustained by the vehicle suspension pads for both the constant force and full simulations are similar for both vehicle systems.

Vehicle accelerations at the front and rear suspension attachment points computed from the full simulation and computed from a Fourier representation of constant force deflections and subsequent transfer function representation of the vehicle are presented in Figures 3.18 and 3.19. The acceleration time histories for the two simulation methods are similar with the maximum acceleration for the 0.05g vehicle predicted by the full simulation reaching 0.06g's and that of the constant force Fourier model reaching 0.64g's. For the 0.1g vehicle the full simulation acceleration approaches 0.116g's and the constant force Fourier model acceleration approaches 0.120g's.

The data illustrates for both vehicles considered the

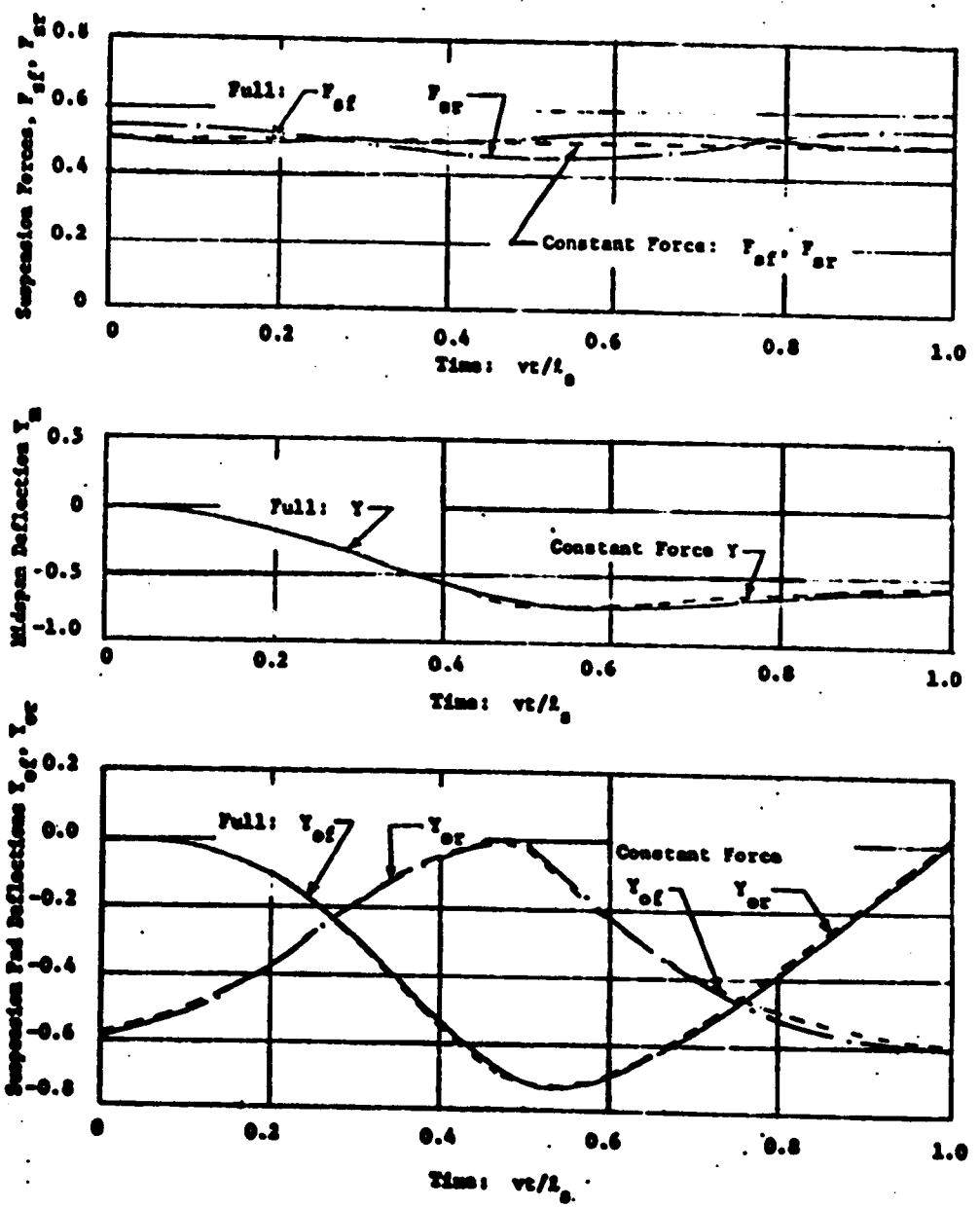

Fig. 3-16. Suspension Forces, Midspan and Suspension Pad Deflections Computed from Full and Constant Force Simulations for 300 mph, 0.05g Vehicle A Traversing a Single Span

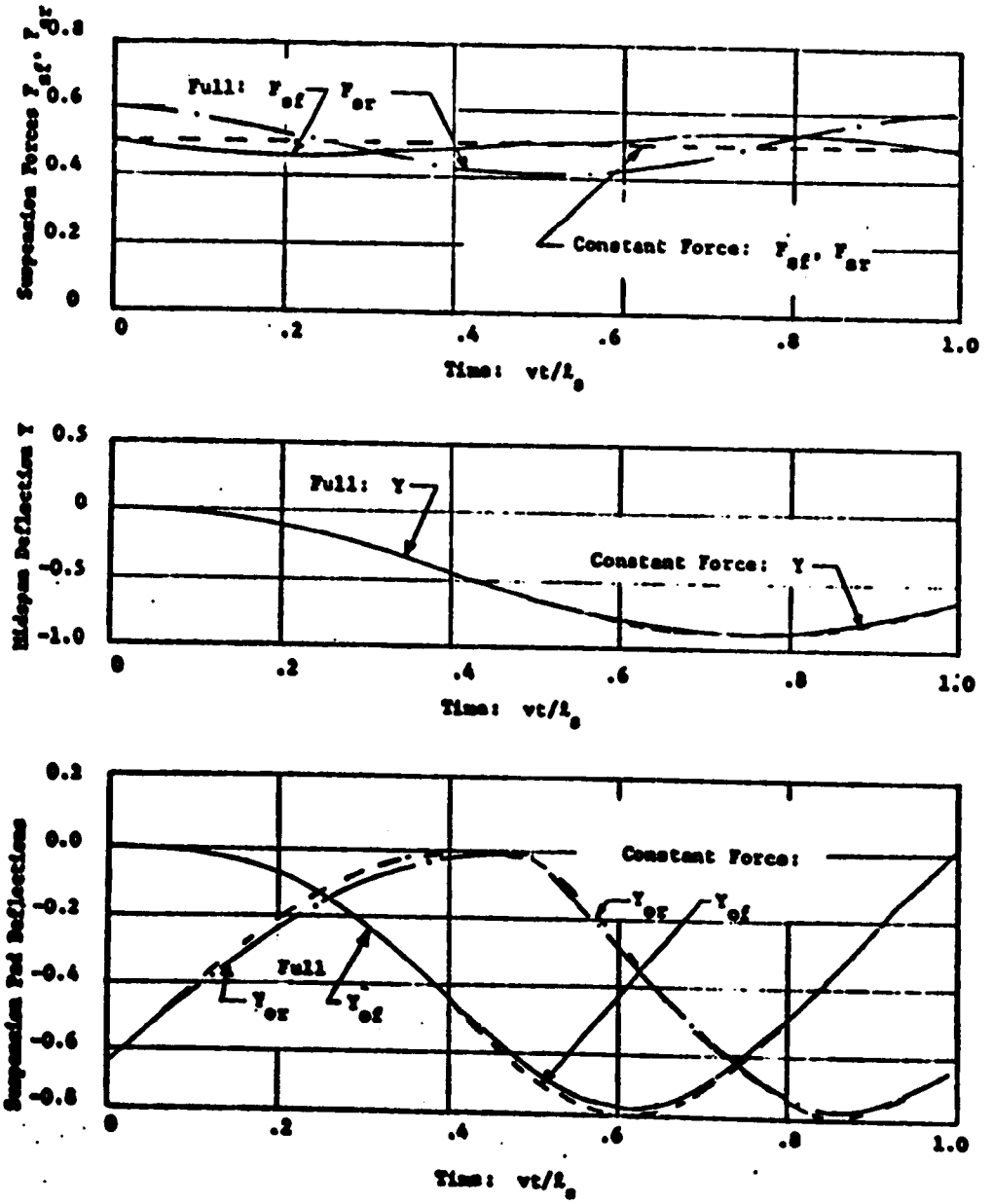

Fig. 3-17. Suspension Force, Midspan and Suspension Pad Deflections Computed from Full and Constant Force Simulations for 300 mph, 0.1g Vehicle B Traversing A Single Span

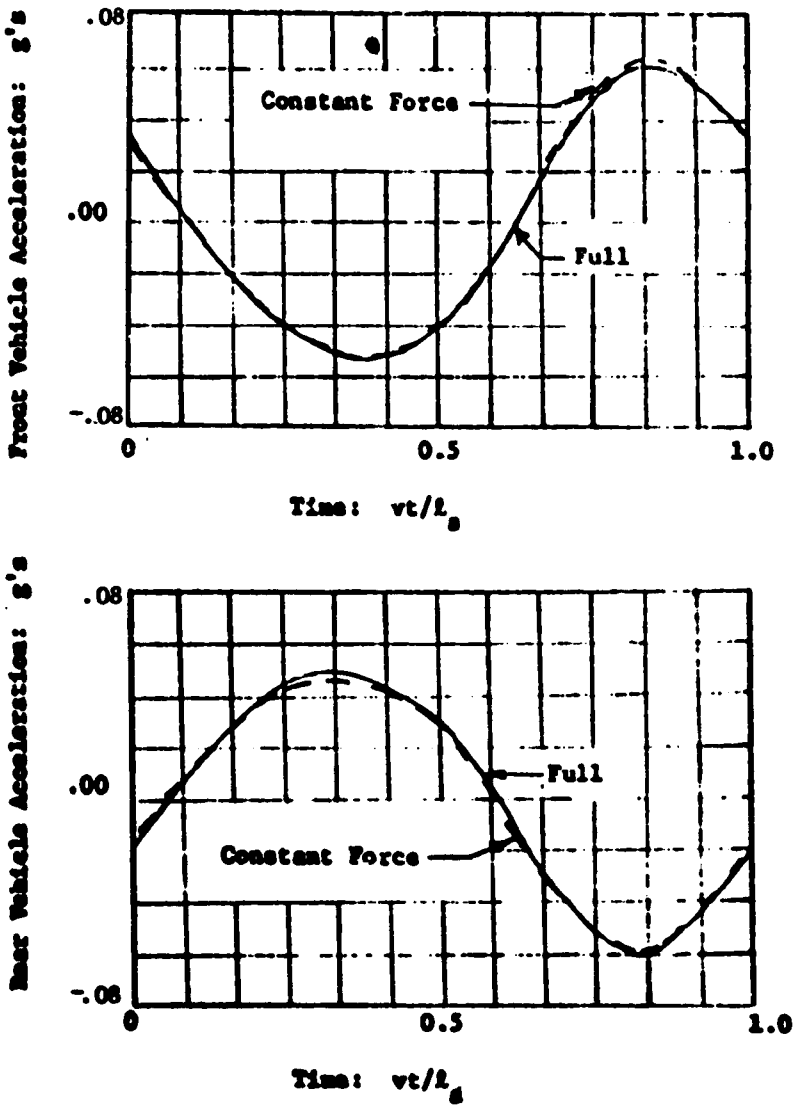

Fig. 3-18. Vehicle A Front and Rear Accelerations Computed from Full and Constant Force Simulations

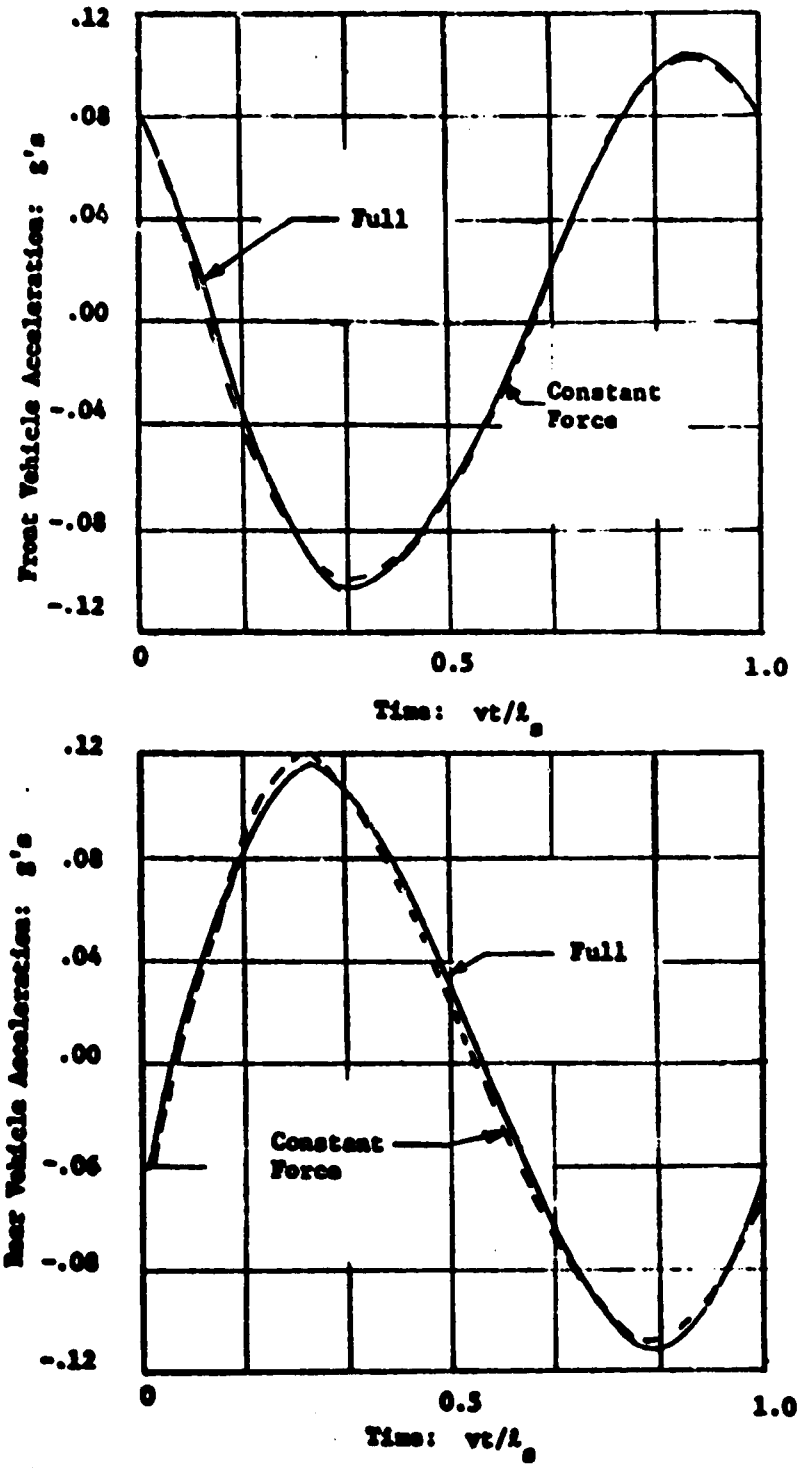

Fig. 3-19. Vehicle B Front and Rear Accelerations Computed from Full and Constant Force Simulations

validity of a constant force vehicle model in system performance computation for high speed, high passenger comfort level vehicles which have a relatively large unsprung mass equal to 25% of the vehicle mass. Additional simulations of the two guideway systems described have indicated that for similar vehicles with unsprung mass ratios less than 0.25 the constant force approximation is also valid.

Parametric data is presented in Appendix G based upon a reduced order vehicle model ($L_a = 0$, $L_p = 0$) which shows the range of parameters for which suspension force variations are limited to 15% if the vehicle sprung mass accelerations are limited to 0.07g. This data for undamped, single span guideways has shown that:

(1) For span encounter frequencies v/ℓ_s less than half the suspension natural frequency f_v, $v/\ell_s < 0.5\ f_v$, the maximum force variation is less than 10% for the full range of crossing velocities $.15 < V_c < 1.5$, unsprung to sprung mass ratios $.15 < M_u < 1.0$ and unsprung to sprung mass natural frequency ratios $2.5 < \Omega_u < 10$ considered. In this range the fully and partially coupled vehicle models agree within 10% in the prediction of vehicle and span dynamics.

(2) For span encounter to suspension frequency ratios $v/\ell_s < f_v$, the maximum force variation is less than 15% for the full range of crossing velocities $.15 < V_c < 1.5$ and unsprung to sprung mass frequency ratios $2.5 < \Omega_u < 10$ if $.15 < M_u < .66$. In this range fully and partially coupled models agree within 15% in the prediction of vehicle and span dynamics.

(3) For span encounted to vehicle suspension frequency ratios $v/\ell_s > f_v$ the suspension force

variation is strongly dependent upon M_u, Ω_u and $v/\ell_s f_v$. The range for which suspension force variations are limited to 15% is displayed in Fig. 3.20 which is reproduced from Fig. G.11.

Using the data in this chapter and Appendix G an initial estimate of the range of system parameters for which the partially coupled vehicle model is useful for preliminary design may be made. As shown by the data presented for many of the advanced transportation of current interest, the partially coupled vehicle model may be used for preliminary design estimates over significant operating regions.

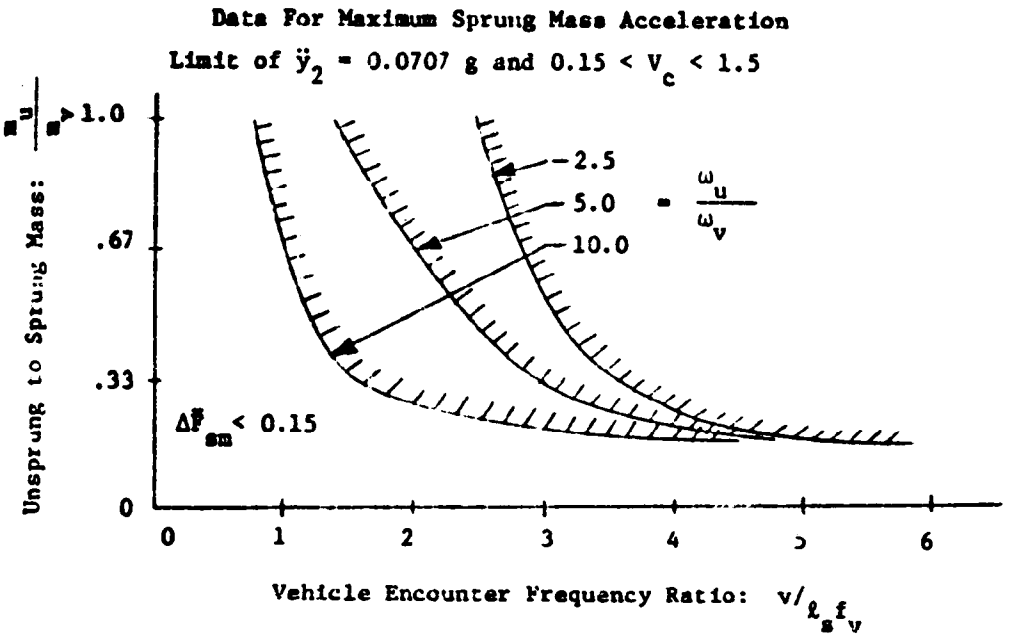

Fig. 3-20. Range of System Parameters for 15% Suspension Force Variation

4. GUIDEWAY DESIGN FOR PASSENGER CARRYING VEHICLES

4.1 The Design Factors

The design of an elevated vehicle-guideway system is influenced by a number of factors including:

(1) Structural loading due to (a) the vehicle live loads, (b) the structure dead loads and (c) environmentally related snow, wind, thermal, earthquake and settlement loads.

(2) Passenger safety and comfort.

(3) Community environmental impact.

(4) Cost.

The design constraints for advanced urban and intercity systems represented by these factors are discussed in [11-14], while the structural loading constraints considered in highway bridge design are summarized in the AASHO document [15]. Of the factors listed, the two for advanced levitated, vehicle systems which are primarily different from highway and rapid transit elevated structure design are the influence of vehicle induced loads on the guideway and the design of a vehicle-guideway system to meet a specific passenger comfort criteria. The distributed suspension forces and the high vehicle speeds (150 - 300 mph for proposed vehicles) produce load conditions which are not readily accounted for in the analysis described in [5]. The passenger comfort specification for classical guideways has traditionally been in the form of a guideway dynamic deflection to span length constraint such as the 1/800 constraint in [5].

Data for urban air cushion vehicle system in Chapter 5 indicates that a simple guideway deflection ratio constraint is an inadequate method of specifying comfort because the level of passenger comfort is strongly dependent upon both the vehicle and the guideway characteristics.

Rather than indirectly specifying passenger comfort in terms of a span deflection to length ratio, the U. S. Department of Transportation has specified passenger comfort in terms of permissible levels of vehicle passenger compartment acceleration over the vehicle operating speed range. The specification used in this report is derived from the International Standards Organization rms acceleration versus frequency criteria illustrated in Figure 4.1, in which a maximum level or rms acceleration is allowed for each frequency component of vehicle acceleration. This criteria applied in this report to the vertical vehicle accelerations produced by vehicle guideway interactions.

For a vehicle-guideway system for which a preliminary design has been completed the computer program listed in Appendix C which is based upon the complete vehicle-guideway interaction model may be used to determine vehicle passenger compartment accelerations, suspension deflections and guideway loads, deflections,

Permissible RMS Acceleration in a One Octave Band -- Extension of One-hour Comfort Criteria of International Organization for Standardization

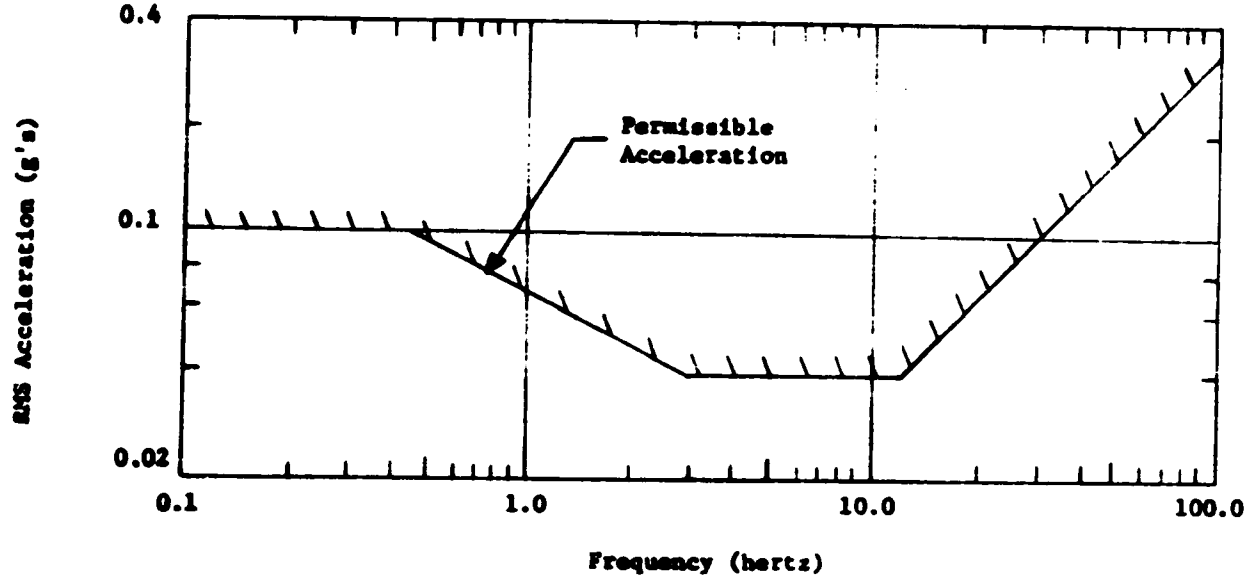

Fig. 4-1. Passenger Comfort Constraint RMS Acceleration Versus Frequency

and guideway loads, deflections, moments and stresses. Complete interaction simulation programs are useful to assess a prototype design capability to meet design specifications; however, they do not provide a simple, direct method for determining the guideway structural properties required to meet a passenger comfort specification as shown in Figure 4.1. In this chapter a method is developed, based upon the constant force simulation which provides a preliminary estimation of the guideway structural properties required to meet the passenger comfort specification given in Figure 4.1* and to meet a given moment or stress level in the guideway. Since the passenger comfort specification of Figure 4.1 tends, for typical advanced systems, to be a more stringent design constraint than dynamic stress or moment it is considered first and then the dynamic stress level is checked to insure it is acceptable.

4.2 A Guideway Design Procedure

A procedure for determining the guideway main support beam structural properties required for a vehicle running at its design operating speed to meet the rms acceleration passenger comfort specification in Figure 4.1 is outlined in this section. The procedure utilizes the computation method described in Section 3.4 to determine the nondimensional acceleration at the vehicle

---

*The design procedure may be used with any passenger comfort specification which specifies rms acceleration as a function of frequency or which uses a weighted sum of rms accelerations at selected frequencies. With some modification it may be adapted for use with criteria which specify peak accelerations.

body front and rear suspension attachment points. These accelerations are considered to be representive of passenger compartment accelerations and are required to meet the specification of Figure 4.1. In the procedure uniform cross-section, simply supported single and multiple spans are considered. The parameters listed in Table 4.1 are assumed to be specified prior to the detailed design of the span cross-section, i.e. the vehicle properties are specified as well as span material, length and general cross-section shape.

With the specification of the span properties in Table 4.1 only two general parameters remain which can be independently specified to describe the span's influence upon the vehicle:

(1) the flexural rigidity*: EI

(2) the mass per unit length*: ρa

For a given span system the flexural rigidity and the mass per unit length have been included in a general way in the nondimensionalization of the span deflections and the vehicle accelerations through y* the nominal deflection of a single pinned end span due to a force equal to the vehicle weight concentrated at midspan:

$$y^* = \frac{2 W \ell_s^3}{\pi^4 EI} \tag{4.1}$$

---

*Note: these actually reduce to ℓ and a since ρ and E are specified in Table 4.1.

TABLE 4.1 SYSTEM PARAMETERS SPECIFIED PRIOR TO SPAN CROSS SECTION DESIGN

(1) The vehicle properties

- (a) Vehicle design operating speed: v
- (b) Vehicle weight: W
- (c) Vehicle pad length: ℓ_p
- (d) Vehicle suspension attachment length: ℓ_a
- (e) Vehicle secondary suspension natural frequency: $\omega_v = 2\pi f_v$
- (f) Vehicle suspension dmaping ratio: ξ_v
- (g) Vehicle suspension stiffness ratio: K
- (h) Vehicle unsprung mass ratio: M_u
- (i) Vehicle inertia ratio: $\bar{I}_v$

(2) Basic span length and general configuration for which a design is required.

- (a) Span length: ℓ_s
- (b) Span configuration: k span
- (c) Material: elastic modulue E and density ρ
- (d) General cross-section shape
- (e) Span damping

and though the first mode beam natural frequency f* of a k span system:

$$f^* = \frac{\pi}{2\ell_s^2} \sqrt{\frac{EI}{\rho a}} = \frac{\pi c_s}{2\ell_s^2} \sqrt{\frac{I}{a}} \tag{4.2}$$

where $c_s = \sqrt{\frac{E}{\rho}}$

With the parameters in Table 4.1 only one additional parameter requires specification so that the nondimensional rms vehicle acceleration($\tilde{Y}_2 = \tilde{\ddot{y}}_2/\omega_v^2 y^*$) may be computed using the Fourier coefficient--transfer function analysis described in Section 3.4--the vehicle crossing frequency ratio V_c:

$$V_c = \frac{v}{\ell_s f^*} = \frac{v}{c_s} \frac{2\ell_s}{\pi} \sqrt{\frac{a}{I}} \tag{4.3}$$

For a given span material the selection of V_c essentially specifies the ratio of I/a for a span. Thus, based upon the general span dynamic information in Chapter 3 a value of V_c can be selected for the vehicle operating speed, implicitly selecting I/a, and then the vehicle nondimensional rms acceleration as a function of frequency can be calculated by the methods in Section 3.4.

Since the rms accelerations at all frequencies are normalized by the same factor, they may be proportionally compared with Figure 4.1 to determine the frequency corresponding to the limiting nondimensional acceleration and the

corresponding limiting dimensional acceleration. If the limiting dimensional acceleration in g's determined from Figure 4.1 is designated $\ddot{y}_{2d}$ and the corresponding frequency ω_d, then directly from the definition of the nondimensional rms acceleration ($\ddot{\tilde{Y}}_2(\omega_d) = \ddot{\tilde{y}}_2(\omega_d)/\omega_v^2 y^*$) the following expression for the span EI required to match the vehicle dimensional rms acceleration $\ddot{\tilde{y}}$ to the desired limiting acceleration $\ddot{y}_{2d}$ is from Fig. 4.1:

$$EI = \left(\frac{8 \times 144}{32.2 \times \pi^2}\right) \left(\frac{\ddot{\tilde{Y}}_2(\omega_d)}{\ddot{y}_{2d}}\right) W \ell_s^3 f_v^2 \qquad (4.4)$$

where EI is in lb-in^2, W is in lbs., $\ddot{y}_{2d}$ is in g's, f_v is in hertz and the corresponding value of y* in feet is:

$$y^* = \frac{\ddot{y}_{2d}}{\ddot{\tilde{Y}}_2(\omega_d)} \quad \frac{32.2}{4\pi^2 f_v^2} \qquad (4.5)$$

With the determination of EI, since the span material properties are known, the cross section area, a, may be determined since I/a was implicitly specified in selecting V_c (4.3) to complete the specification of the two independent span parameters

While the direct application of the procedure outlined above will determine the span structural properties required to meet the passenger comfort specification of Figure 4.1, the span I/a and area a, may not correspond to a convenient standard section beam.

For steel I or box beams a set of standard size and cross-section beams are available. For prestressed concrete spans a number of general shapes, configurations and sizes are also available. The use of standard sections or sections which are easily fabricated may lead to a reduction in guideway cost compared to the use of nonstandard sections. To design a beam so that a standard span section or a given specific type of section is obtained for a given beam material imposes an additional constraint upon beam design which relates the cross-section inertia I and the inertia to area ratio I/a. The particular relationship between I and I/a depends upon the span material and general cross section configuration. In this report only prestressed concrete spans are considered in detail.*

The relationships between I and I/a and between I and span height, h, for prestressed concrete guideway structures which have been designed by a number of organizations are contained in Figure 4.2. All the spans represented have been designed for span lengths between 75 and 100 ft. Also plotted in the Figure is the relationship between I and I/a and between I and the span height, h, for the twin I-beam span sketched in Figure 4.3. The data for all the spans generally clusters about the curve for the twin I-beam span for both I versus I/a and I versus h.

*Cost estimates for urban tracked air cushion vehicle guideways [11] indicate that concrete spans in the designs considered to date lead to a lower cost structure than steel spans. Although only concrete spans are considered in detail, the design may be easily extended to other types of beams.

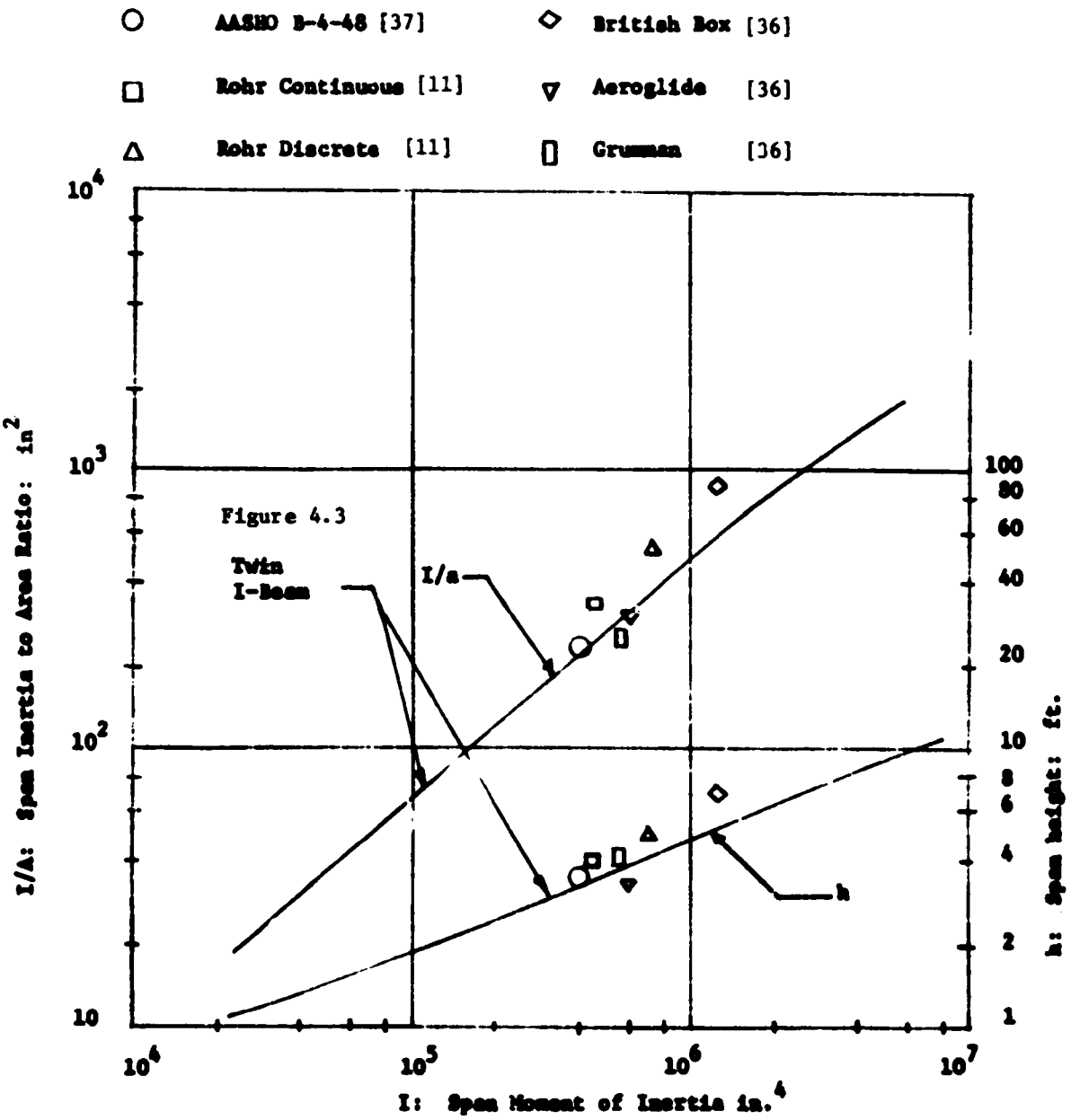

Fig. 4-2. Span Cross Section Moment of Inertia, Area and Height Relationships for Several Guideway Configurations

For Twin I-Beam Span

w = 5 ft., c = 10.0 inches, h'= 5.0 inches

h: variable

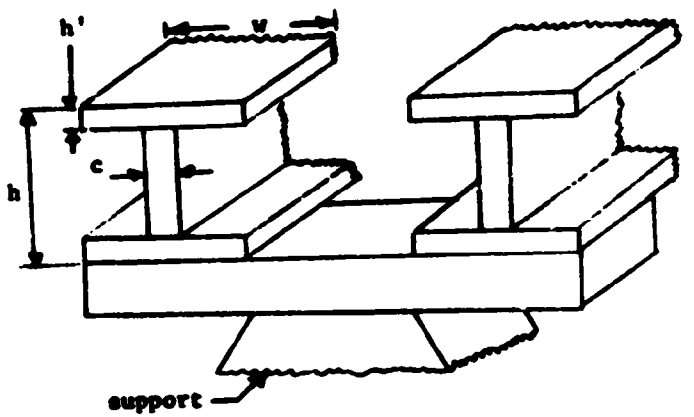

Fig 4-3. The Twin I-Beam Span Configuration

Spans which for a given I have a larger I/a require less material and have a higher natural frequency than spans of the same material with lower values of I/a. The value of I/a for a given I is an indication of the span efficiency of material utilization. All the spans which have a larger I/a for a given I than the twin I-beam span also are greater in height at a given I than the twin I-beam span. Since the twin I beam span is representative of the data in Figure 4.2 it is used for purposes of illustration in the design examples discussed in this report.

The design of a guideway structure to meet both the passenger comfort criteria in Figure 4.1 and to provide a beam design which corresponds to a given class of beams as defined by a specified relationship between I and I/a such as is shown in Figure 4.2 may be accomplished by using the design steps outlined above in an iterative manner. Thus for a given class of beams for which a relationship between I and I/a is specified an iterative design procedure which will identify* the particular beam required so that the ride comfort specification of Figure 4.1 is satisfied at the vehicle operating speed may be summarized as indicated in Table 4.2.

The procedure outlined in Table 4.2 is an iterative design procedure. The number of iterations required to achieve a structure

*The possibility exists that for a given limited class of beams it is not possible to satisfy the passenger comfort constraint of a given vehicle system.

TABLE 4.2

DESIGN PROCEDURE STEPS

Step 1: From the initial vehicle and span specification data corresponding to the quantities in Table 4.1 compute: $L_p = \ell_p/\ell_s$, $L_a = \ell_a/\ell_s$.

Step 2: Select an initial value of V_c and determine the Fourier suspension deflection coefficients from the data in Appendix F or using the computer program listed in Appendix D for each $\hat{\omega}_i = \frac{iv}{\ell_s f_v k}$ of interest; usually $i = 1$ to $2k$ is sufficient.

Step 3: Determine the vehicle nondimensional rms front and rear accelerations as a function of the frequencies $\hat{\omega}_i$ either using equations (3.23) and (3.24) or using the computer program listed in Appendix D.

Step 4: Using the passenger comfort specifications of Fig. 4.1 determine which nondimensional rms acceleration $\ddot{\tilde{Y}}_{2f}(\frac{2\pi iv}{\ell_s k})$, $\ddot{\tilde{Y}}_{2r}(\frac{2\pi iv}{\ell_s k})$ at which frequency $\omega_i = \frac{2\pi iv}{\ell_s k}$ provides the limiting acceleration constraint, and determine the corresponding limiting dimensional acceleration $\ddot{y}_{2d}$ from the plot in Fig. 4.1.

Step 5: Using equation 4.4 compute the span EI and then using the value of E, determine I.

Step 6: For a given class of spans refer to Fig. 4.2 (or an equivalent Figure for the desired span class) and determine the span area a.

Step 7: Compute the span crossing frequency ratio V_c from equation (4.3) and compare it with the initial value selected in Step 2. Select a new value of V_c and return to Step 2 and perform steps 2 through 7 again. The iterative design should be repeated until convergence is reached on values of the span I and a which meet desired levels of design accuracy.

Step 8: After the design values of I and a have been determined, compute y^* from (4.5). The maximum span deflection and stress may be computed using the definition $y_m = Y_m y^*$ and equation A.78 from the information in Appendix F in which the nondimensional deflection and stress are given or from the Appendix D computer program.

---

*When guideway surface irregularities as well as deflections are considered, the steps outlined here represent only a part of the overall design process. Additional design steps must be considered to treat both surface irregularity and deflective generated vehicle accelerations.

design which for two successive iterations is within desired levels of design accuracy can be minimized with a good selection of the initial value of the crossing frequency, V_c. The design data developed in Chapter 5 for both 150 mph and 300 mph systems can provide a good initial estimate of the value of V_c for the design of systems which have similar operating conditions to those represented. The procedure has been implemented in the computer program described in Appendix E, which iteratively searches for the beam design from a family of beams such as defined in Figure 4.2 which satisfy a prescribed passenger comfort criteria such as defined in Figure 4.1. Fourier coefficient data is also provided in Appendix F so that for many cases of interest a preliminary design can be performed with paper and pencil techniques.

To illustrate the design procedure outlined in Table 4.2, the design of a guideway for an 80,000 lb., 80 ft. air cushion vehicle operating at a speed of 150 mph is considered. The vehicle is assumed to have air cushion suspensions which extend along 75% of its length and which have an effective suspension natural frequency of 2.0 hertz and damping ratio of 0.25. The design of the guideway main support beams for a 100 ft. three span system is considered for the basic twin I-beam span configuration illustrated in Figure 4.2. For the design example the system parameters which may be specified prior to the structure design are summarized in Table 4.3

TABLE 4.3

DESIGN EXAMPLE PARAMETERS SPECIFIED PRIOR

TO SPAN CROSS SECTION DESIGN

(1) Vehicle Properties

(a) Design operating speed: $v = 150$ mph

(b) Weight: $W = 80{,}000$ lbs.

(c) Pad length: $\ell_p = 30$ ft.

(d) Attachment length: $\ell_a = 50$ ft.

(e) Suspension frequency: $f_v = 2$ hertz

(f) Suspension damping ratio: $\xi_v = 0.25$

(g) Suspension stiffness ratio: $K = 10$

(h) Unsprung mass ratio: $M_u = 0.0$

(i) Inertia ratio: $\bar{I}_v = 1.0$

(2) Span Properties

(a) Length: $\ell_s = 100$ ft.

(b) Configuration: $k = 3$ span

(c) Material: concrete: $E = 5 \times 10^6$ lb/in^2, $\rho = 150$ lbs/ft^3

(d) Span damping: $\xi_m = 0.0$

TABLE 4.4

SPAN PROPERTIES RESULTING FROM DESIGN EXAMPLE

$I = 1.9 \times 10^6$ in.^{4} $\quad$ $a = 2.49 \times 10^3$ in.^{2}

$h = 6.21$ ft. $\quad$ $f_1 = 4.6$ hertz

$y_m = 0.15$ in. $\quad$ $\sigma_t = 212$ psi

The steps in the design procedure are:

Step 1: Compute L_p and L_a:

$$L_p = \ell_p/\ell_s = 0.3 \text{ and } L_a = \ell_a/\ell_s = 0.5$$

Step 2: Select a trial V_c and determine the deflection coefficients:

For 150 mph systems operating on 100 ft. guideways, an initial value* of $V_c = 0.66$ is selected. This value of V_c places the initial design below a crossing frequency where span dynamic resonant effects and span damping are important in the response. Directly from Appendix F, the span deflection Fourier coefficients may be selected and their corresponding frequencies calculated. The first $2k = 6$ deflection coefficients are:

n	a_f	b_f	a_r	b_r	$\hat{\omega}_i = \frac{vi}{\ell_s f_v k}$
1	-0.060	-0.013	-0.040	-0.045	0.37
2	-0.004	-0.007	-0.002	-0.005	0.73
3	0.182	0.091	-0.183	0.096	1.10
4	0.024	0.005	-0.002	-0.024	1.46
5	0.028	0.002	0.034	-0.009	1.83
6	0.002	0.021	0.000	-0.007	2.2

*Data in Appendix F is tabulated for $V_c = 0.33$, 0.5, 0.66, and 0.83 and 1.0

As noted from the table, the coefficients for $\hat{\omega}_3$, which correspond to the nondimensional crossing frequency of a single 100 ft. span*, are significantly larger than all other coefficients and make the most significant contribution to the deflections under the vehicle suspensions.

Step 3: Determine the rms accelerations as a function of $\hat{\omega}_1$: For each $\hat{\omega}_1$, the nondimensional vehicle body accelerations at the front $\hat{\ddot{Y}}_{2f}$ and rear $\hat{\ddot{Y}}_{2r}$ suspension attachment points may be determined using the computer program of Appendix D as:

$\hat{\omega}_1$	$(\omega_1/2\pi)$ (hertz)	$\hat{\ddot{Y}}_{2f}$	$\hat{\ddot{Y}}_{2r}$
0.37	.73	0.0067	0.0067
0.73	1.46	0.0057	0.0048
1.10	2.2	0.0805	0.3870
1.46	2.92	0.0698	0.0337
1.83	3.66	0.0494	0.0354
2.2	4.4	0.0669	0.0539

The largest rms nondimensional acceleration occurs at the single span crossing frequency $(\omega_3/2\pi) = 2.2$ hertz and corresponds to $\hat{\ddot{Y}}_{2r} = 0.387$.

---

*The first coefficient corresponds to the crossing frequency of the complete k span system.

Step 4: Determine the limiting rms acceleration and frequency from Figure 4.1:

The limiting acceleration and frequency can be found from Figure 4.1 by dividing each nondimensional acceleration at a given frequency obtained in Step 3 by the corresponding dimensional acceleration in Figure 4.1. The largest acceleration ratio provides the limiting acceleration. By inspection it is noted that the limiting nondimensional acceleration corresponds to $\tilde{\ddot{Y}}_{2r} = 0.178$ at $(\omega_3/2\pi) = 2.2$ hertz and corresponds to $\ddot{y}_{2d} = 0.045$ g's in Figure 4.1. For this design case the limiting rms acceleration occurs at the single span crossing frequency.*

Step 5: Determine the required span EI:

Directly from(4.4) EI may be calculated as:

$$EI = 9.66 \times 10^{12} \text{ lb} - \text{in}^2$$

$$I = 1.93 \times 10^{6} \text{ in}^4$$

Step 6: Determine the span cross-section area: a

For the twin I beam span configuration the area a and height h corresponding to the I calculated above may be determined from Figure 4.2 as:

$$a = 2.50 \times 10^{3} \text{ in}^2$$

$$h = 6.25 \text{ft.}$$

---

*For almost all the design cases considered in this report, the limiting rms acceleration occurs at the single span crossing frequency ω_k.

Step 7: Compute the resulting crossing frequency V_c:

Using (4.3) V_c may be computed as:

$$V_c = 0.49$$

This crossing frequency is less than the initial design crossing frequency of 0.66. It is quite close to a crossing frequency of 0.5 for which data exists in Appendix F. Thus, a second design iteration using $V_c = 0.5$ should be performed. The results of performing the design of $V_c = 0.5$ are:

(i) The limiting acceleration occurs at $(\omega_3/2\pi) = 2.2$ hertz with $\ddot{Y} = 0.38$ and corresponds to $\ddot{y}_{2d} = 0.045$ g's

(ii) $EI = 9.52 \times 10^{12}$ lb - in^2

(iii) $a = 2.49 \times 10^3$ in^2 and $h = 6.21$ ft.

(iv) $V_c = 0.489$

With this second iteration, the design span cross section properties I and are within 2% of the values computed with the first iteration, also the value of V_c on the second iteration is 0.489 which is close to the value of 0.5 used to compute the data. Thus, two iterations of the design procedure have produced results which are of sufficient accuracy for preliminary design purposes and the design can continue to Step 8.

Step 8: Compute the span deflection and stress:

The maximum span deflection is

$$y_m = Y_m\, y^* = 0.15 \text{ in.}$$

where y^* is computed from (4.5) and Y_m is listed in Appendix F. and the maximum dynamic stress due to a vehicle passage computed from (A.78) is

$$\sigma_t = 212 \text{ psi}$$

where $\tilde{M}_{tm}$ is taken from the data in Appendix F.

The span properties resulting from the design are summarized in Table 4.4. It is noted that the dynamic stress is small and, in fact, the passenger comfort constraint is more stringent than a stress constraint.

The rapid convergence of the design procedure in the example results from the fact that at values of $V_c < 0.66$ span dynamic effects are not very significant and the deflections generated under the vehicle suspensions are not a strong function of V_c. For design cases in which $V_c < 0.66$ convergence is usually very rapid. At higher values of V_c the dynamic suspension deflections are influenced more strongly by V_c and several iterations may be required to achieve a design of acceptable accuracy.

The design procedure results in the specification of a guideway so that the passenger comfort specification of Figure 4.1 is satisfied at the vehicle design operating speed. It is possible that the acceleration at a lower speed would exceed the

rms acceleration specification. Three factors in the present case tend to limit this possibility:

(1) As the vehicle speed decreases, the acceptable level of rms acceleration which occurs at the crossing frequency increases since the original frequency corresponds to $(\omega_k/2\pi) = 2.2$ hertz which is on the left "corner" of the specification in Figure 4.1.

(2) For frequencies lower than 2.2 hertz the magnitude of the vehicle transfer functions decreases with decreasing speed.

(3) The magnitude of the deflections under the vehicle decreases slightly with decreasing speed.

To illustrate the influence of these three factors the rms accelerations corresponding to the first six fundamental Fourier frequencies have been plotted in Figure 4.4 for vehicle speeds of 150, 135, 120, 105, and 90 mph over the guideway summarized in Tables 4.3 and 4.4. The data illustrates the general trend of decreasing acceleration as speed decreases. They also illustrate that at all speeds the rms acceleration corresponding to the single span crossing frequency, i.e., ω_3, is greater by a factor of at least four than the accelerations at any other frequency. For all cases, the maximum rms accelerations at speeds below 150 mph are less than the 0.045 g's acceleration

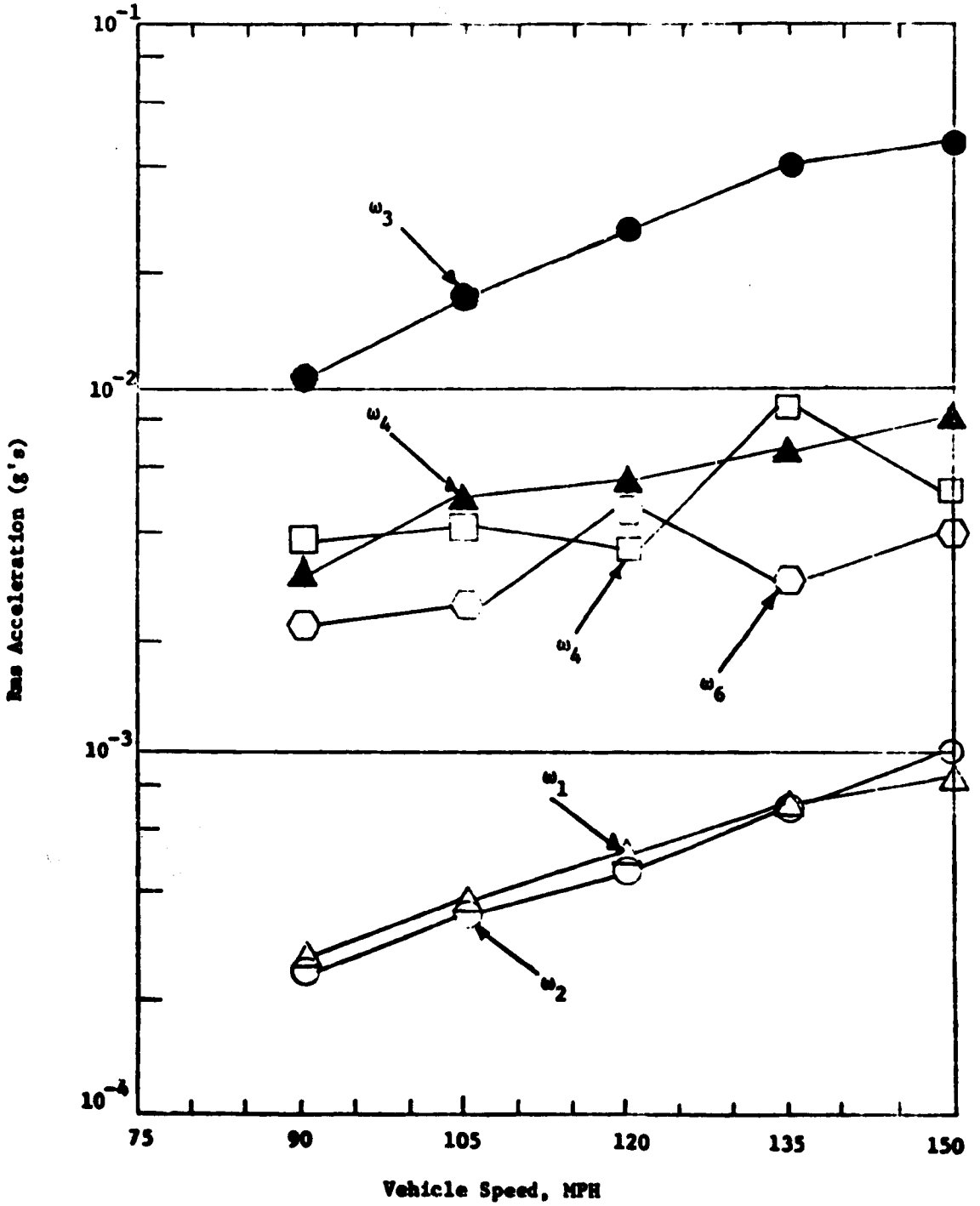

Fig. 4-4. RMS Acceleration for Six Fundamental Frequencies for Selected Vehicle Speeds

at 150 mph for other systems it is possible that the accelerations at lower speeds may be greater than those at the design speed and may exceed the passenger comfort specification of Figure 4.1. It is recommended that after a preliminary design for the vehicle-guideway system is performed, a check of vehicle accelerations for speeds lower than the design speed be made.* If the lower speed accelerations exceed acceptable levels, then it may be necessary to alter the guideway design. Such a modification can be accomplished using the design procedure to design a guideway to meet an acceptable acceleration level at the speed desired.

---

*The computer program listed in Appendix D may be used directly to determine rms acceleration levels as a function of speed.

5. AIR CUSHION VEHICLE GUIDEWAY DESIGN DATA

5.1 Design Scope

In this chapter design data is developed for air cushion vehicle guideways to illustrate the influence of vehicle speed, weight, body mass distribution and suspension design and span length, configuration and camber upon guideway structural requirements. The design data is developed so that the vehicles will meet the passenger comfort requirement specified in Figure 4.1, i.e. so that vehicle body accelerations at the suspension attachment points are equal to or less than those specified in Figure 4.1. For each design case the maximum dynamic midspan stress and deflection have been calculated. In all cases the stress levels have been found to be acceptable and the passenger comfort constraint has represented the most stringent span design constraint considered.

In the first part of the study, the three air cushion vehicle configurations summarized in Table 5.1 have been considered. For each vehicle the air cushions are distributed along 75% of the vehicle length and have been modeled as two effective equivalent cushions, one located at the front of the vehicle and the second at the rear*. The effective vehicle body attachment point of these cushions has been assumed to be at the cushion midpoint. For each vehicle configuration suspension natural frequencies of one and two hertz have been considered. Current

---

*In a practical configuration the two effective cushions may each consist of several smaller cushions or cushion compartments.

TABLE 5.1
THREE AIR CUSHION VEHICLE CONFIGURATIONS AND THE GENERAL SPAN CONFIGURATION

Vehicle Configurations

Parameter	Vehicle 1	Vehicle 2	Vehicle 3
weight: W: lbs	40,000	80,000	120,000
total length: ℓ_v: ft	40	80	120
pad length: ℓ_p: ft	15	30	45
suspension attachment length: ℓ_a: ft	25	50	75
suspension frequency: f_v: herts	1 or 2	1 or 2	1 or 2
suspension damping ratio: ξ_v	0.25	0.25	0.25
suspension stiffness ratio: K	10	10	10
unsprung mass ratio: M_u	0.0	0.0	0.0
vehicle inertia ratio: $\bar{I}_v$	1.0	1.0	1.0

Semi-continuous Span Configurations

Parameter	1 Span	2 Spans	3 Spans
Material	Concrete	Concrete	Concrete
E: lb/in^2	5×10^6	5×10^6	5×10^6
ρ: lb/ft^3	150	150	150
General Cross Section	Twin I-beam	Twin I-beam	Twin I-beam
Span damping:	0	0	0

urban air cushion designs for 150 mph systems have secondary suspension natural frequencies somewhat greater than 2 hertz. In more advanced suspensions which may use active control, it is anticipated that suspension frequencies in the 1 hertz range will be achieved.

The suspension damping ratios for all three vehicles have been selected as 0.25. This damping ratio has been shown to be nearly optimum for a number of passive air cushion vehicle configurations designed to minimize vehicle acceleration for operation on at grade guideways characterized by random roughness [31]. Also in [10] a damping ratio of 0.25 has been shown to represent a good* selection of damping ratio for vehicles which must operate over the crossing frequency range of $0.25 < V_c < 1$. Only design data for $\xi_v = 0.25$ is discussed in this report, and further evaluation of the influence of suspension damping on span requirements is recommended.

The suspension primary to secondary stiffness ratio has been selected at $K = 10$ to represent a typical air cushion vehicle, while the unsprung mass ratio has been set to $M_u = 0.0$ to reflect the small unsprung mass ratios which are characteristic of current urban vehicle designs. For the vehicles considered in the first part of the study, the vehicle mass is assumed to be essentially uniformly distributed and $\bar{I}_v = 1.0$.

---

*Lower values of damping result in increased vehicle accelerations at crossing frequencies near the suspension heave and pitch natural frequencies, while higher values of damping tends result in increased accelerations for $V_c > 0.5$.

Design data is developed for the three vehicle configurations running on single, 2 and 3 span prestressed concrete guideways* with a twin I-beam cross-section. The twin I-beam configuration is representative of the family of box, I-beam, and II-beam configurations. The specific configuration considered in the design is the twin I-beam configuration illustrated in Figure 4.3 which has the I/a and h versus I relationship illustrated in Figure 4.2. In the design the height of the beam is allowed to vary while other cross-section dimensions are maintained constant. By selecting beam cross section dimensions which vary with height, for smaller values of h, i.e. $h < 6.0$ ft., beams could be designed which have a larger I/a ratio at a given I than the configuration considered to further reduce the material requirements; also for larger values of $h > 10.0$ ft. beams could be designed which have a larger I at a given h than the beam considered to reduce the height requirements. The design of beams with cross-section dimensions which are a function of span height has been considered in [34] and found not to significantly alter the results presented in this chapter for beams with constant cross-section for the full range of heights considered.

The span considered in the design is standard prestressed concrete with the typical elastic modulus and density specified in Table 5.1. The span material damping is assumed to be zero. Span damping in typical guideway structures is small [10]

---

*Data in [11] indicates that concrete structures cost less than steel structures for the typical air cushion vehicle guideways considered to date.

with $\xi_m < 0.05$. For the designs considered in this section, the effects of span damping are essentially negligible since the vehicle crossing frequency ratios are less than 1.5. The use of $\xi_m = 0.0$ will result in little error and will, in any event, result in a conservative set of span requirements.

The design of guideways for the vehicle configurations in Table 5.1 has been performed using the design procedure outlined in Section 4.2. This procedure provides a design so that the comfort specification of Figure 4.1 is satisfied at the vehicle design operating speed. The design results are summarized in the following section.

5.2 Air Cushion Guideway Design Data

Design data for 40,000, 80,000 and 120,000 lb. air cushion vehicles with 1 and 2 hertz suspension natural frequencies are summarized in Tables 5.2, 5.3, and 5.4 for 150 mph design speeds and in Tables 5.5, 5.6, and 5.7 for 300 mph design speeds. For each design case the span flexural rigidity (EI) and corresponding values of area (a), height (h), frequency (f_1), deflection to length ratio (y_m/ℓ_s), stress (σ_t) and the cubic yards of concrete per mile required for the systems to meet the passenger comfort specification are tabulated. As illustrated by all the data, the dynamic stress levels are quite low with no stress levels exceeding 775 psi, and the passenger comfort specification has represented a more stringent design constraint than stress. The deflection to span length ratios

TABLE 5.2

GUIDEWAY DESIGNS FOR 150 MPH, 40,000 LB. URBAN VEHICLE

	f_v (hertz)	1.00			2.00		
	ℓ_s (ft)	50	100	150	50	100	150
SINGLE SPAN	EI (lb-in^2)	7.8×10^{11}	3.8×10^{12}	9.5×10^{12}	2.1×10^{12}	1.21×10^{13}	1.78×10^{13}
	a (in^2)	1540	2020	2480	1800	2630	2920
	h (ft)	2.2	4.3	6.2	3.3	6.8	8.0
	f_1 (hertz)	6.6	3.2	2.0	9.9	4.9	2.5
	y_m/ℓ_s	1/3850	1/2780	1/2630	1/8580	1/10,460	1/4960
	σ_t (psi)	286	378	386	192	160	266
	cubic yards per mile	2080	2750	3370	2440	3570	3970
2-SPAN	EI (lb-in^2)	5.1×10^{11}	3.0×10^{12}	6.4×10^{12}	1.53×10^{12}	8.5×10^{12}	1.18×10^{13}
	a (in^2)	1460	1930	2260	1710	2420	2610
	h (ft)	1.90	3.9	5.3	2.9	5.9	6.7
	f_1 (hertz)	5.4	2.9	1.72	8.7	4.3	2.2
	y_m/ℓ_s	1/2980	1/2950	1/2510	1/9640	1/20240	1/4900
	σ_t (psi)	314	324	345	150	142	226
	cubic yards per mile	1980	2620	3070	2320	3290	3550
3-SPAN	EI (lb-in^2)	4.5×10^{11}	2.6×10^{12}	5.8×10^{12}	1.40×10^{12}	7.6×10^{12}	1.01×10^{13}
	a (in^2)	1430	1870	2210	1680	2360	2530
	h (ft)	1.81	3.6	5.1	2.8	5.7	6.4
	f_1 (hertz)	5.2	2.7	1.65	8.4	4.1	2.0
	y_m/ℓ_s	1/2720	1/2630	1/2270	1/9160	1/9430	1/4420
	σ_t (psi)	328	340	366	153	148	237
	cubic yards per mile	1950	2540	3000	2280	3210	3630

TABLE 5.3

GUIDEWAY DESIGNS FOR 150 MPH, 80,000 LB. VEHICLE

	f_v (hertz)	1.00			2.00		
	ℓ_s (ft)	50	100	150	50	100	150
SINGLE SPAN	EI (lb-in^2)	6.3×10^{11}	7.2×10^{12}	1.80×10^{13}	1.06×10^{12}	1.33×10^{13}	2.2×10^{13}
	a (in^2)	1490	2330	2920	1610	2100	3070
	h (ft)	2.1	5.5	8.0	2.5	7.1	8.6
	f_1 (hertz)	5.9	4.0	2.5	7.5	5.1	2.7
	y_m/ℓ_s	1/1730	1/3690	1/3490	1/3550	1/6880	1/6310
	σ_t (psi)	586	370	377	353	253	225
	cubic yards per mile	2020	3160	3970	2190	3660	4170
2-SPAN	EI (lb-in^2)	2.9×10^{11}	6.2×10^{12}	1.35×10^{13}	6.9×10^{11}	1.03×10^{13}	1.57×10^{13}
	a (in^2)	1370	2250	2710	1510	2530	2810
	h (ft)	1.54	5.2	7.1	2.1	6.4	7.5
	f_1 (hertz)	4.3	3.8	2.3	6.2	4.7	2.4
	y_m/ℓ_s	1/1220	1/5250	1/3780	1/2810	1/8120	1/4400
	σ_t (psi)	624	242	311	376	193	282
	cubic yards per mile	1860	3050	3680	2060	3430	3820
3-SPAN	EI (lb-in^2)	3.1×10^{11}	5.3×10^{12}	5.3×10^{13}	5.6×10^{11}	9.5×10^{12}	1.42×10^{13}
	a (in^2)	1380	2170	2630	1470	2480	2750
	h (ft)	1.57	4.9	6.8	1.97	6.2	7.3
	f_1 (hertz)	4.4	3.6	2.2	5.7	4.5	2.3
	y_m/ℓ_s	1/1040	1/4540	1/3390	1/2580	1/7790	1/4010
	σ_t (psi)	746	264	330	378	196	299
	cubic yards per mile	1870	2950	3570	2000	3370	3730

TABLE 5.4

GUIDEWAY DESIGNS FOR 150 MPH, 120,000 LB. VEHICLE

	f_v (hertz)	1.00			2.00		
	ℓ_s (ft)	50	100	150	50	100	150
SINGLE SPAN	EI (lb-in^2)	1.27×10^{12}	8.1×10^{12}	2.1×10^{13}	3.8×10^{12}	1.69×10^{13}	2.5×10^{13}
	a (in^2)	1650	2390	3050	2020	2870	3190
	h (ft)	2.7	5.8	8.6	4.3	7.8	9.1
	f_1 (hertz)	8.1	3.2	2.7	12.6	5.6	2.9
	y_m/ℓ_s	1/3650	1/4660	1/3230	1/11910	1/9940	1/3840
	σ_t (psi)	368	306	435	177	193	391
	cubic yards per mile	2250	3240	4150	2750	3890	4330
2-SPAN	EI (lb-in^2)	8.4×10^{11}	7.5×10^{12}	1.78×10^{13}	2.6×10^{12}	1.01×10^{13}	1.41×10^{13}
	a (in^2)	1550	2380	2900	1870	2530	2750
	h (ft)	2.3	5.6	7.9	3.6	6.4	7.3
	f_1 (hertz)	6.8	4.2	2.5	10.9	4.6	2.3
	y_m/ℓ_s	1/3780	1/5780	1/4800	1/11750	1/8120	1/3810
	σ_t (psi)	300	240	272	152	193	314
	cubic yards per mile	2110	3230	3940	2540	3430	3730
4-SPAN	EI (lb-in^2)	7.8×10^{11}	5.8×10^{12}	1.56×10^{13}	2.4×10^{12}	8.6×10^{12}	1.30×10^{13}
	a (in^2)	1540	2210	2810	1850	2420	2680
	h (ft)	2.3	5.1	7.5	3.5	5.9	7.0
	f_1 (hertz)	6.6	3.7	2.4	10.5	4.3	2.3
	y_m/ℓ_s	1/3320	1/4270	1/3960	1/11170	1/7090	1/3290
	σ_t (psi)	335	292	313	156	205	350
	cubic yards per mile	2090	3000	3820	2510	3280	3640

TABLE 5.5

GUIDEWAY DESIGNS FOR 300 MPH, 40,000 LB. VEHICLE

f_w (hertz)		1.00			2.00		
ℓ_s (ft)		50	100	150	50	100	150
SINGLE SPAN	EI (lb-in^2)	1.38×10^{12}	7.6×10^{12}	1.89×10^{13}	2.9×10^{12}	1.95×10^{13}	6.0×10^{13}
	a (in^2)	1680	2360	2970	1910	2990	4100
	h (ft)	2.8	5.7	8.2	3.8	8.3	12.9
	f_1 (hertz)	8.3	4.1	2.6	11.3	5.9	3.9
	y_m/ℓ_s	1/4880	1/4340	1/4310	1/12070	1/13130	1/14870
	σ_t (psi)	285	323	313	154	156	214
	cubic yards per mile	2280	3210	4030	2590	4060	5560
2-SPAN	EI (lb-in^2)	1.02×10^{12}	5.1×10^{12}	1.43×10^{13}	2.0×10^{12}	1.40×10^{13}	3.6×10^{13}
	a (in^2)	1600	2150	2760	1790	2730	3530
	h (ft)	2.5	4.8	7.3	3.3	7.2	10.6
	f_1 (hertz)	7.4	3.5	2.3	9.8	5.2	3.3
	y_m/ℓ_s	1/4650	1/3340	1/3270	1/11920	1/13700	1/14020
	σ_t (psi)	266	353	368	137	190	186
	cubic yards per mile	2170	2920	3740	2430	3710	4800
3-SPAN	EI (lb-in^2)	9.2×10^{11}	5.1×10^{12}	1.5×10^{13}	1.91×10^{12}	1.21×10^{13}	4.2×10^{13}
	a (in^2)	1580	2160	2800	1770	2630	3710
	h (ft)	2.4	4.8	7.5	3.2	6.8	11.3
	f_1 (hertz)	7.0	3.5	2.4	9.6	4.9	3.4
	y_m/ℓ_s	1/4630	1/3030	1/4160	1/11720	1/12230	1/15550
	σ_t (psi)	257	393	296	136	137	179
	cubic yards per mile	2140	2930	3800	2410	3570	5040

TABLE 5.6

GUIDEWAY DESIGNS FOR 300 MPH , 80,000 LB. VEHICLE

f_v (hertz)		1.00			2.00		
ℓ_s (ft)		50	100	150	50	100	150
SINGLE SPAN	EI ($lb\text{-}in^2$)	1.67×10^{12}	1.14×10^{13}	3.7×10^{13}	2.7×10^{12}	3.9×10^{13}	1.08×10^{14}
	a (in^2)	1730	2600	3560	1890	3640	4880
	h (ft)	3.0	6.7	10.7	3.7	11.0	16.2
	f_1 (hertz)	9.1	4.8	3.3	11.1	7.6	4.8
	y_m/ℓ_s	1/3000	1/6030	1/6360	1/6390	1/21370	1/22130
	σ_t (psi)	499	273	276	286	127	180
	cubic yards per mile	2340	3540	4830	2560	4940	6630
2-SPAN	EI ($lb\text{-}in^2$)	8.6×10^{11}	8.8×10^{12}	2.7×10^{13}	1.47×10^{12}	2.8×10^{13}	7.5×10^{13}
	a (in^2)	1560	2430	3260	1690	3300	4370
	h (ft)	2.3	6.0	9.4	2.9	9.6	14.1
	f_1 (hertz)	6.8	4.4	7.9	8.6	6.7	4.2
	y_m/ℓ_s	1/2030	1/5910	1/6330	1/4410	1/25930	1/21140
	σ_t (psi)	568	249	245	323	91	164
	cubic yards per mile	2120	3300	4430	2200	4490	5490
3-SPAN	EI ($lb\text{-}in^2$)	7.4×10^{11}	8.0×10^{12}	2.4×10^{13}	1.47×10^{12}	2.5×10^{13}	6.7×10^{13}
	a (in^2)	1520	2390	3180	1700	3170	4240
	h (ft)	2.2	5.8	9.1	2.9	9.0	13.5
	f_1 (hertz)	6.4	4.2	2.8	8.6	6.4	4.1
	y_m/ℓ_s	1/1830	1/6290	1/5860	1/5530	1/21909	1/18940
	σ_t (psi)	591	227	255	259	106	176
	Cubic yards per mile	2070	3240	4320	2300	4300	5760

TABLE 5.7

GUIDEWAY DESIGNS FOR 300 MPH, 120,000 LB. VEHICLE

f_v (herts)		1.00			2.00		
ℓ_s (ft)		50	100	150	50	100	150
SINGLE SPAN	EI (lb-in^2)	2.5×10^{12}	1.11×10^{13}	4.7×10^{13}	4.9×10^{12}	4.0×10^{13}	1.36×10^{14}
	a (in^2)	1850	2590	3810	2140	3650	5270
	h (ft)	3.6	6.6	11.7	4.7	11.0	17.8
	f_1 (herts)	10.7	4.8	3.6	14.0	7.6	5.2
	y_m/ℓ_s	1/6340	1/4250	1/7300	1/15650	1/20740	1/21750
	σ_t (psi)	277	385	264	149	131	202
	cubic yards per mile	2520	3520	5180	2900	4960	7160
2-SPAN	EI (lb-in^2)	1.81×10^{12}	7.4×10^{12}	3.5×10^{13}	3.4×10^{12}	3.1×10^{13}	9.9×10^{13}
	a (in^2)	1760	2350	3510	1970	3390	4780
	h (ft)	3.2	5.6	10.5	4.0	9.9	15.8
	f_1 (herts)	9.3	4.1	3.2	12.0	7.0	4.7
	y_m/ℓ_s	1/6460	1/4570	1/7650	1/15170	1/21980	1/26840
	σ_t (psi)	261	303	225	131	112	145
	cubic yards per mile	2290	3290	4760	2670	4600	6500
3-SPAN	EI (lb-in^2)	1.54×10^{12}	7.2×10^{12}	3.3×10^{13}	3.1×10^{12}	2.7×10^{13}	8.7×10^{13}
	a (in^2)	1710	2330	3460	1940	3260	4690
	h (ft)	2.9	5.5	10.3	3.9	9.4	15.0
	f_1 (herts)	8.7	4.0	3.2	11.7	6.6	4.5
	y_m/ℓ_s	1/3890	1/3900	1/7480	1/13,270	1/19830	1/23320
	σ_t (psi)	247	350	226	145	117	159
	cubic yards per mile	2320	3160	4700	2630	4420	6250

for the 150 mph case lie between 1/1040 and 1/11,900 and for the 300 mph case lie between 1/1830 and 1/26,800. These ratios vary considerably depending upon the span and vehicle configuration. The use of a single deflection to length ratio specification to indirectly specify passenger comfort as is done in classical design procedures [15] would produce a marked variation in passenger comfort levels obtained in the design of the cases considered. The deflection ratio required to achieve a given level of passenger comfort is a strong function of suspension natural frequency as shown in Table 5.2 where for the 100 foot span the 80,000 lb. vehicle with a 2.0 hertz natural frequency suspension requires a ratio of 1/6880 while the vehicle with a 1 hertz suspension requires a ratio f 1/3690. For a number of the 300 mph vehicles with 2 hertz suspension designs, the span deflections required to achieve passenger comfort are so small as to be difficult to obtain and maintain in guideway construction, i.e., less than 0.1 inches on a 150 ft. single span for 120,000 lb. vehicle and a lower frequency suspension, an increase in acceleration or other design modification would be required to achieve a practical design.

The influence of suspension frequency, span length and vehicle size and weight upon the span materal requirements for a 150 mph urban vehicle and a 300 mph intercity vehicle are summarized in Figures 5.1 and 5.2. The data illustrates that both the vehicle and span configuration may strongly influence guideway material requirements in systems designed to satisfy a passenger

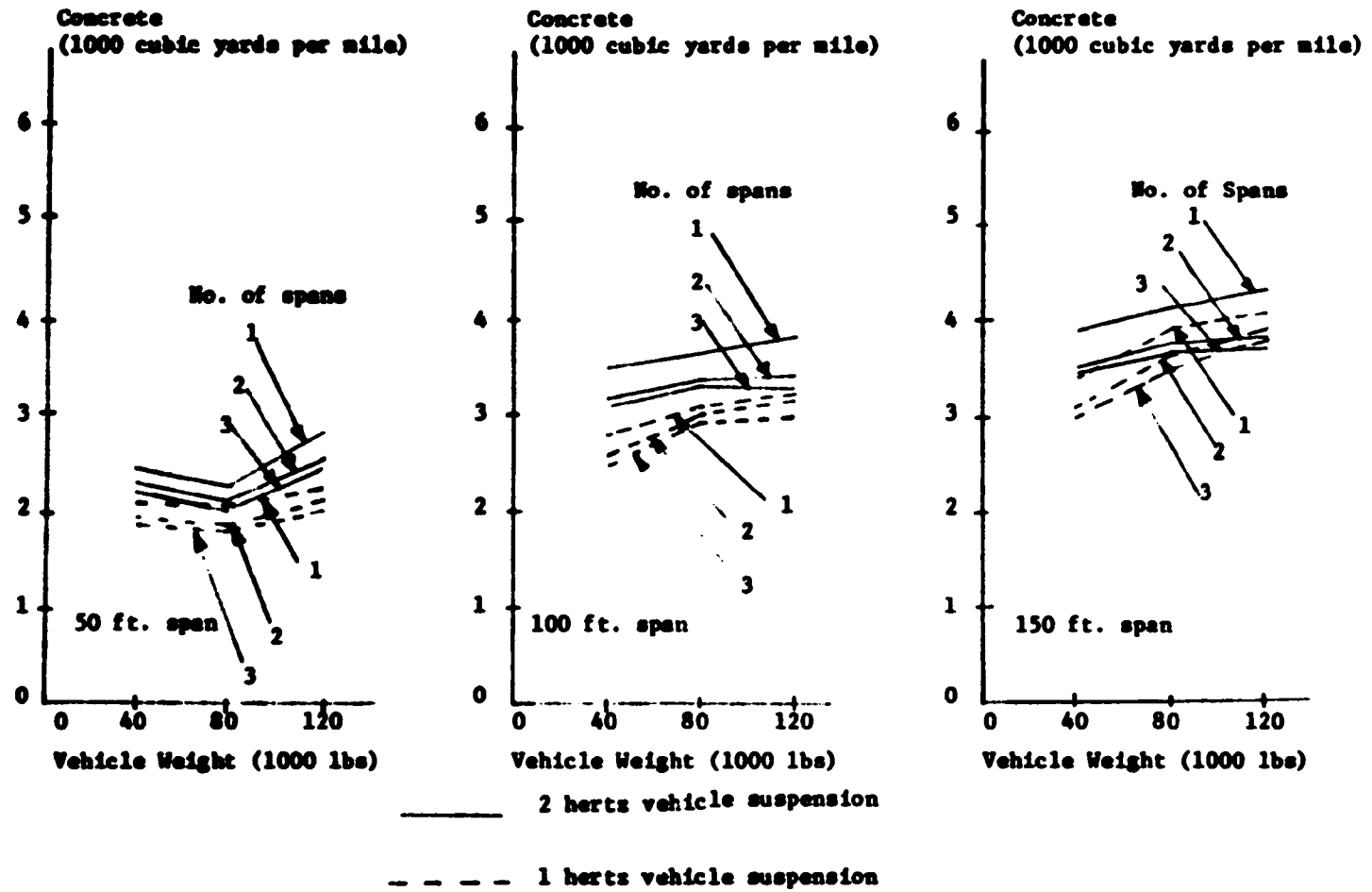

Figure 5-1. Span Material Requirements for a 150 mph System

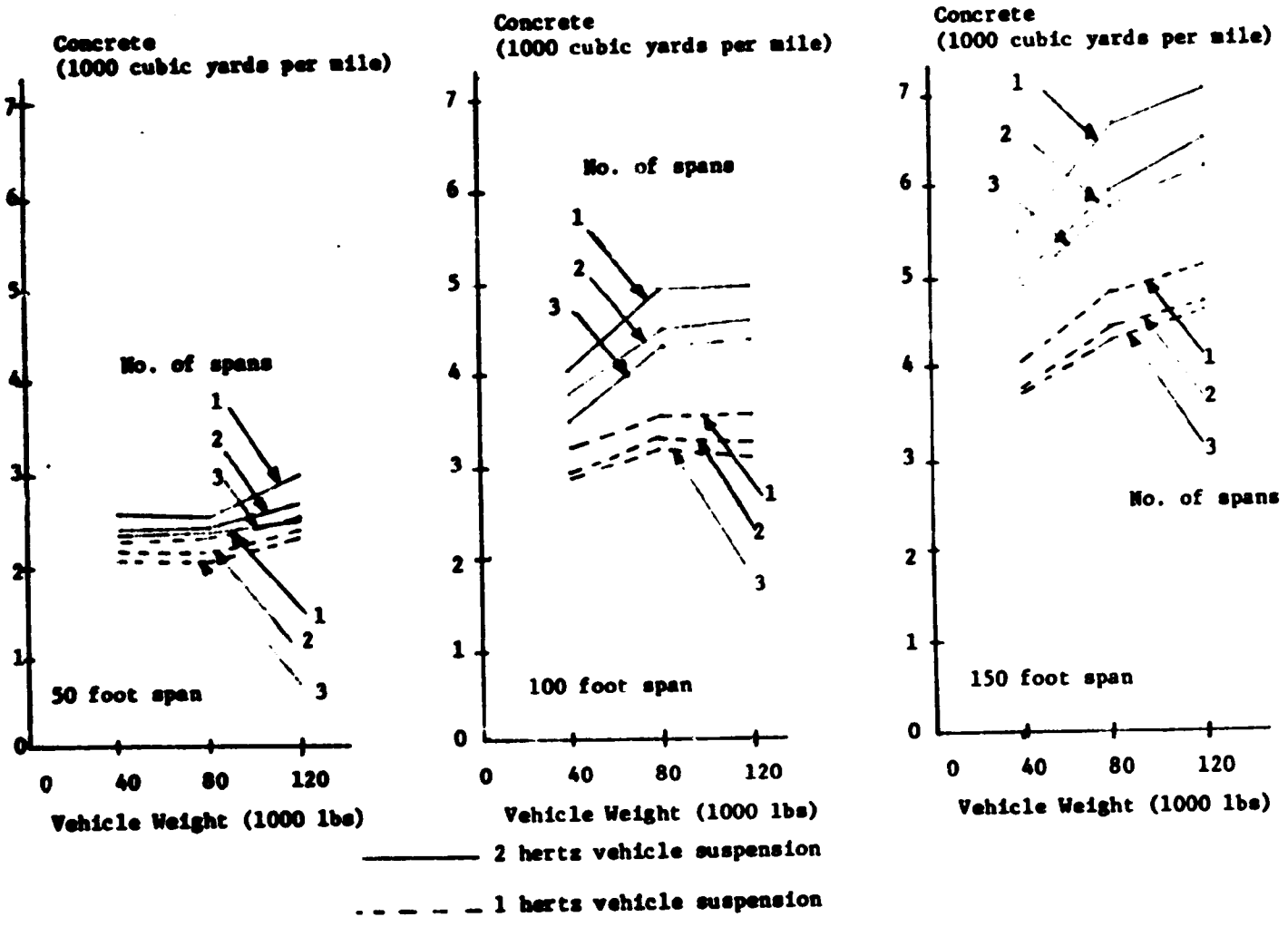

Figure 5-2. Span Material Requirements for a 300 mph System

comfort constraint such as given in Figure 4.1. The data specifically shows for the vehicle configuration parameters:

(1) Vehicle Suspension Natural Frequency

In all 300 mph and in all 150 mph design cases except for the 150 mph 120,000 lb. vehicle crossing 150 ft. 2 and 3 multispan systems* a reduction in suspension natural frequency from 2.0 to 1.0 hertz reduces the span material requirements. The effect is more pronounced for the higher speed cases as noted by comparing Figures 5.1 and 5.2. For an 80,000 lb. vehicle crossing 100 ft. single spans at 300 mph a reduction in suspension natural frequency from 2.0 to 1.0 hertz reduces material requirements by 29% while at 150 mph operation a reduction of 14% is obtained. It is noted that for several of the 300 mph 120,000 lb. vehicles equiped with 2 hertz suspensions span heights of greater than 15 ft. are required for 150 ft. spans, and either a reduction in suspension frequency, span length or other design change is required to achieve a practical design.

(2) Vehicle Size

Vehicle size, keeping the weight per unit length constant**, may have an influence upon span material requirements. While in many cases the data shows as vehicle total length and weight increase, span material requirements increase, in a number

*This configuration has system parameters such that the vehicle pitch mode is strongly excited at 150 mph operation on 150 ft. spans with 120 ft. vehicle and a 1 hertz suspension.

** For a given size vehicle as the weight per unit length increases, the span material requirements increase.

of cases the vehicle total weight and length may increase with either no increase or even a small decrease in span material requirements. This factor occurs because,as the vehicle length changes, the phasing between the front and rear suspensions is also changed. In a number of cases, the suspension phasing has a more significant effect upon span requirements than vehicle total weight.

(3) Vehicle Speed

For guideways designed for a 300 mph vehicle, span materials requirements are greater than or equal to those of a corresponding 150 mph vehicle. For an 80,000 lb., 2.0 hertz suspension vehicle crossing 100 ft. single spans, operation at 300 mph requires 1.35 times as much span material as that required for 150 mph operation. For some configurations, only small increases are required, i.e. for 120,000 lb., 1.0 hertz suspension vehicle crossing 100 ft. single spans only 1.06 times as much material is required for 300 mph operation compared with 150 mph operation.

For the Span:

(4) Span Configuration

In every design case multispan beam configurations required less material than single span configurations. In the majority of cases a greater reduction in material is obtained by replacing a single span, by a two span beam, rather than by re-

placing a 2 span beam by a three span beam. For an 80,000 lb., 2.0 hertz suspension vehicle crossing 100 ft. spans, at 150 mph a 2 span system requires 94% and a 3 span system 92% of the material of a single span system while at 300 mph a 2 span system requires 91% and a 3 span system 87% of the material of a single span system.

(5) Span Length

For a given vehicle, as the span length increases, the cross section material requirements increase*. For an 80,000 lb. 2 hertz suspension vehicle crossing a single span, at 150 mph the span material requirements per unit length of 100 ft. and 150 ft. spans are respectively 1.7 and 1.9 times greater than a 50 ft. span and at 300 mph, 100 ft. and 150 ft. span requirements are respectively 1.9 and 2.4 times greater than a 50 ft. span.

All of the design data discussed has been developed for the specific passenger comfort specification of Figure 4.1. Since the designs are essentially limited by this constraint, they are sensitive to the levels of permissible acceleration specified. An indication of the sensitivity of span material requirements to the acceleration level has been determined for an 80,000 lb. vehicle with a 2 hertz suspension natural frequency crossing a 100 ft. single

*In guideway design, the cost of the spans must be balanced against the support costs. As span length increases more span material is required, but fewer supports are required.

span system. At a 150 mph operating speed, if the permissible acceleration level is increased from the 0.045 g's represented by the specification to 0.09 g's, the span material requirements are reduced by 15%. At a 300 mph operating speed if the permissible level of acceleration is increased from 0.04g's to 0.08 g's, the span material requirements are reduced by 15%. The specification of the levels of passenger comfort in an advanced system thus has a significant influence upon the guideway requirements.

In addition to the parametric data presented for all three size air cushion vehicles, data has been developed for the 80,000 lb. vehicle equiped with a 1.0 hertz natural frequency suspension to illustrate the influence of guideway camber and vehicle body mass distribution (pitch inertia) on system requirements.

The data illustrating the influence of camber on guideway requirements is summarized in Table 5.8. Camber in a guideway may result from a number of factors including thermal effects, dead-load and/or by purposely constructing the guideway with an initial shape. For typical guideways, specified amounts of positive camber* can reduce the guideway "net dynamic deflection presented to the vehicle"and can compensate for the dynamic deflection due to the vehicle.

---

*The initial shape of the span results in an upward deflection which contacts the dynamic downward deflection due to a vehicle passage.

For a given vehicle, span and vehicle speed, an optimum camber shape exists which will minimize the excitation generated in the vehicle due to the span motion. Thus, in high performance systems, precamber may allow either a more comfortable ride or permit a reduction in span material requirements. In addition to intentional camber, because of thermal gradients resulting from environmental conditions, thermal camber will occur in guideway spans. For a 100 ft. single span defined in Figure 4.3 which is 4.3 ft. high, a uniform thermal gradient of $5^{\circ}F$ results in a deflection of 0.21 in*. This deflection is comparable to the dynamic deflection due to a vehicle passage and may significantly influence ride quality. Because multispan guideways have significantly reduced thermal camber in comparison to single spans [13], multispan structures may be used to reduce thermal camber effects to levels which will not strongly influence system performance. The influence of a specified camber on single and multispan guideway-vehicle performance may be assessed with the guideway simulation and design computer programs in Appendicies C, D, and E.

The data in Table 5.8 has been developed for a periodic cosine camber shape. The nondimensional camber amplitude $\bar{A}_c$ is normalized by y* the midspan deflection due to a concentrated

*Note the experimental data in[11] which confirms the large thermal camber deflections occuring in single spans due to solar heating and night cooling.

TABLE 5.8

INFLUENCE OF CAMBER ON SPAN REQUIREMENTS

	v (mph)	150		300	
	camber	None	Compromise	None	Compromise
SINGLE SPANS	$\bar{A}_c$	0.0	0.60	0.0	0.60
	min. allowable $\bar{A}_c$	——	0.45	——	0.40
	max allowable $\bar{A}_c$	——	0.80	——	0.90
	EI (lb-in^2)	7.2×10^{12}	4.3×10^{12}	1.14×10^{13}	7.5×10^{12}
	a (in^2)	2330	2070	2600	2360
	h (ft)	5.5	4.5	6.7	5.7
	f_1 (hz)	4.0	3.3	4.8	4.1
	y_m/ℓ_s	1/3690	1/2670	1/6030	1/3180
	σ_t (psi)	370	420	270	440
	cubic yards/mile	3160	2810	3540	3200
3-SPAN BEAMS	$\bar{A}_c$	0.0	0.40	0.0	0.40
	min. allowable $\bar{A}_c$	——	0.28	——	0.05
	max. allowable $\bar{A}_c$	——	0.48	——	0.75
	EI (lb-in^2)	5×310^{12}	3.0×10^{12}	3.0×10^{12}	5.3×10^{12}
	a (in^2)	2170	1920	2390	2180
	h (ft)	4.9	3.8	5.8	4.9
	f_1 (hz)	3.6	2.9	4.2	3.6
	y_m/ℓ_s	1/4540	1/2260	1/6290	1/3610
	σ_t (psi)	260	410	230	330
	cubic yds/mile	2950	2600	3240	2960

Vehicle: 80,000 lb with a 1.0 hertz suspension natural frequency of the configuration specified in Table 5.1.

Span: 100 ft. of the configuration specified in Table 5.1 and Fig. 4.3.

force equal to the vehicle weight. The data compares the span structural requirements for designs with and without (i.e. initially flat) camber which meet the passenger comfort specification of Figure 4.1. The cambered designs have been selected so that for a variation in camber over a tolerance band, the passenger comfort constraint is satisfied. This tolerance band is indicated as minimum and maximum allowable $\bar{A}_c$ in Table 5.8. The data in the table shows that for both 150 and 300 mph operation a positive precamber of $\bar{A}_c = 0.6$ for single span systems provides a design which meets passenger comfort, utilizes 11% for 150 mph operation and 9.6% for 300 mph operation less material than uncambered guideways and allows at least a 33% decrease or increase in camber amplitude before the passenger comfort specification is exceeded. For the three span system a camber amplitude of $\bar{A}_c = 0.4$ utilizes 12% for 150 mph operation and 8.6% for 300 mph operation less material than uncambered guideways and allows at least $\pm$ 20% increase or decrease in camber amplitude before the passenger comfort specification is exceeded. Thus, the use of precamber on single and multispan guideways can both reduce span material requirements and provide a tolerance to the effects of thermal camber.

Data to illustrate the influence of vehicle body mass distribution is summarized in Table 5.9 for an 80,000 lb. vehicle traversing 100 ft. single spans. A value of nondimensional inertia $\bar{I}_v$ equal 1.0 corresponds to a uniformly distributed body, while a value of 3.0 corresponds to the mass concentrated at the two suspension attachment points. For a zero pad length vehicle $\bar{I}_v = 1.0$

TABLE 5.9

INFLUENCE OF VEHICLE PITCH INERTIA $\bar{I}_v$ ON SPAN REQUIREMENTS

v (mph)		150			300		
$\bar{I}_v$		1.0	2.0	3.0	1.0	2.0	3.0
SINGLE BEAMS	EI (lb-in^2)	7.2×10^{12}	3.9×10^{12}	2.8×10^{12}	1.14×10^{13}	7.1×10^{12}	5.8×10^{12}
	a (in^2)	2330	2030	1900	2600	2330	2210
	h (ft)	5.5	4.3	3.8	6.7	5.5	5.1
	f_1 (hz)	4.0	3.2	2.8	4.8	4.0	3.7
	y_m/ℓ_s	1/3690	1/2410	1/1480	1/6030	1/3160	1/2440
	σ_t (psi)	370	441	626	273	429	512
	cubic yds/mile	3160	2760	2580	3540	3160	3010
3-SPAN BEAMS	EI (lb-in^2)	5.3×10^{12}	2.4×10^{12}	1.79×10^{12}	8.0×10^{12}	4.7×10^{12}	4.0×10^{12}
	a (in^2)	2170	1840	1750	2390	2120	2040
	h (ft)	4.9	3.5	3.1	5.8	4.7	4.3
	f_1 (hz)	3.6	2.6	2.3	4.2	3.4	3.2
	y_m/ℓ_s	1/4540	1/1780	1/1400	1/6290	1/2940	1/1980
	σ_t (psi)	264	526	590	227	413	573
	cubic yds/mile	2950	2500	2380	3240	2870	2770

Vehicle: 80,000 lb with a 1.0 hertz suspension natural frequency of the configuration listed in Table 5.1.

Span: 100 ft. of the configuration specified in Table 5.1 and Figure 4.3

yields a pitch natural frequency 1.73 times the heave natural frequency while $\bar{I}_v = 3.0$ yields a vehicle with equal pitch and heave natural frequencies. In the urban air cushion vehicle [11], the distribution of mass, especially the compressors and the linear induction motor, and suspension distribution yields a vehicle with nearly equal pitch and heave natural frequencies.

Table 5.9 summarizes guideway structural requirements as a function of vehicle pitch inertia for vehicles designed to meet the passenger comfort specification of Figure 4.1. The data shows for the 100 ft. single span that an increase in pitch inertia $\bar{I}_v$ from 1.0 to 3.0 allows a reduction in span material requirements of 18% for 150 mph operation and 15% for 300 mph operation compared to those of a uniformly distributed mass vehicle. For the three span system an increase in pitch inertia $\bar{I}_v$ from 1.0 to 3.0 reduces span material by 19% for 150 mph operation and by 14% for 300 mph operation compared to the requirements of a uniformly distributed mass vehicle. For the vehicles and span configurations considered in this report, vehicle pitch motion produces an important contribution to vehicle body accelerations, thus reduction of the pitch frequency by increasing the pitch inertia results in less pitch acceleration and the span structural rigidity may be reduced.

For vehicles with lengths much shorter than the span length in which principally the vehicle heave motion is excited, an increase in pitch inertia will not significantly alter span requirements.

6. SUMMARY AND CONCLUSIONS

This report provides analysis techniques, a design procedure and design data for passenger carrying vehicle single and multispan guideways. Three documented computer programs have been developed to aid in design:

(1) Fully Coupled Vehicle-Guideway Simulation-Appendix C

This is a computer simulation based upon numerical integration which determines the response of a completely coupled vehicle-guideway system as a function of time. The vehicle model includes vehicle body mass and pitch inertia, front and rear secondary suspensions with stiffness and damping characteristics and primary suspensions with stiffness and finite pad length characteristics. The guideway model includes single and multispan cambered beams with distributed stiffness, mass and damping properties supported on rigid piers. In the model the time varying vehicle accelerations and suspension deflections and forces are computed as well as span deflections, moments and stresses.

(2) Partially Coupled Computer Simulation-Appendix D

This program determines vehicle accelerations versus time, rms accelerations versus frequency, suspension deflections and guideway deflections, moments and stresses using a partially coupled vehicle-guideway model. The model allows full coupling between the vehicle and the guideway but assumes that the vehicle suspension forces on the guideway are constant and equal to the vehicle weight. All other features of the vehicle-guideway model are similar to those of the model described above. This partially coupled model is valid for many high performance transportation systems as described in Chapter 3 and allows computation of system characteristics in less than one quarter the time required for the full simulation program.

(3) Guideway Design Program - Appendix E

This program is based upon the partially coupled vehicle-guideway model and determines guideway main support beam structural properties required for a vehicle-guideway system to provide specified levels of passenger comfort. The program is set up for prestressed concrete twin I-beam type structures but may be easily modified for other types of structures.

In addition to the working computer programs, general design data for vehicle-elevated guideway systems has been developed which show:

(1) For vehicle operating speeds v

(a) less than 0.5 $\ell_s f^*$ for single span structures

(b) less than $\ell_s f^*$ for multiple span structures

(c) less than 1.5 $\ell_s f^*$ for continuous span structures

The span deflections, due to a vehicle passage, are quasi-static and multispan deflections (for 3 or greater spans) are 70% while continuous span deflections are 53% of comparable single span structures. In these operating ranges span dynamics are relatively insentive to span damping.

(2) For vehicle operating speeds v that approach 2 $\ell_s f^*$ resonance conditions occur in multiple and continuous spans. The span deflections are influenced strongly by span damping and for a damping ratio of 0.02, maximum deflections in three and continuous spans caused by the passage of a concentrated force are respectively 3.7 and 4.6 times the quasi-static deflections.

(3) As vehicle loads are distributed across suspension pads, guideway deflections are reduced. In the quasi-static operating range, vehicles crossing single spans with pad lengths 50% and 100% of a span length reduce span deflections respectively by more than 20% and 40% compared to concentrated force vehicles.

Specific design data has been developed for 40,000, 80,000 and 120,000 lb. 150 mph and 300 mph air cushion vehicle guideway. This data was developed using the design program of Appendix E for prestressed concrete twin I beam structures traversed by vehicles which meet the passenger comfort.

specifications of Figure 4.1, i.e. rms vehicle body accelerations are less than 0.045 g's in the 2.5-12 hertz frequency range. The conclusions reached from this specific study include:

(1) For all designs, the passenger comfort constraint is more stringent than vehicle induced stress constraints. The maximum induced span dynamic stress is less than 775 psi for both low and high speed vehicle systems. The guideway designs are directly dependent upon the passenger comfort level required. For an 80,000 lb. 150 mph vehicle with a 2 hertz suspension natural frequency traversing a single 100 ft. span guideway, if the permissible rms acceleration is increased from 0.045 g's to 0.09 g's span material requirements may be reduced by 15%.

(2) For system designs constrained by passenger comfort, vehicle characteristics may strongly influence guideway requirements. Vehicle suspension natural frequency and damping, vehicle body mass distribution (pitch inertia) and vehicle suspension attachment point location may all influence span requirements as well as total vehicle size and weight, vehicle speed and suspension pad length. For an 80,000 lb. vehicle crossing a 100 ft. single span system at 300 mph, a reduction in suspension natural frequency from 2.0 to 1.0 hertz allows a reduction in span requirements of 29% while an increase in pitch inertia from that of a uniform mass distribution to a body with an effective mass distribution concentrated at the suspension attachment points allows a reduction in span material of 14%.

(3) Span configuration and camber may strongly influence span structural requirements. In all cases studied the use of multiple span guideways required less span material than single span structures designed for the same operational vehicle. For an 80,000 lb. vehicle with a 2.0 hertz suspension crossing 100 ft. spans at 300 mph, a two span system requires 91% and a three span system 87% of the material of a single span system.

The use of cambered spans for single and three span systems can result respectively in 11% and 12% material reduction in comparison to uncambered spans and can, also, provide a tolerance of ± 33% variation in camber due to thermal effects from the precamber amplitude and still met ride quality specifications for 150 mph vehicles.

This report has provided design programs and data which are directly useful in determining guideway structural requirements based upon the vertical deflections induced in straight guideway spans by a vehicle passage. Extension of the work to provide design information for:

(1) The guideway vertical, angular and lateral misalignment tolerances required to provide acceptable ride quality.

(2) The structural design of curved and possibly superelevated sections of guideway.

(3) The lateral support surface structural requirements.

(4) The torsional restraint structural requirements.

(5) The pier-span interface structural requirements.

(6) Vehicle vertical and lateral optimized suspensions and vehicle body mass distribution and flexibility characteristics.

would provide additional valuable information for advanced transportation system designers. In addition, an important contribution to vehicle-guideway design would be provided by the correlation of analytical design techniques with experimental data for vehicle-guideway dynamic interactions.

7. REFERENCES

1. Anderson, J. E., Dais, W. L., Carrad, W. L., Kornhauser, A. L. "Personal Rapid Transit," Department of Conferences and Institutes, University of Minnesota, Minneapolis, Minnesota, 1971.

2. "High Speed Rail Systems," Technical Report FRA-RT-70-36, TRW Systems Group, Redondo Beach, California, 1970.

3. Wickens, A., "The British High-Speed Train," ASME Paper No. 73-ICT-16, 1973.

4. Isozaki, S., Hope, R., "J. N. R. Prepares for the 21st Century," Railway Gazette International, V. 128, No. 10, 1972.

5. Van Dorn, N. H., "The Aerotrains Are Coming," ASME Paper No. 73-ICT-101, 1973.

6. Lampros, Alex, "Status of the Tracked Air Cushion Research Vehicle (TACRV)," ASME Paper No. 73-ICT-23, 1973.

7. Winkle, G., "The Transrapid System," IEEE Northeast Region Electronics Region Conference Paper, Boston, Massachusetts, 1972.

8. Wilkie, D. F., "Dynamic Characteristics and Control Requirements of Alternative Magnetic Levitation Systems," ASME Paper No. 73-ICT-17, 1973.

9. Ohno, E., Iwamoto, M., Yamada, T., "Characteristics of Superconductive Magnetic Suspension and Propulsion for High-Speed Trains," Proceedings of IEEE, Vol. 61, No. 5, 1973.

10. Chiu, W. S., Wormley, D. N., Smith, R. C., Richardson, H. H. "Coupled Dynamic Interactions between High Speed Ground Transport Vehicles and Discretely Supported Guideways," Tech. Report No. FRA-RT-71-76, Department of Mechanical Engineering, Mass. Institute of Technology, Cambridge, Mass., July, 1970.

11. "Urban Tracked Air Cushion Vehicle Program—Phase I," Report 1, Rohr Corporation, Chula Vista, California, 1972.

12. "Urban Tracked Air Cushion Program--Phase 1," Report 1. LTV Corporation, Arlington, Texas, 1972.

13. Birkeland, P. W., Magura, D. D., McCullough, B. F. Meisenholder, S. G., Weidlinger, P., "Investigation of Low Cost Guideway Concepts for Tracked Air Cushion Vehicles", Tech. Report, TRW Systems/ ABAM Systems, Redondo Beach, California, Draft copy dated May 1973.

14. Giraud, R., "A Preliminary Design Study for a Tracked Air Cushion Research Vehicle", Tech. Report No. 7-35337, Vol. 1 and Vol. 2, Aeroglide Systems, New York, New York, February 1969.

15. Standard Specifications for Highway Bridges, The American Association of State Highway Officials, Washington, D. C., 1965.

16. Pulgrano, L., "Tracked Air Cushion Research Vehicle— Vehicle/Guideway Dynamic Analysis", Technical Report No. PMT-B4-R71-07, Grumman Aerospace Corporation, Bethpage, New York, March, 1971.

17. Kaplan, A., Lipner, N., Roberts, F. B. and Strom, R. O., "Train Elevated Guideway Interactions", Tech. Report No. FRA-RT-70-23- TRW Systems Group, Redondo Beach, California, February, 1970.

18. Lipner, N., Evensen, D.A., and Kaplan, A., "Dynamic Response of Continuous Beam Elevated Guideway", Report No. FRA-RT-71-42 (Vol. 1 and Vol. 2), TRW Systems Group, Redondo Beach, California, July 1970.

19. Wang, C. H., "Elevated Guideway Structures -- Continuous Beams" Tech. Report No. FRA-RT-71-54, TRW Systems Group, Washington D. C., June 1970.

20. Meisenholder, S. G., "Dynamic Requirements for a Suspended Vehicle System for High Speed Ground Transportation", AIAA Paper No. 72-405, April, 1972.

21. Royal, J. W. and Zuckerberg, H., "TACV Vibration Analysis Program", Tech. Report No. KHL-TSC-73-1039, DOT, Transportation Systems Center, Cambridge, Massachusetts.

22. Wilson, J. F. and Biggers, S. B., "Dynamic Interactions between Long, High Speed Trains of Air Cushion Vehicles and their Guideways", A. S. M. E. Transactions, JOURNAL OF DYNAMIC SYSTEMS, MEASUREMENT, AND CONTROL, No. 1, Series G, Vol. 93, March 1971.

23. Biggers, S. B. and Wilson, J. F., "Dynamic Interactions of High-Speed Tracked Air Cushion Vehicles with their Guideways", ASME Transactions, JOURNAL OF DYNAMIC SYSTEMS, MEASUREMENT, AND CONTROL, No. 1, Series G, Vol. 95, March 1973.

24. Biggers, S. B., "Guideway Camber and Three-Stage Passive Suspension for Improved Tracked Air Cushion Vehicle Ride Quality", ASME Transactions, JOURNAL OF DYNAMIC SYSTEMS, MEASUREMENT, AND CONTROL, No. 1, Series G, Vol. 95 March, 1973.

25. Wilson, J. F., "Dynamic Interactions between Moving Loads and the Supporting Structures, with Application to Air Cushion Vehicle--Guideway Design," Report No. FRA-RT-72-27, Department of Civil Engineering, Duke University, Durham, North Carolina. (PB205 325)

26. Richardson, H. H. and Wormley, D. N., "Transportation Vehicle/Beam-Elevated Guideway Dynamic Interactions: A State of the Act Review", ASME Transactions, JOURNAL OF DYNAMIC SYSTEMS, MEASUREMENT AND CONTROL, Vol. 96, Series G, No. 2, June, 1974.

27. Meisenholder, S. G. and Weidlinger, P. "Dynamic Interaction Aspects of Cable-Stayed Guideways for High Speed Ground Transportation", ASME, Transactions, JOURNAL OF DYNAMIC SYSTEMS, MEASUREMENT AND CONTROL, Vol. 96, Series G, No. 1, June, 1974.

28. Smith, C. C. and Wormley, D. N. "Response of Continuous Periodically Supported Guideway Beams to Traveling Vehicle Loads ", ASME Transactions JOURNAL OF DYNAMIC SYSTEMS, MEASUREMENT AND CONTROL, to appear in a 1974 issue.

29. Smith, C. C., Gilchrist, A. J., and Wormley, D. N. "Multiple and Continuous Span Elevated Guideway-Vehicle Dynamic Performance" JOURNAL OF DYNAMIC SYSTEMS, MEASUREMENT AND CONTROL, to appear in a 1974 issue.

30. Katz, R. M., Nene, V. D., Ravera, R. J., Skalski, C. A., "Performance of Magnetic Suspensions for High Speed Vehicles Operating Over Flexible Guideways," ASME Transactions, JOURNAL OF DYNAMIC SYSTEMS, MEASUREMENT AND CONTROL, Vol. 96, Series G, No. 2, June, 1974.

31. Anderes, J. R. and Ravera, R. J. "Vehicle/Guideway Interaction Dynamics Simulation for TLRV and PTACV-Phase 1", Technical Report No. MTR-6710, MITRE Corp., June, 1974.

32. Wormley, D. N., Garg, D. P. and Boghani, A. B., "Nonlinear and Finite Pad Length Performance of Vehicle Air Cushion Suspensions". Technical Report No. RPL-72-72966-1, Department of Mechanical Engineering, Massachusetts Institute of Technology, Cambridge, Massachusetts, 1972.

33. Richart, F. E. Vibrations of Soils and Foundations Prentice-Hall, Englewood, N.J., 1970.

34. Gilchrist, A. J. "Design of Multispan Elevated Guideway Structures for Urban and Intercity Transport Vehicles" Ph.D. Thesis, Department of Mechanical Engineering, Massachusetts Institute of Technology, Cambridge, Mass., 1974.

35. Schultz, D. G., and Melsa, J. L. State Functions and Linear Control Systems, McGraw-Hill, N.Y., N.Y., 1967.

36. Gifford, E. W. H. and partners, "A Study of Three Guideway Systems," Technical Report No. DOT-FR-9-0032, (for Tracked Hovercraft, Limited), London, England, 1970.

37. Rowe, R. E., Concrete Bridge Design, John Wiley and Sons, New York, New York.